UNIVERSITÀ DEGLI STUDI DI MILANO
Scuola di Dottorato in Scienze Biologiche e Molecolari
XXVII Ciclo

Alterations of choline phospholipid metabolism in ovarian cancer: study of the activity and expression of choline kinase as a prognostic value

SSD: MED16; BIO/11

Anna Granata

PhD Thesis

Scientific tutor: Dr.ssa Delia Mezzanzanica

Thesis performed at Fondazione IRCCS Istituto Nazionale Tumori di Milano, Dipartimento Oncologia Sperimentale e Medicina Molecolare, Molecular Therapies Unit.

Academic year: 2013-2014

Contents

PART I

Summary

Epithelial ovarian cancer (EOC) is a highly lethal malignancy due to late diagnosis and early relapse associated with development of chemoresistance. So far, the origin of drug resistance is not completely understood and several mechanisms seem to be responsible for this process including the ability of cancer cells to modify/reprogram cellular metabolism. Aberrant choline metabolism, characterized by increased phosphocholine (PCho) levels sustained by enhanced choline kinase (ChoK) activity, is a new cancer metabolic hallmark that can be monitored by Magnetic Resonance Spectroscopy (MRS) and that reflects the interactions between oncogenic signaling and cellular metabolism. EOC possesses an altered MRS-choline profile, characterized by increased PCho content to which mainly contribute over-expression and activation of Choline kinase-alpha (ChoKα). The project aimed to investigate the biological and clinical relevance of increased ChoK expression and activity in EOC. We showed that transient CHKA silencing induced: a significant reduction in PCho accumulation as assessed by MRS analysis; an inhibition of in vitro cell growth; down modulation of genes related to inflammation and EOC aggressiveness; a significantly reduced cell motility and invasion and a significant increase of sensitivity to platinum, paclitaxel and doxorubicin even in a drug-resistant context. Since the dynamics of biological effects related to CHKA silencing could not possibly be detectable by transient RNAi, we stably downregulated ChoKα mRNA expression using a lentiviral vector, expressing GFP and specific CHKA shRNA, in two EOC cell lines, INTOV11 and SKOV3. In both transduced cell lines, we confirmed the data obtained with the transient downmodulation, as reduction of PCho content, inhibition of in vitro cell growth, reduction of invasive potential and migration capability. Furthermore, a significant decrease of in vivo tumor growth (sub-cutaneous

injection) was evident in both sh-CHKA cellular models as compared to their controls. The global metabolic profiles of sh-CHKA and control EOC cell lines, performed with the Metabolon technology platform, revealed in both cellular models an alteration of glutathione metabolism, commonly characterized by a decrease of reduced glutathione (GSH) content in shCHKA cells as compaired to their controls. Interestingly, sh-CHKA showed an increased sensitivity to drug treatment (platinum and doxorubicin) suggesting that CHKA knocking down may change antioxidant cellular defense thus increasing drug sensitivity. Since the GSH intracellular levels are well known to interfere with treatment efficacy of several DNA damaging drugs, we have investigated whether the alteration of GSH/GSSG levels dependent upon CHKA silencing is the mechanism by which response/resistance to DNA-damaging drugs is affected. Artificial reduction of intracellular GSH in wild type EOC cells phenocopied CHKA silencing effects while restoration of GSH levels in CHKA silenced cells caused a recovery of the wt phenotype by rescuing drug resistance. The concurrent modulation of active ROS species following CHKA silencing demonstrates the direct involvement of oxidative stress pathway regulation by ChoKα expression.

Finally, in order to investigate the putative role of CHKA in EOC pathogenesis we performed an in silico analysis on seven public data sets of gene expression profile, including 698 EOC patients and we found a progressive increase of CHKA expression along EOC grading. Interestingly the CHKB expression in the same samples showed an opposite trend. Given these premises, we propose that a metabolic approach to EOC treatment might have the potential to address some of the issues that contribute to the high EOC lethality and open the way for the validation of ChoKα as a new therapeutic target to be used alone or in combination with conventional drugs for EOC treatment.

Introduction

1. Ovarian Cancer

1.1 Clinical aspects

Although its incidence is quite low, EOC is the leading cause of death from gynecologic cancers (1). Symptoms associated with EOC are typically nonspecific and their association to the tumor is often not recognized therefore, more than two thirds of EOC cases are diagnosed when the disease has progressed to late stages (III/IV) (2), dropping 5-year survival rate to approximately 33%. Besides stage and histologic grade at diagnosis, the presence or absence of residual disease after debulking surgery remains an important prognostic factor for EOC. Surgery is followed by a combination of platinum - and taxane-based chemotherapy as first-line treatment for advanced EOC, yielding response rates of over 80% (3). However, most of the patients will eventually relapse with a median progression-free survival of 18 months. The length of the disease-free period following response to platinum compounds can be used to categorize patients into groups with different prognosis: platinum-sensitive, -resistant and -refractory disease (4). Many efforts have been made to overcome chemoresistance following front-line treatment. Different drug combinations are indeed available to treat relapsing patients, including some molecular targeted agents like: angiogenesis, PARP or tyrosine kinase inhibitors (5); however, clinical responses to these drugs are only partial and new approaches to improve EOC patients treatment with better design of therapeutic trials are still needed (6).

1.2 Histological subtypes and origins of EOC

Historically, EOCs were thought to arise from ovarian surface epithelial cells, leading to four major cell types: serous, endometrioid, clear cell and mucinous. Although differences in biology and response to therapy were recognized, it was thought that these cell types reflected morphologic variants of the same disease, and cell type was not a selection criteria for type of treatment. There are now increasing evidences that major EOC cell types arise from distinct, often non ovarian, precursor lesions (Figure 1) (7). Recent pathological, immune-histochemical and molecular studies have changed this view, "*Shifting the paradigm*" (8), from one disease model toward a set of unique diseases of diverse origin and biology, linked primarily by ovarian localization, with profound therapeutic implications. The EOC are primarily classified by cell types in: high grade serous, mucinous, endometroid and clear cells corresponding, according to the molecular (assessed by gene expression profile) and morphological features similar to those of the different epithelia in the organs of the female reproductive tract (Figure 1).

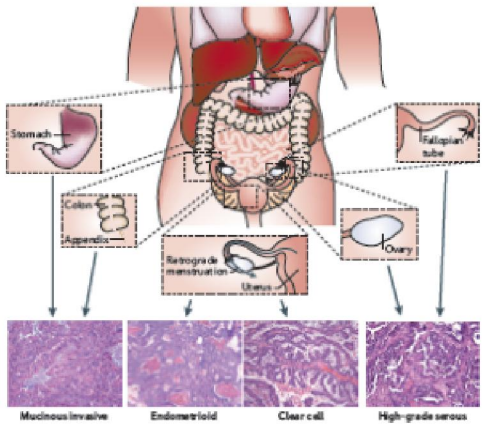

Figure 1. The origins of ovarian cancer (*from Vaughan S. et al 2011*).

- **Serous EOC:** the most common type. It derives from epithelial cells covering ovary surface and/or from the distal fallopian tube, even if at the moment the real contribute of this two compartments to the origin of this tumor is not completely understood (7),(9).
- **Mucinous EOC:** represent 5–10% of all malignant ovarian neoplasms, are characterized by cells resembling either those of the endocervical epithelium or, more frequently, those of the intestinal epithelium (intestinal type).
- **Endometrioid EOC:** the second most common malignant EOC, are characterized by cells resembling those of the endometrium and they are associated with endometriosis.
- **Clear Cell EOC:** little is known about the development and progression of this type of EOC. In some cases they are associated to endometriosis, atypical noninvasive endometriosis has been shown to be linked to Clear Cell Carcinoma (CCC) through demonstration of identical mutations in both components.

Based on cell type, origin and molecular features a new paradigm for the pathogenesis and origin of EOC has been now proposed on the basis of a dualistic model of carcinogenesis. Accordingly, EOC have been categorized into two categories corresponding to the two main pathways of tumorigenesis, designated as types I and II (Figure 2).

Type I tumors comprise Low grade serous Carcinomas (LGSCs), endometroid, clear cell and mucinous carcinomas. These tumors constitute only 25% of EOC with a 5 year survival of about 55%. They are generally indolent, with a good prognosis, tumor masses are localized to one ovary (stage I) and are associated

with frequent KRAS, BRAF, CTNNB, PTEN and PIK3C genetic alterations, with rare mutations in TP53 gene (8).

Type II tumors comprise High Grade serous Carcinomas (HGSC). These cancers present at more advanced stages and grow aggressively, constitute approximately 75% of ovarian tumors, and are responsible for 90% of EOC deaths. They are driven by multiple areas of amplification and deletion; almost all HGSC have mutations in the p53 gene, and 40% of these cancers also showed mutations or epigenetic alterations in BRCA1 or BRCA2 genes. (8),(10). Carcinomas diagnosed in the past as poorly differentiated, high-grade endometrioid or mixed, exhibiting p53 mutations, are best classified as Type II.

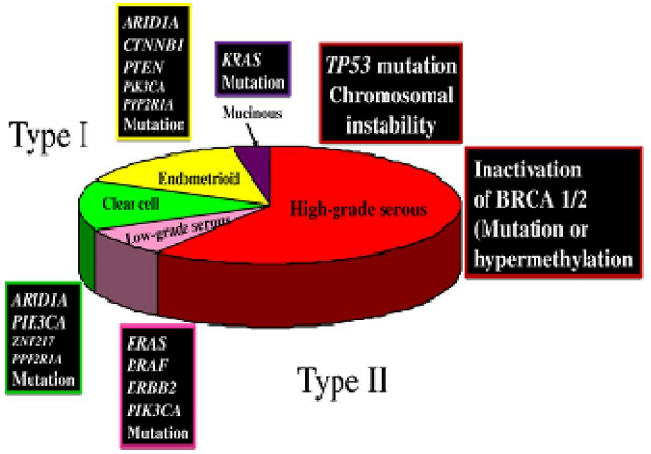

Figure 2. The histologic types of EOC and their associated molecular genetic change (*from Kurman and Shih, Hum Path 2011*).

2. Alteration of cellular metabolism: a new cancer hallmark.

Cancer is a complex and heterogeneous disease characterized by specific genomic alteration and deregulation of important molecular events related to apoptosis, cell cycle control, cell differentiation, response to growth-promoting/inhibiting signals and migration capability. All these alterations are included in the first classification of cancer hallmarks (11). This classification has been recently revised to include two other important cancer features: stemness and metabolism alteration (12). The introduction of magnetic resonance spectroscopy (MRS) for tumor studies helped to identify a potential source of novel indicators of tumor progression and response to therapy: among them the abnormal choline metabolism, characterized by increased phosphocholine (PCho) and total choline-containing compounds (13) has been identified in different type of tumors including EOC (14).

2.1 Choline transporters

Choline is an essential nutrient that is derived from diet and transported into the cells. Four different types of choline-transporting transmembrane systems have been implicated in cancer: high-affinity choline transporters (CHTs), choline transporter-like proteins (CTLs), organic cation transporters (OCTs) and organic cation/carnitine transporters (OCTNs). CTL1 was shown by microarray analysis to be expressed in cancers of the central nervous system, breast and prostate, as well as in leukemia, and to be highly expressed in melanoma, renal and colon cancer (15). Human pulmonary adenocarcinoma tissues overexpress CTL1 and to a lesser extent OCT3, compared with matched normal tissues (16). In breast cancer cells the increased PCho level is predominantly determined by enhanced Cho transport mediated by OCT2 and CHT1 (17).

2.2 Phosphatidylcholine metabolism

Phosphatidylcholine (PtdCho) is the most important membrane lipid in eukaryotic cells. The biosynthesis of PtdCho in eukaryotes is done by two distinct pathways: cytidine disulphate (CDP)-choline pathway (also known as Kennedy pathway) and phosphatidylethanolamine (PE) methylation pathway. The de novo synthesis of PtdCho from choline via the CDP–choline pathway is present in all mammalian cells and consists of three steps: in the first reaction, choline kinase (ChoK) converts choline to phosphocholine (PCho). In the second reaction of the pathway, CTP-PCho-cytidylyltransferase (CT) converts CTP and PCho to CDP–choline. In the third and final step, CDP – choline: 1,2-diacyl glycerol choline phosphotransferase (CPT) converts CDP–choline and Diacylglycerol (DAG) to PtdCho (Figure 4)(18). In addition to the Kennedy pathway, hepatocytes have an additional pathway to make PtdCho by methylation of PE (Figure 5) (19). Another PtdCho biosynthetic pathway is related to sphingomyelin metabolism (SM) (Figure 5). This pathway is often involved in the process of apoptosis. Since PtdCho donates PCho to ceramide in the final step of SM synthesis, inhibition of PtdCho synthesis may lead to a decrease of SM and accumulation of pro-apoptotic ceramides (19).

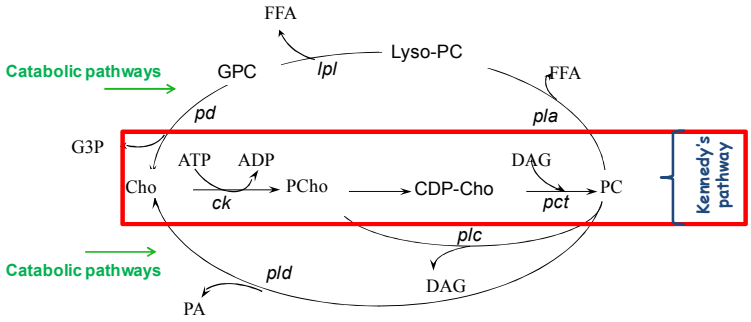

Figure 4: Schematic representation of PtdCho biosynthesis and catabolism. Metabolites: CDP-Cho, cytidine diphosphate choline; Cho, choline; DAG, diacylglycerol; FFA, free fatty acid; G3P, sn-glycerol-3-phosphate; GPC, glycerophosphocholine; PA, phosphatidate; PCho, phosphocholine. Enzymes: ck, choline kinase; ct, cytidylyltransferase; lpl, lysophospholipase; pct, phosphocholine transferase; pd, glycerophosphocholine phosphodiesterase; pla, phospholipase A1 and phospholipase A2; plc, phospholipase C; pld, phospholipase D. (*Modified from Iorio et al 2005*)

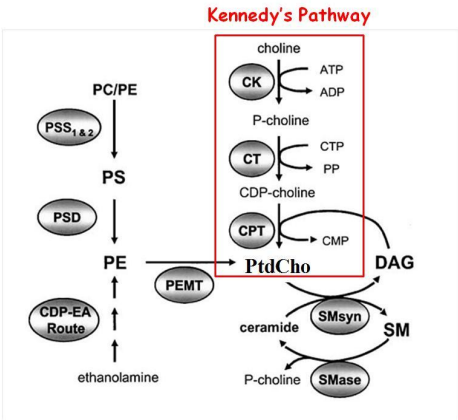

Figure. 5:.Pathways for the synthesis of PtdCho, PE and SM. Abbreviations: CK, choline kinase; CPT, cholinephosphotransferase; CT, CTP:phosphocholine cytidylyltransferase; DAG, diacylglycerol; PtdCho, phosphatidylcholine; PE, phosphatidylethanolamine; PEMT, phosphatidyl- ethanolamine-N-methyltransferase; PS, phosphatidylserine; PSD, phosphatidylserine decarboxylase; PSS1&2, phosphatidylserine synthase1&2; SM, sphingomyelin; SMase, sphingomyelinase; SMsyn, sphingomyelin synthase. *(Modified from Zheng Cui et al 2002).*

We focused our attention on Kennedy pathway, because we and others identified several enzymes such as choline kinase-α (CHKα), phosphocholine cytidylyl-transferase (CCT), phosphatidylcholine specific phospholipase D (PC-PLD) and phosphatidylcholine phospholipase C (PC-PLC), as overexpressed and/or activated in cancer suggesting their potential use as prognostic markers.

2.3 PtdCho biosynthetic pathway (Kennedy's Pathway).

Choline kinase (Chok) catalyses the first reaction of Kennedy's Pathway: phosphorylation of free choline using ATP as a phosphate donor, to produce PCho (see Fig 4). Chok was first described in 1953 by Wittenberg and Kornberg (20)and first cloned in 1992 (21). At least three isoforms of Chok exist in mammalian cells, encoded by two genes: CHKA and CHKB (22). The two functional isoforms, Chokα1 and Chokα2, are derived from CHKA by alternative splicing. Distribution of isoform's dimer population is still not known but ChoKα is the major form of Chok which positively correlates with malignant phenotype of cancer cells (23). Studies with knockout mice demonstrate that CHKA, but not CHKB loss, is embryonically lethal suggesting that CHKB cannot compensate for the loss of CHKA, which is necessary to sustain PtdCho biosynthesis (24). Overexpression of Chokα, but not of Chokβ, has been reported in several human tumour-derived cell lines of multiple origins, as well as in biopsies of lung, colon and prostate carcinomas compared with matched normal tissue from the same patient (23),(25),(26). Besides expression, also Chokα activity was shown to be increased in colon (27), in breast (28) and in ovarian (29) carcinomas compared with normal tissue. This large body of literature suggests that Chokα expression and activity is

associated with increased cancer cell proliferation and malignancy, making it a potential prognostic marker for some cancers.

Phosphocholine cytidylyltransferase (ct) catalyses the synthesis of CDP choline and PPi from PCho and cytidine triphosphate (CTP) (see Figure 4). CDP-choline is the most highly activated Cho intermediate of the Kennedy pathway, directly used to form the membrane lipid PtdCho. This enzyme exists as an inactive soluble form and as an active lipid-bound form in the nuclear membrane. Four highly homologous isoforms of this enzyme exist in mammalian cells: ctα (also known as PCYT1A), which is ubiquitously expressed and active as a homodimer; and ctβ1, ctβ2 and ctβ3 (which are splice variants of PCYT1B) that exhibit tissues pecific expression. In the literature is reported that an increasing of Chokα and ct expression and activity in colon cancer results in elevated PCho and PtdCho levels, thereby facilitating enhanced cell growth and proliferation (13).

2.4 PtdCho catabolic pathways

PC-specific phospholipase D (PC-PLD) is one of the enzyme involved in PtdCho catabolism; it catalyzes PtdCho hydrolysis producing phosphatidic acid and intracellular free Choline. Two isoforms of mammalian PC-PLD have been isolated and sequenced: PLD1 predominantly localized to Golgi membranes, and PLD2 associated to both Golgi and plasma membranes. Location of both PLD enzymes may depend on the cell type and physiological state of the cells. PLD1 and PLD2 are crucial in cell proliferation, survival signaling, cell transformation and tumor progression (13). Increased expression and activity of PLD1 has been well documented in gastric and breast cancer. Recently it has been reported a strong correlation between expression of Chokα and PLD1 with breast cancer malignancy. These two enzymes were found to be interactive: down-regulation of either one of the two enzymes induced increased expression

of the other one and their simultaneous silencing in a breast cancer cell line increased apoptosis. These data support multiple targeting of enzymes in choline phospholipid metabolism as a strategy for cancer treatment (30).

PC-specific phospholipase C (PC-PLC) also mediates PtdCho hydrolysis producing PCho and DAG, an important second messenger for cells. Since the 1990s, a growing body of evidence has pointed, to the implication of PC-PLC in proliferation, differentiation, and apoptosis of mammalian cells. Indeed, this enzyme has been implicated in many cellular processes crucial for cell signaling (31),(32).

Additional catabolic enzymes, such as PC-specific phospholipase A1 (**PC-PLA2**), PC-specific phospholipase A2 (**PC-PLA2**), lysophospholipase, GPC phosphodiesterase (**GPC-PDE**), may also be important in sustaining the cholinic phenotype by altering levels of PCho, GPC and Cho. GPC-PDE catalyzes the degradation of GPC to free choline and glycerol-3-phosphate. GPC-PDE probably participates in the regulation of choline phospholipid metabolism in breast cancer in cooperation with CHKA and PLD1 (33). The expression of cytosolic phospholipase A2 (PLA2; also known as PLA2G4A) was decreased in breast cancer cells(13) and may modulate the cellular MRS-detected GPC levels (24).

3 Aberrant choline metabolism in EOC

My research group in collaboration with the Istituto Superiore di Sanità in Rome, by analyzing tumor cells MRS spectra profiles, identified for the first time in EOC an abnormal concentration of PCho. Analysis of expanded total choline spectral profiles showed that the relative areas of signal components due to individual choline metabolites (GPC, PCho, and choline) changed in the progression from non-tumoral ovarian surface epithelial cells or immortalized cell variants (EONT) to EOC cells (14), with PCho becoming predominant in carcinoma cells (Figure 6).

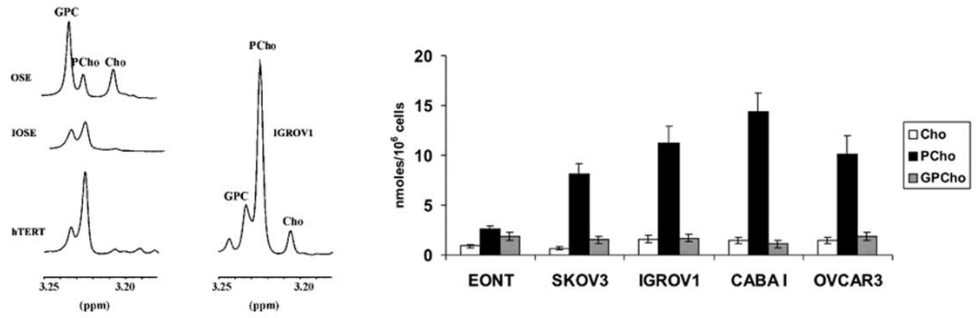

Figure 6. Altered Choline metabolism in EOC cells. ***left panel*** **:** Representative expanded region of H1NMR spectra profiles (700 MHz) of total choline in aqueous extracts of EONT (OSE and immortalized cells variants IOSE and hTERT) cells and EOC cell line (IGROV1). ***Right panel:*** Quantification of aqueous metabolites (mean±SD) in EOC and EONT cells. *(Modified from Podo , NMR 2011).*

Major contribution to PCho accumulation may derive from alternative or combined activation of enzymes involved in PtdCho biosynthesis and/or catabolism: Chok and PC-PLC. By multidisciplinary approaches, it has been

found that in EOC cells there is an iper-expression and iper-activation of Chok compared to the normal counterpart (Figure 7).

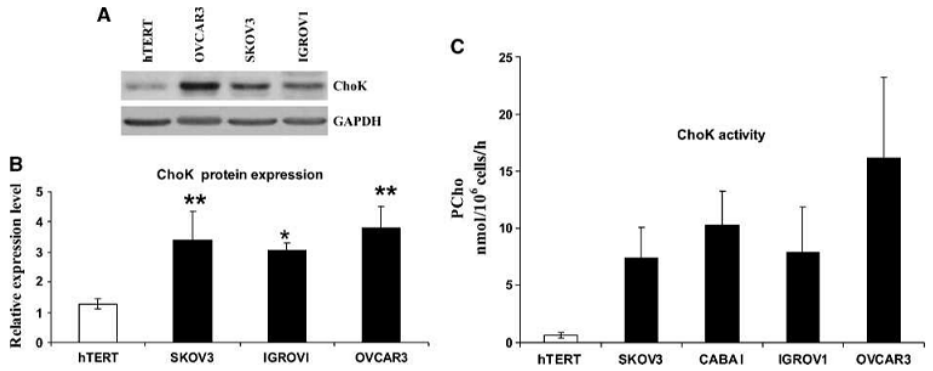

Figure 7: ChoK activity and expression are increased in EOC cells. **A:** ChoK protein expression by Western blotting. **B:** Chok densitometric evaluation referred to GAPDH, relative to EONT cells. **C:** Chok enzymatic activity in EOC cells compared to EONT cells. (*Modified from Iorio et al, 2010*)

Gene expression analysis of the enzyme involved in metabolic and catabolic pathway showed that only CHKA was iper-expressed whereas the expression of others enzyme involved in Kennedy's pathway, as well as choline transporters and enzyme involved in catabolic pathway (PLD, PLA1 and PLA2) remained unchanged (Figure 8).

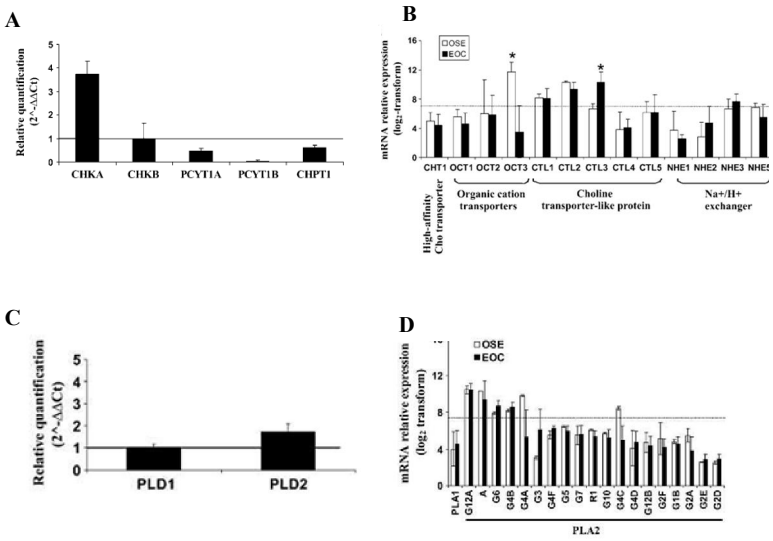

Figure 8: Gene expression of enzymes involved in PtdCho biosynthetic and catabolic pathways. A: RT-qPCR analysis of enzymes' expression in EOC (OSE cells used as an internal calibrator; horizontal line at quantification level = 1). For each gene, the mean value (±SD) of the analyzed EOC cell lines is reported. **B:** microarray analysis of choline transporters (dotted line, sensitivity threshold). **C:** RT-qPCR analysis of PLD1 and PLD2 in EOC cells (OSE used as an internal calibrator; horizontal line at quantification level = 1). **D:** Gene expression of PLA1 and of PLA2 isoforms. The dotted line represents sensitivity threshold. *(Modified from Iorio et al 2010).*

Among the enzymes involved in catabolic pathways only PC-PLC is directly involved in PCho accumulation. Currently, the mammalian PC-PLC has not been cloned and its sequence is unknown. The only available knowledge is related to its protein expression and activity in cancer cells. Indeed, this enzyme is iper-expressed and iper-activated in EOC cell compared to normal counterparts (29),(31) . EOC cell exposure to the PC-PLC inhibitor D609, abolished the activity of this enzyme and reduced intracellular PCho level

(without altering GPC and free Cho contents) suggesting that PC-PLC contributes to the intracellular PCho pool in EOC (Figure 9).

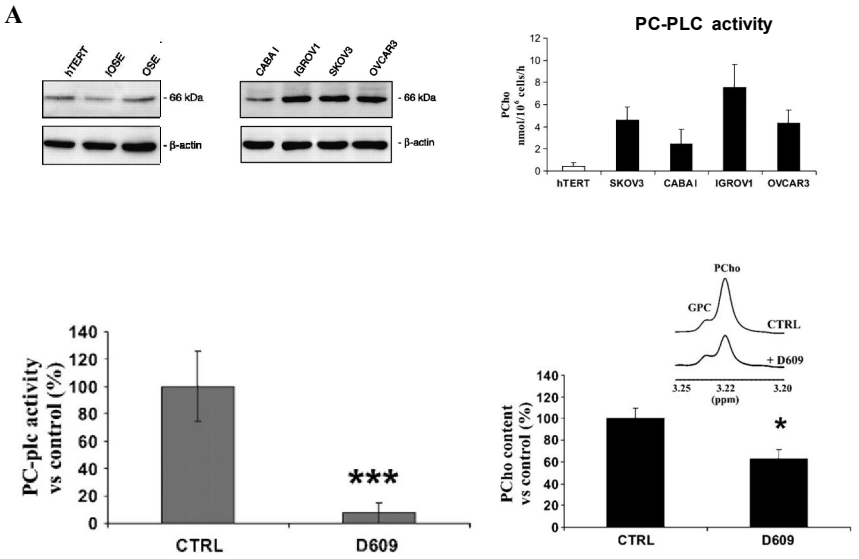

Figure 9: Activation of PC-PLC in EOC cells. A: Expression (left) and activity (right) of PC-PLC in cell lysates of nontumoral (OSE, IOSE, hTERT) and EOC cell lines. **B:** PC-PLC activity (left) and PCho content (right) in OVCAR3 cells following incubation in the absence (CTRL) or presence of D609 (53µg/mL, 24 h). Inset: representative ^{1}H NMR tCho profile in aqueous extracts showing PCho drop following D609 treatment (*Modified from Spadaro et al, 2008 and Iorio et al 2010*).

4 Choline kinase as a novel therapeutic target

Several studies have demonstrated that ChoKα plays an important role in cell transformation inducing in vivo tumorigenesis (34), (28). Furthermore, ChoKα is overexpressed in different type of tumors, including colon, breast, lung, prostate, ovary (25),(35),(14),(29). Based on these observations, ChoKα has been proposed as a novel molecular target to develop a new antitumoral

strategy. Available ChoKα inhibitors (ChoKIs) are derivates of the Hemicolinium-3 (HC3), a known ChoK inhibitor with a high neurotoxicity in vivo (36),(37). MN58b was identified as a first generation of HC3 derivate with potent antiproliferative activity in vitro and efficient antitumoral activity in vivo in nude mice xenografts (38). MN58b has been used as model for a new generation of compounds (39),(40). A second generation of ChoKIs has been synthesized to improve tolerability in mice. TCD-717 has been selected among several molecules because it provided the best results in vitro and in vivo (38). TCD-717 is currently undergoing a Phase I clinical trials for toxicity testing in cancer patients. Both drugs, MN58b and TCD-717, being derived from HC3 are considered choline competitive inhibitors at choline binding pocket and at the moment are not commercially available. A small molecule (CK37) is also available as able to inhibit tumor growth in preclinical models (41). Silencing of CHKA has been proposed as an alternative strategy to inhibit Chokα, to be used alone or in combination with conventional drugs. Silencing of CHKA in human breast cancer cells by RNA interference (RNAi) decreased cellular 1H-MRS-detectable PCho levels and cell proliferation with induction of differentiation in highly invasive and metastatic human breast cancer cells and tumour xenografts (42). Non-invasive 31P-MRS detected a reduction in PCho levels following intravenous injection of a lentiviral vector that delivered short hairpin RNA targeting CHKA in a breast cancer xenograft model (43). ChoKα inhibition is highly specific for tumor cells, since primary cells are reversibly arrested in G1 and are able to recover their growth kinetics once the drug is removed. In fact, the targeting of ChoK by RNA interference (RNAi), results in decreased PCho and tCho levels in human breast cancer cells while leaving human mammary epithelial cells unaffected (44) opening an important therapeutic window for the development of a pharmacological intervention

directed to this enzyme. These data suggest that inhibiting Chokα in solid tumors might represent a new anticancer approach.

5 Mechanisms of cancer cell resistance to chemotherapy

Drug induced resistance is frequently observed in clinical oncology and can significantly limit the clinical response to subsequent chemotherapy. Cancer patients respond significantly to selected anticancer agents during initial treatment. However, most of the cancers acquire resistance to the drug following long term treatment, thus compromising patient's response. Cancer cells undergo continuous genetic changes in order to escape natural mechanisms and drug-induced death. Continuous use of chemotherapy induces selective pressure on tumor cells, with possible development of drug resistance in cell sub-populations that can lead to "Multidrug resistance phenomenon". Cancer cell resistant to one drug can display cross-resistance to numerous drugs, having different structures and mechanisms of action. Multidrug resistance (MDR) increases disease aggressiveness and significantly reduces survival rates. MDR has been associated with multiple alterations including: a) decreased drug accumulation due to altered expression of drug trasporters (ABC family); b) increased detoxification by Thiols; c) increased tolerance to DNA damage; d) mismatch repair deficiency; e) reduced susceptibility to drug induced apoptosis and activation of survival pathways (45). Cancer cells can also inherently possesse resistance to wide variety of drugs; this is called "Intrinsic Resistance" and is potentially due to genetic and epigenetic alternations, such as activation of oncogenes and inactivation of tumor suppressor genes. p53 is a well known and extensively characterized tumor suppressor gene (46). It is the key candidate in the regulation of apoptosis induced by various stimuli. It is

also involved in cell cycle regulation by controlling G1 check point and in maintenance of genomic stability. Many anticancer drugs exert their action by inducing DNA damage, which in turn activates p53 apoptotic pathway, eventually leading to cell death. However, 50% of cancers have defects in p53 pathway, due to p53 point mutations or deletions (46). Growing evidences suggest association between intrinsic resistance and the presence of cancer stem cells in the tumor population (47). Cancer stem cells have been shown to constitutively express drugs transporters, DNA repair genes, and to be resistant to apoptosis. Presence of tumor stem cells may therefore provide a source for disease recurrence and metastasis. Standard chemotherapy for EOC is based on platinum compounds that exert their anticancer effects via multiple mechanisms. The most prominent one involves the generation of DNA lesions which can be recognized by multiple repair pathways leading to the activation of signaling cascade with proapoptotic outcomes that are often impaired in resistant cancer cells. My laboratory has contributed in defining the central role of p53 status in tumor escape from death receptor apoptotic related (48),(49),(50),(51). However, genetic and epigenetic alterations in the components of this complex signaling network have been also associated with variable levels of resistance to cisplatin (52), (53).

6 The relationship between cellular metabolism and drug resistance

Cancer cells posses a unique metabolic profile since they are more dependent on aerobic glycolysis, fatty acid synthesis and glutamine metabolism. Increasing evidence supports the idea that dysregulated cellular metabolism is linked to drug resistance in cancer therapy. Several glycolytic enzymes as glucose transporters (GLUTs), hexokinase (HK), pyruvate kinase (PK), lactate dehydrogenase A (LDHA) have been found iperexpressed and iperacrivated in cancer cells. In different tumor types these alterations are related to drug

resistance being involved in repressing pro-apoptotic signaling or activating compensatory pathways (54). Also the regulation of oxidative stress is an important factor in both tumour development and respons to anticancer therapies. Reactive oxygen species (ROS) and tumor biology are intertwined in a complex network, making it difficult to understand which came
first, whether oxidants are required for tumor cell growth or whether oxidant stress can be exploited therapeutically. Imbalances of cellular redox state may render cells vulnerable to chemotherapeutic agents (55). Many conventional antitumor agents have been shown to trigger cancer cell death by inducing oxidative stress; therefore, targeting oxidative-stress related pathway is considered a promising tool to overcome drug resistance. The major player in controlling the intracellular redox balance is reduced Glutathione (GSH) a thiol peptide which tightly regulates cell redox status through its antioxidant and reducing activities (56). Combining chemotherapeutic agents with targeted disruption of dysregulated cellular metabolism represents a promising strategy to overcome drug resistance and improve the efficacy of current chemotherapeutic agents in cancer patients (57).

7 Role of glutathione in cancer progression and chemoresistance

ROS are physiologically produced by aerobic cells and their production increases under conditions of cell injury (58). Physiological levels of ROS mediate crucial intracellular signaling pathways and are essential for cell survival. However, an excess of ROS formation generates cell damage and death. To prevent cell damage, the increase of ROS induces an adaptive response, consisting in a compensatory up-regulation of antioxidant systems, aimed to restore the redox homeostasis. Oxidative stress has long been implicated in cancer development and progression suggesting that antioxidant

treatment may provide protection from cancer (58). On other hand, pro oxidant therapies, including ionizing radiation and chemotherapeutic agents, are widely used in clinics, based on the rationale that a further oxidative stimulus added to the constitutive oxidative stress in tumor cells should, in fact, cause the collapse of the antioxidant systems, leading to cell death (59) . Among the enzymatic systems involved in the maintenance of the intracellular redox balance, a main role is played by glutathione (GSH) (60) that participates, not only in antioxidant defense systems, but also in many metabolic processes (61). Elevated GSH levels are observed in various types of tumors, and this makes the neoplastic tissues more resistant to chemotherapy (62),(63). Moreover, the content of GSH in some tumor cells is typically associated with higher levels of GSH-related enzymes, such asγ-glutamylcysteine ligase (GCL) and γ-glutamyl-transpeptidase (GGT) activities, as well as a higher expression of GSH-transporting export pumps (58) resulting in tumor cell drug resistance (64) . Three mechanisms have been proposed for the role of GSH in regulating cisplatin (DDP) resistance: (i) GSH may serve as a cofactor in facilitating Multidrug Resistance Protein (MRP) mediated DDP efflux in mammalian cells; (ii) GSH may serve as a redox-regulating cyto-protector based on the observations that many DDP-resistant cells over-express GSH and γ-GCS; and (iii) GSH may function as a copper (Cu) chelator. Additionally, GSH is involved in the control of cell cycle regulation, proliferation and apoptosis (65). Changes in GSH levels affect mitochondrial pore permeability, depletion of GSH leads to the release of cytochrome c and cell death, thus rendering GSH an attractive target that could ameliorate the success of conventional cancer therapies (56). Interestingly, glutathione levels are higher in ovarian tumors than in healthy ovarian tissue, and increased in patients who are nonresponsive to therapeutic intervention (66).

Aim of the Project

ChoKα is considered an important posible therapeutic target in many type of cancer, including EOCs. In fact, ChoKα expression and activity have a primary role in EOC in sustaining the "cholinic phenotype", defined by aberrantly increased PCho levels in tumor cells. ChoKα inhibition in appropriate cellular models will help to elucidate the biological and clinical relevance of its increased expression and activity. This study is mainly committed to investigate:

a) The functional role of ChoKα in the biology of EOC, knowing that ChoKα expression and activation increased during EOC progression. Therefore, the goal of this section will be to modulate the ChoKα expression by transient and stable silencing and analyze the metabolic and biological silencing effects. In particular, we will focus the attention on its possible druggability by investigating the mechanisms related to drug sensitivity/resistance dependent on Chokα expression.

b) The prognostic role of Chokα analyzing CHKA genes expression according to EOC phenotypes in publicly datasets**.**

The results of this study will contribute to elucidate the complex network that modulates the response to chemoresistance in EOC cells and help to identify new players that could be exploited to develop novel therapeutic approaches

SECTION 1. CHOLINE KINASE ALPHA SILENCING REGULATES CELL AGGRESSIVENESS AND DRUG SENSITIVITY IN EOC.

Results and Discussion

1.1 Transient CHKA silencing reduces Chokα expression and PCho accumulation.

In order to evaluate the role of ChoKα in EOC growth and progression, we silenced its expression in two EOC cell lines, with well known ChoKα activity and expression, INTOV11 and SKOV3 (67). Chokα expression was inhibited, as first approach, by specific transient RNA interference. Silencing efficacy was evaluated 72h after transfection both at transcript and protein level, obtaining a significant reduction of ChoKα mRNA and protein expression ranging from 60% to 70% in INTOV11 and SKOV3 respectively as compared to their relative controls (Figure 1A). A proportional drop in PCho content was observed in siCHKA cells, as assessed by MRS profiles, confirming the dependence of EOC cholinic phenotype on elevated ChoKα expression and activity (Figure 1B). Accordingly, the overall tCho contents also decreased (41.4% and 44 % in silenced INTOV11 and SKOV3 cells respectively). GPC absolute concentration, although highly variable, was not significantly changed by CHKA knock-down. No changes were observed in GPC in CHKA-silenced INTOV11 cells compared with their controls. Except for CHKA down modulation, none of the genes associated to the biosynthetic Kennedy's Pathway resulted perturbated after transient CHKA silencing. The analysis of Chokβ isoform mRNA expression in CHKA-silenced cells showed that levels of CHKB transcript remained unchanged as compared to controls in both EOC cell lines (Figure 1C), demonstrating also the specificity of our siRNA pool for α isoform.

1.2 CHKA silencing inhibits cell proliferation without affecting survival signalling pathways.

ChoKα silencing was accompanied by 35% inhibition of cell growth in both cell lines (Figure 2A), a 35-38% reduction in S-phase (proportional to growth inhibition) and a slight G1 cell cycle arrest as assessed by BrdU incorporation and Propidium Iodide staining (Figure 2B). These biologic effects were evident only in EOC cell lines and not in the non-tumoral ovarian I64-hTERT cell line in spite of the comparable cellular turnover of the two cellular models and of the efficient decrease of ChoKα expression at both mRNA and protein levels (Figure 3A and 3B) and cellular PCho drop (Figure 3C) following CHKA silencing. Indeed, no significant effects on cell proliferation were observed in the non tumoral cell line I64-hTERT (Figure 3D). Our results, in agreement with data published in the literature, for other type of non tumoral cells (44), further support the concept of ChoKα as the major player in supporting cholinic phenotype only in tumor cells (13).

The effects related to CHKA transient silencing in EOC appeared to have perturbation on EOC cell behavior different than that observed in other cellular models. In fact, we did not observe a reduction of Akt phosphorylation in a PI3K-independent way (68), nor an attenuation of MAPK and PI3K/AKT signaling (69) (Figure 4). Furthermore, although cell proliferation was reduced in both cell lines after *CHKA* silencing, neither decrease of cell viability nor apoptosis were observed in silenced cells. In this respect, EOC seems to behave differently than other tumor types in which targeting ChoK by siRNA technology (70),(71) or by pharmacological inhibitors (72),(73) was able to induce an apoptotic effects.

1.3 Modulation of gene expression profiling associated to CHKA silencing

Since the biological outcomes observed in siCHKA EOC cell lines were not super imposable to features described in other tumor models, we investigated alteration of global gene expression profile upon CHKA silencing to possibly identify the main pathways affected. By class comparison analysis of INTOV11- and SKOV3- CHKA silenced *vs.* control cells, we identified 476 differentially expressed genes in CHKA silenced as compared to control cells, 252 of them being down-regulated. Importantly, apart from CHKA, none of the genes associated to the biosynthetic Kennedy's Pathway resulted perturbed after transient CHKA silencing and *CHKB* gene was not included among the modulated genes thus confirming the data obtained by RT-qPCR (see Figure 1C).

The 15 genes most consistently up or down regulated following CHKA silencing are reported in Table 1. Microarray data were validates by Real time PCR or Bioplex analysis for six selected genes (Figure 5 A and B). Among the most relevant co-repressed genes we focused our attention on Cyclin A1 (CCNA1), related to regulation of cell cycle progression and cytokines genes (IL6 and IL8) related to inflammation and EOC aggressiveness. We observed a consistent and reproducible decrease of IL6 and IL8 mRNA levels associated to a decrease of protein release in conditioned supernatant of siCHKA cells (Figure 5C). It is now established that in EOC IL6 and IL8 expression is induced by lysophosphatidic acid (LPA) (74), (75),(76) a biolipid that, by upregulating these cytokines, stimulates tumor cell invasion and metastasis. Interestingly, LPA can be produced by phosphatidic acid (PA), a breakdown of PtdCho by PC-PLD, an enzyme involved in the catabolic pathway of PtdCho (14),(77). Down-modulation of these cytokine following CHKA silencing might be then related to a lower availability of LPA, derived from possibly

altered PtdCho turnover. Form a metabolic point of view, among the most up-regulated genes, we identified as gene of interest Osteoprotegerin (TNFRSF11B; OPG), a soluble decoy receptor for receptor activator of nuclear factor-kappa B ligand (RANKL); Acyl-CoA synthetase (ASCM3), needed for fatty acid synthesis and accumulation of cytoplasmic lipid droplets (78),(42); Phosphatidic acid phosphatase 2A (PPAP2A), a biolipid mediator that converts phosphatidic acid to diacylglycerol. It has been reported that an increase of PPAP2A activity, due to a gene up-modulation, could terminate Raf-1 and the MAP-kinase pathway signaling overall affecting cell proliferation (79).

1.4 CHKA silencing modulates cell functions related to cell movement and affects drug sensitivity.

To derive the possibly deregulated pathways following CHKA silencing, a dataset consisting of the 476 differentially expressed genes was analyzed with Ingenuity Pathway Analysis (IPA) Tool, revealing 25 significantly altered pathways: the network identified with the highest score included CHKA among the focus molecules (Figure 6). The biological functions associated to this network were related to cell morphology, cellular assembly and organization, cellular function and maintenance. The molecular and cellular functions affected by CHKA silencing were related to *cell death*, *cellular growth and proliferation* and *cellular movement* (Figure 7A). Interestingly, as shown by the z-score heatmaps (Figure 7B), *Cellular movement* and *cellular growth and proliferation* functions were predicted to be decreased whereas cell death function was predicted to be increased in CHKA-silenced cells as compared to their controls. The predicted alterations of these pathways were supposed to lead EOC cells towards a less tumorigenic behavior.

Indeed, following CHKA knockdown, a decreased proliferation was evident (see Figure 2) and a clear delay in wound closure was observed in both CHKA-silencing cell lines using the classic scratch assay (Figure 8A). Since the significantly reduced cell motility observed in CHKA silenced cells as compared to their control cells could be partially due to a reduced proliferation capability, to possibly exclude effects of CHKA silencing related to proliferation rather than migration, scratch assay was also performed in the presence of Actinomycin D obtaining comparable inhibitory effects. Indeed we observed an inhibition of wound repair of 46% in INTOV11 and 45% in SKOV3 CHKA-silenced cell lines, thus suggesting that results observed were mostly related to alterations of the migratory rather than proliferative phenotype (Figure 8B).

Also, CHKA silenced cells showed a dramatic rearrangement of F-actin fibers with a significant reduction of oriented actin stress fibers and focal adhesion sites (Figure 9), further suggesting that CHKA silenced cells are less prone to movement and migration as compared to their control cells. To confirm these indications, we then assessed migration capability by using two assays both based on the Boyden chamber principle but having different detection methods to account for methodological variability and in presence of Actinomycin D to exclude bias related to proliferative effects. Results obtained showed a 43-47% inhibition of migration in INTOV11 and SKOV3 CHKA-silenced cells as compared to their relative controls when migration was detected by fluorimetric assay; comparable results were obtained when Actinomycin D was added to culture medium (Figure 10 A). Also a 37-65% inhibition of migration was detected in INTOV11 and SKOV3 cells as compared to their relative controls when migration was detected by quantification of SRB staining (Figure 10 B). Furthermore, CHKA-silenced cells showed a significantly reduced (72% and

79% in silenced INTOV11 and SKOV3 respectively) invasive potential through matrigel as compared with their control cells (Figure 11).

Furthermore, although we did not show any direct effect of ChoKα down-regulation on cell death, to possibly confirm the IPA-predicted modulation of *cell death* function, we evaluated sensitivity to drug treatments upon CHKA silencing. As compared to their relative untreated cells, we observed a significant increase of sensitivity to cisplatin (DDP) treatment associated with CHKA silencing in both INTOV11 and in the DDP-resistant SKOV3 cell line (Figure 12A). Importantly, we observed also a sensitization of the CHKA-silenced cells to the other two drugs, Paclitaxel and Doxorubicin, that are currently in use in the clinical practice for EOC treatment in combination with platinum compounds (Figure 12B and C). In agreement with the increased drug sensitivity, CCNA1 down-modulation following *CHKA* silencing might then impair the ability of cells to arrest cell cycle to repair DNA following DNA damage. CCNA1 is indeed a down-stream target of p53 able to mediate a G2/M cell-cycle arrest (80). A cell sensitization to drug treatment (5-fluoruracil) after CHKA silencing has been already reported also in breast (81) and colorectal cancer cells (38).

Conclusion and Future Perspectives

Aberrant choline metabolism, characterized by an increased intracellular PCho pooling and sustained by increased activity/expression of ChoKα, is a new metabolic hallmark for different cancer types (13). Our previous studies significantly contributed to define its relevance also in EOC, showing that tumor cells have an increased expression and over activation of its enzyme (14), (29). The results collected in this section showed that specific CHKA transient silencing induces a decrease of cell proliferation, a reduction of migration and

invasion capability and increases sensitivity to drug treatment. These biological effects were evident only in EOC cell lines and not in non tumoral ovarian cells, suggesting that Chokα sustains the "*cholinic phenotype*" only in tumor cells. When considering the biological relevance of CHKA knockdown it should be taken into account that the specific EOC molecular context may require longer time and a more persistent CHKA down regulation to achieve a more effective modulation of cell behavior. A transient inhibition of CHKA in EOC could be not sufficient alone to maintain overtime the biological effect of its silencing. Furthermore, in a previous study we also showed that the alterations of EOC tCho MRS spectral profile is sustained also by activation of enzymes involved in PtdCho catabolic pathways like PC-PLC (14),(31),(29),(32). Therefore a simultaneous inhibition of the enzymes involved in both the biosynthetic and the catabolic pathways could be more appropriated in these cellular models to obtain a stronger biological effect.

The increased sensitivity of EOC cell lines to drug treatment when interfering with Chokα expression, has an important biological relevance to support the concept of targeting metabolism to improve efficacy of existing standard chemotherapeutic approaches (82) and opens the way to validate ChoKα as a druggable target.

SECTION 2. CHOLINE KINASE ALPHA KNOCKDOWN SENSITIZES OVARIAN CARCINOMA CELLS TO ANTITUMOR AGENTS BY IMPARING GLUTATHIONE DEPENDENT ANTIOXIDANT DEFENSE.

Results and Discussion

2.1 Molecular and functional characterization of stable CHKA silencing

Since the dynamics of biological effects related to CHKA silencing could differ from other cancer types and could not possibly be detectable by transient RNAi, we stably downregulated ChoKα expression using a lentiviral vector, expressing GFP and specific ChoK shRNA (Figure 13 A). Stable CHKA silencing caused: i) reduction of CHKA-mRNA (61% and 68% for INTOV11 and SKOV3 respectively as compared to their relative control (Figure 13B), ii) down modulation of ChoKα protein expression (40% and 41% for INTOV11 and SKOV3 transduced cell lines, respectively) (Figure 13C), iii) a significant drop of PCho content in silenced cells (Figure 13D).

The indirect evidence of decreased ChoKα activity (evaluated as decrease of PCho content) in sh-CHKA cells was confirmed by the direct measurement of enzymatic activity in both EOC models. Indeed, consistently with the reduction of PCho levels in sh-CHKA transduced cells a significant decrease of 77% and 97% of ChoK enzymatic activity as compaired to controls was detected both for INTOV11 and SKOV3 cell lines (Figure 13E). We clearly showed that the depletion of CHKA expression was associated to a drop in PCho content and CHK activity, indicating in these EOC cells a predominant role of the alpha isoform in the build-up of PCho in these cancer cells. Furthermore, we did not observe any significant changes in the levels of PtdCho in CHKA-silenced cells, suggesting that the phospholipid homeostasis was not substantially altered under these experimental conditions. A 44.4% and 49.63% in vitro growth

inhibition was obtained for sh-CHKA INTOV11 and sh-CHKA SKOV3 respectively as compared to their relative controls (Figure 14 A). With the stable transfection approach we were able to assess the inhibition of foci formation: 10 days after cell seeding, the INTOV11 and SKOV3 sh-CHKA cells showed a 38% and a 61.6% reduction in colony formation (Figure 14B). We also confirmed in sh-CHKA transduced cells a 40% and 51% reduction of migration capability (Figure 14C) and 41% and 45% inhibition of invasive potential (Figure 14D) compared with their control cells, in INTOV11 and SKOV3 models, respectively.

2.2 CHKA stable silencing inhibits EOC xenotraplants growth

Given the strong inhibitory effects on in vitro cell proliferation by CHKA stable silencing, we evaluated potential inhibitory effects in *in vivo* experiments. Nude mice were injected subcutaneously with $3x10^{\wedge 6}$ sh-CHKA or control cells (ΔLuc). Tumor volumes were monitored and a significant inhibition of tumor growth was observed for both EOC silenced cell lines (Figure 15 A). Tumors derived from control and CHKA silenced xenografts were analyzed at molecular and enzymatic level. RTqPCR (Figure 15B) confirmed the stable CHKA downmodulation. The decrease of PCho accumulation is evident in the CHKA-shRNA transduced tumors (Figure 15C). The percentage of reduction of PCho accumulation has reached 60% in both models.

Our results showed that CHKA stable silencing significantly affected EOC *in vivo* growth supporting the hypothesis that EOC aggressiveness could be due, at least in part, also on the expression and activity of this enzyme. In spite of safety concerns involving use of lentivirus as a mode of gene delivery, these studies, conducted in breast and ovary, may be the bases for future gene therapy trials targeting Chokα in tumors. Indeed, our collaborators using the same

approach, demonstrated for the first time, the therapeutic potential of CHKA down regulation *in vivo* in a human breast cancer xenograft model (43).

2.3 Metabolic impact of CHKA silencing

Global biochemical profiles, performed with the Metabolon technology platforms, were determined comparing ΔLuc and sh-CHKA cells for INTOV11 and SKOV3 EOC models collected 24 and 72 hours after plating. The first evidence from metabolic profile was the distinct separation between the two cell lines consistent with fundamental metabolic difference between the two phenotypically different cell lines. The greatest metabolic changes were observed 72h post seeding where a number of metabolites were found to be down-regulated in CHKA silenced cells (Table 2). The complete heatmap of significantly altered metabolites for each cell line is reported in Table 3 We identified as commonly altered in the two sh-CHKA models, metabolic pathways mainly related to amino acid, lipid and nucleotide metabolism (Table 4). We found of particular interest the altered glutathione metabolism characterized by decreased content of glutathione and its precursor cysteine. Indeed, in both cellular models, CHKA stable silencing resulted in a significant decrease in cysteine levels as compared to the relative controls (ΔLuc) (Figure 16A), coupled with an alteration of glutathione metabolism, commonly characterized by a 3-fold decrease of reduced glutathione (GSH) and a 2-fold decrease of oxidized glutathione (GSSG) content (Figure 16B). A 30-40% reduction of GSH/GSSG ratio indicated an overall decrease in GSH content in sh-CHKA cells as compared to their controls (Figure 16C). To independently validate this observation, we transiently silenced CHKA expression on INTOV11 and SKOV3 and quantified GSH and GSSG levels using the luminescence-based system GSH/GSSG-Glo assay, obtaining a 2 fold reduction

of GSH/GSSG ratio in silenced (si-CHKA) cells compared to their relative controls (Figure 16D). To verify whether an altered expression of the cysteine transporter (Sxc) could account for the decrease in cysteine observed in sh-CHKA cells, we analyzed the expression of the transporter subunit xCT both at mRNA and protein level, but we did not observe any alteration following CHKA silencing thus excluding a decrease in cysteine uptake (Figure 17). Further analysis will be performed to assess whether CHKA silencing impact on expression of enzymes involved in trans-sulfuration pathway or enzymes involved in glutathione synthesis.

To exclude that this metabolic change was a cell line-dependent effect but was extensible to other EOC cellular models, CHKA was silenced in four different EOC cell lines, IGROV1, A2774, OAW42 and OVCAR5, with heterogeneous ChoKα protein expression levels and PCho intracellular accumulation (Figure 18 A and B). In all tested cell lines, CHKA transient silencing induced an average 60% decrease of ChoKα protein expression (Figure 18 C) and a significant 2 fold decrease of the GSH/GSSG ratio (Figure 18 D). To exclude a non specific off target effects, GSH decrease after CHKA silencing was validated also with an independent CHKA specific siRNA pool (Figure 18E).

2.4 CHKA silencing by modulating intracellular GSH levels affects cell sensitivity to drugs.

The mechanisms of cytotoxic drug resistance in EOC remained unclear. Among the various mechanisms, high intracellular GSH levels have been shown to contribute in developing resistance to chemotherapeutic drugs including DDP and doxorubicin, two drugs targeting DNA. Consistently, increased GSH contents has been observed in different tumour types and a relationship with resistance to a number of drugs has been described (56). GSH acts as scavenger of free radicals and peroxides accumulating in the cell during oxidative stress

like the hypoxic condition in tumour tissues, where GSH plays a protective role. Therefore, treatments causing GSH depletion are expected to render cancer cells more susceptible to chemotherapeutic agents, while sparing normal cells.

GSH is well known to regulate redox state through its antioxidant and reducing activities. Our observations suggested that CHKA knocking down, by altering GSH intracellular levels, may cause an increase in ROS levels thus impairing antioxidant cellular defense and possibly response to drug treatment. Indeed, we assessed the ROS intracellular levels measuring by flow cytometry the CM-H2DCF-DA probe fluorescent signal in control and si-CHKA cells. A 3-fold and a 6-fold increase in intracellular ROS levels was detected in INTOV11 and in SKOV3 siCHKA cells respectively as compared to their corresponding controls (Figure 19). Interestingly, as I reported in Section 1 of my results, CHKA silencing in INTOV11 and SKOV3 increased sensitivity to DDP and doxorubicin treatment (see Figure 12) and this effect was reproducible in four additional EOC cell lines following CHKA down modulation (Figure 20).

We therefore investigated whether the alteration of GSH/GSSG levels dependent upon CHKA silencing was the mechanism by which cell sensitivity was modulated. Thus, to phenocopy the effects of CHKA-silencing, we reduced basal intracellular glutathione levels treating wild type INTOV11 and SKOV3 cells with a non toxic concentration of Buthionine Sulphoximine (BSO), a well known inhibitor of gamma-glutamylcysteine synthetase. As hypothesized, this GSH-depleting agent significantly increases DDP and doxorubicin sensitivity mimicking the pattern of sensitization observed after CHKA silencing (Figure 21). As complementary approach, we examined if we could rescue the resistant phenotype in INTOV11 and SKOV3 siCHKA cells restoring GSH intracellular levels. The glutathione tripeptide itself is not cell permeable, therefore to increase its intracellular content we loaded cells with a membrane/lipid

permeable derivative, Glutathione Reduced Ethyl Ester (GEE) and we evaluated the capability of GEE treatment to recover intracellular GSH levels in siCHKA cells. After CHKA silencing, cells were loaded with 10μM GEE for 8h and then incubated for 48h in the absence of this agent, resembling the time-schedule of the drug treatment. GSH/GSSG levels were monitored and quantified at the end of silencing (t0), after loading (8h GEE) and at the end of experiments. CHKA silencing caused in both cell lines the expected 2-fold decrease of GSH/GSSG ratio as compared to relative controls (Figure 22, t=0). We observed that GEE treatment effectively recovered GSH levels in both siCHKA cell lines (Figure 22 A, green histograms) and such an increase was maintained up to 48h after the end of GEE loading. Most importantly GSH reloading in siCHKA cells substantially affected intracellular ROS levels, by lowering their amount to levels comparable to drug treated control cells (Figure 22 B) . Significantly, GEE treatment reverted drug sensitization associated with CHKA silencing, almost completely retrieving the dose-response curve typical of wt and control cells (Figure 22C).

2.5 CHKA silencing does not affect Glutathione metabolism and/or drug sensitivity in non - tumoral ovarian cells.

As I reported in the first section of results, the biological effects of CHKA silencing were evident only in cancer cells. Interestingly, GSH levels have been reported to be higher in ovarian tumors that in normal ovarian tissue (66),(83). Thus, to assess the specific biological impact of GSH regulation by CHKA expression in EOC cell lines, we evaluated the GSH/GSSG ratio in the non-tumoral ovarian cell line I64-hTERT and its possible alteration following CHKA silencing.

The GSH/GSSG ratio was significantly higher in EOC cells than in I64-hTERT (Figure 23A) and knock-down of CHKA did not impact on GSH intracellular

levels (Figure 23B) and drug sensitivity of I64-hTERT cells (Figure 23C). GSH depletion by BSO resulted in a sensitization of I64-hTERT cells to DDP but no differences were detected between silenced and non silenced cells (Figure 24A and B). Indeed, GEE treatment caused a moderate increase in the GSH levels in I64-hTERT (Figure 24C), and accordingly no differences were observed in drug sensitivity of siCHKA, GEE-treated cells (Figure 24D).

Conclusion and Future Perspectives

The results reported in this section demonstrated that stable silencing of CHKA in two different EOC cell lines reduced in vitro cell proliferation, migration and invasion capability and affected EOC *in vivo* growth supporting the hypothesis that EOC aggressiveness could be due in part to iper expression and over activation of this enzyme. In fact, following CHKA knocking down the cells showed a less aggressive phenotype.

On the other hand, the analysis of global metabolic profiling identified an altered glutathione metabolism characterized by a decreased cysteine and GSH content. The reduction of GSH content is expected to perturb redox homeostasis in EOC cells and renders tumor cells more susceptible to chemotherapeutic treatment. Accordingly, we observed that CHKA targeting, either by shRNA as well as siRNA, increased ROS intracellular levels and sensitivity to cisplatinum and doxorubicin treatment and these effects were mediated by the reduction of GSH content, even in drug resistant EOC model. Interestingly, alteration of GSH levels and increased sensitivity to drug treatment were found in different EOC cellular models, despite the different Chokα expression, but not in non tumoral EOC cells. Targeting mechanisms upon which cancer cells are expected to be dependent (CHKA expression and cellular ROS homeostasis)

could explain the differential response of cancer and non transformed cells to CHKA knock-down.

As well known, cancer cells acquire specific genetic and epigenetic alterations that involves hyperactivation of oncogenes and/or inactivation of oncosuppressor genes. Some genetic changes support survival of cancer cells by creating specific signalling sustaining metabolic pathways. However, the overall deregulation of cellular processes and functions is frequently associated with enhanced cellular stress and malignant cells have to adapt to this phenotype, becoming dependent on a number of non-oncogenic functions to survive (84). Similarly, a dependency associated with ROS homeostasis has been shown to constitute a selective liability of malignant cells also in xenograft tumor models (85). Identifying such dependencies represent a promising alternative for the development of new therapeutic strategies to successfully target metabolic enzymes minimizing adverse effects on normal tissues. Synergisms of CHKA knockdown with conventional treatment might open interesting clinical perspective as it could represent an alternative strategy to increase the treatment efficacy also by reducing the clinical dose of drugs and limiting the damage of normal cells.

SECTION 3. EVALUATION OF PROGNOSTIC ROLE OF CHOLINE CHINASE ALPHA IN EOC: BIOINFORMATICS ANALYSIS.

Results and Discussion

The over expression of ChoKα in many cancer types has also generated interest in phospholipid metabolism as a diagnostic or therapeutic target in oncology (13),(28). ChoKα over-expression has been reported and proposed as an indicator of reduced patient survival in human lung and bladder carcinomas (35),(86).

My group in past years analyzed, for the first time in EOC, the CHKA mRNA expression in EOC surgical specimens (29). Gene expression analyses were performed on 21 frozen EOC surgical specimens, 2 OSE cells preparation and 8 different EOC cell lines. The mRNA relative expression levels of ChoKα measured in clinical tissue samples were significantly higher than those in OSE cells (Figure 25A) overall these expression levels were however lower than those detected in EOC cell lines. The different gene expression levels of ChoKα between tumor samples and cell lines may derive from stromal contamination and/or from in vitro culture conditions. The increased although heterogeneous expression of ChoKα was also confirmed at protein level by Western blot analysis of lysates of surgical specimens randomly selected from those analyzed for gene expression (Figure 25 B).

In order to investigate the putative prognostic role of CHKA in EOC we performed ~~a~~ preliminary *in silico* analysis on available public data sets of gene expression profiling of EOC tumors (see Table 5 for detailed description). We firstly performed a metanalysis of metabolism-related genes expression in high grade serous EOC compared to OSE cells. To this end we selected a total of 119 genes involved in KEGG hs-glycerophospholipid pathway (hsa:00564) or reported to be directly involved in Kennedy's pathway ((87)), and we compared

their expression profile between OSE and tumor samples on a joined dataset derived from Bowen, Mok and Bonome dataset. (88),(89), (90). Complete heatmap is reported in Figure 26. 96 out of the 119 metabolism-related genes were identified in the dataset and 71 of these genes resulted differentially expressed (FDR <0.06) between the two groups (OSE cells vs EOC tumors). Interestingly, OSE cells showed a higher CHKB expression as compared to EOC samples, whereas CHKA expression was higher in tumors respect to OSE cells (Figure 26). We then analyzed the expression profile of this selected gene-set in the Anglesio dataset (91) that comprise Low malignant potential (LMP) and Malignant tumors. LMP serous EOCs are thought to arise by the transformation of tumors of borderline malignancy and activating mutations in members of RAS pathway (KRAS, BRAF, ERB2) are found in the majority of these tumors (92). LMP EOCs show a relatively high grow capacity, are usually not invasive but resistant to conventional chemotherapy (93). With this analysis we identified a cluster of genes overexpressed in LMP and one overexpressed in malignant tumors (Figure 27**A**). CHKA and CHKB were among the differentially expressed genes between the two groups and whereas CHKB showed higher expression in LMP EOCs, CHKA was overexpressed in malignant EOCs (Figure 27**B**). Of note, this finding was further confirmed when we analyzed the Tothill dataset (94) that includes a higher number of patients comprising LMP, Malignant type I and malignant type II tumors. By this analysis we found 111 metabolism-related genes present on the array, 42 of which were significantly differentially expressed (FDR<0.05) (Figure 27 **C**). Interestingly, CHKA and CHKB were among them and maintained the same expression pattern as above described (see arrows in the heatmap of Figure 27 C).

Given these data, we hypothesized that increased CHKA expression could be associated with increased tumor aggressiveness. We therefore analyzed the expression of the two enzyme isoforms in 3 datasets King (95), Berchuck (96) and Tothill (94) which included malignant tumors of different grading. In accordance with our hypothesis, we observed a general increase of CHKA expression with tumor grading in all datasets whereas CHKB expression showed an opposite trend (Figure 28).

Conclusion and future perspectives

By applying these preliminary bioinformatics analysis, we firstly validated that CHKA is over expressed in tumor samples compared to OSE cells, whereas CHKB in the same samples showed an opposite trend. Moreover, we found a progressive increase of CHKA expression along with tumor aggressiveness although the number of samples analyzed was limited by the availability of datasets including OSE cells, LPM and malignant EOC tumors.

For the future we plan to: i) confirm these results performing further analysis in newly collected case materials; ii) validate the prognostic relevance of CHKA and CHKB expression performing survival analysis; iii) investigate the putative causal relationships at the basis of the complex network of interactions between CHKA-CHKB and metabolism related genes.

FIGURES AND TABLES

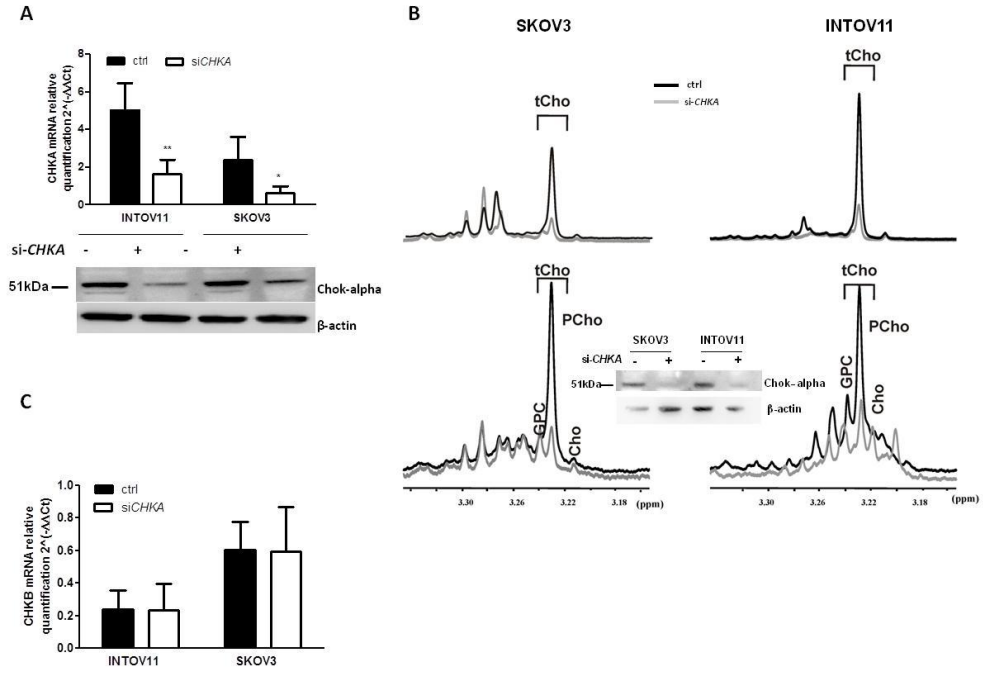

Figure 1. Transient *CHKA*-silencing efficiently down-modulates ChoKα expression and intracellular PCho content in EOC cell lines.

A: CHKA silencing was confirmed at mRNA (RT-qPCR, upper panel; data are the mean±SD of 5 independent experiments) and protein expression level (lower panel: Western Blotting of a representative experiment is reported). **B:** Representative examples of alterations induced by si-*CHKA* on the ^{1}H-MRS tCho profile and its PCho component. Black lines: control cells; grey lines: silenced cells. Inset in lower panel: western blot of control and si-CHKA EOC cells probed with specific antibody to ChoKα. GPC, glycerophosphocholine; PCho, phosphocholine; tCho, total choline-containing compounds. The PCho/tCho ratio was 0.75±0.20 in both cell types before silencing. **C:** RT-qPCR for ChoK β-isoform. Data are the mean±SD of 5 independent experiments. *GAPDH* was amplified as endogenous control and I64-hTERT cells preparations were used as calibrator.

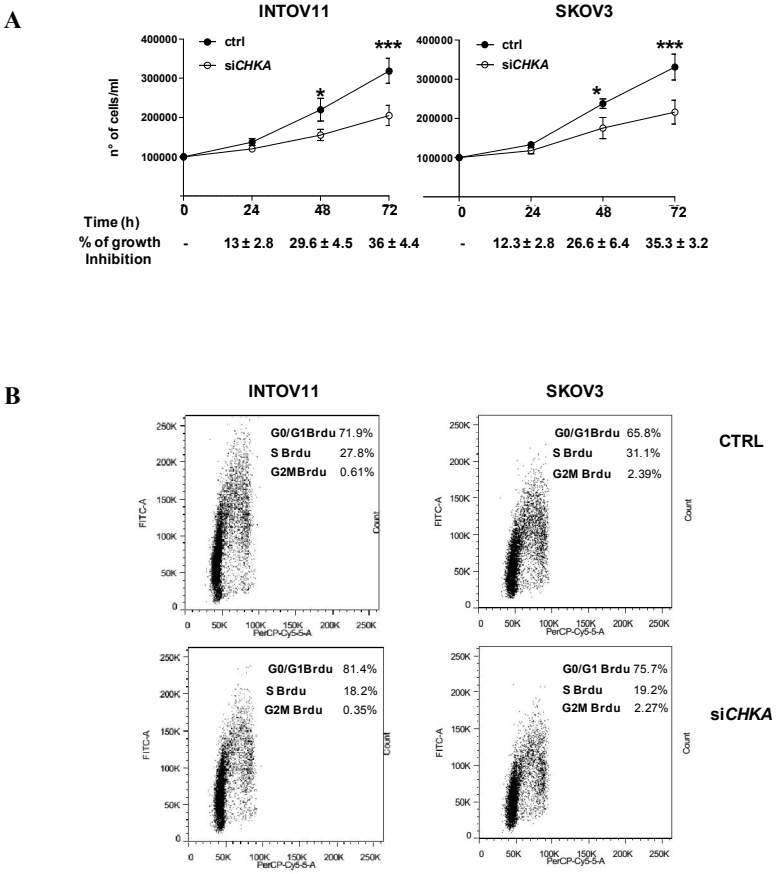

Figure 2: Cell proliferation upon CHKA silencing

A: Proliferation curves. Viable cells were counted 24, 48 and 72h post-transfection. Cells were seeded in triplicates at 1×10^5 /well on 12-well plates. After transfection, proliferation was assessed at each time-point by Trypan Blue exclusion assay using Countess automated cell counter. Cell viability was evaluated as percentage of alive cells in the total cell population. Mean percentage of growth inhibition of CHKA-silenced vs. control cells is reported below. **B:** Representative experiment of BrdU incorporation 72h after transfection. Cells were pulsed with 10 μM 5'-bromo-2'-deoxyuridine (BrdU) for 1 hour at 37°C, harvested and serially washed in PBS. Following fixing with 70% ethanol, cells were processed using BrdU Labelling and detection kit according to manufacturer's protocol. Samples were double-stained by incubation with 5 μg/ml Propidium Iodide and 0.5 mg/ml RNAse for 30 min, then they were analyzed with FACS Canto and the data processed using FlowJo 7.6.4 Analysis Software.

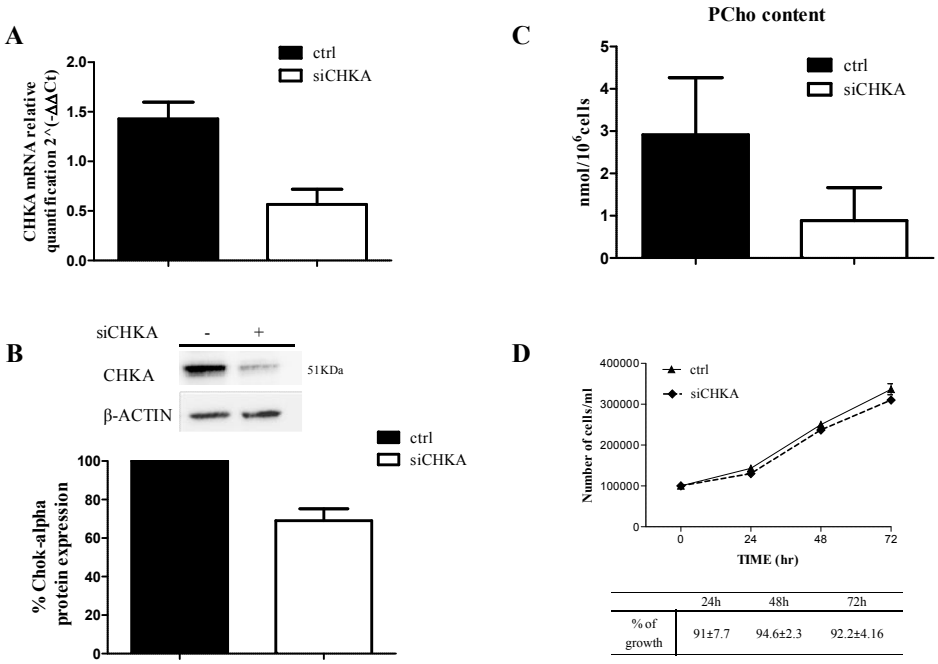

Figure 3. Effects of *CHKA* downmodulation in non tumoral I64-hTERT cells.

A: RT-qPCR for *CHKA* expression on silenced and control cells. GAPDH was amplified as endogenous control and I64-hTERT wild type cells were used as calibrator. **B. Upper panel:** Representative Western blotting analysis of ChoKα expression on silenced and control cells. β-actin protein levels were used as loading control. **Lower panel:** Densitometric analysis of ChoKα protein levels normalized to β-actin. Relative percentage of ChoKα protein expression is shown respective to control cells set to 100%. **C:** Quantification of PCho intracellular concentrations obtained from ^{1}HMRS spectra of water-soluble cell extracts. **D:** Proliferation curves of control and *CHKA*-silenced cells. Viable cells were counted 24, 48 and 72 h after transfection. Mean percentage of growth of *CHKA*-silenced vs. control cells is reported below.

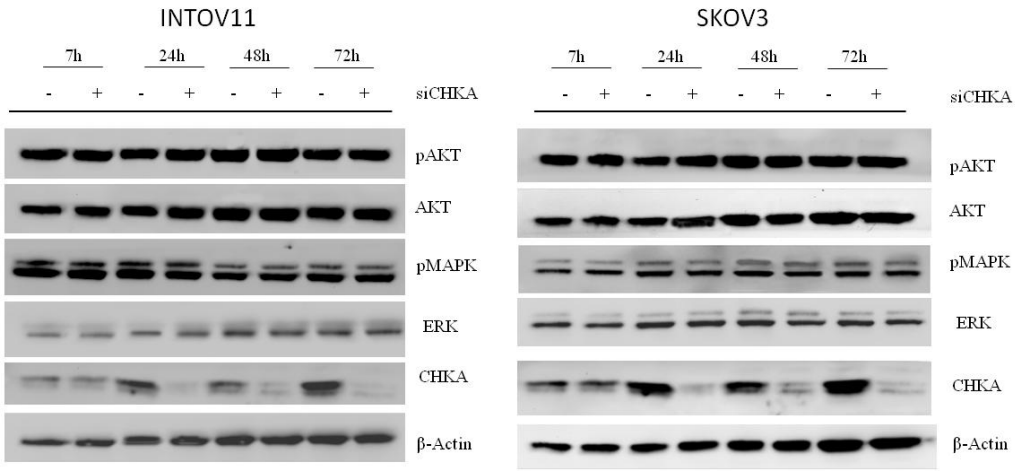

Figure 4: Effects of *CHKA* silencing on survival pathways activation.

Western blots of the time course of *CHKA* knockdown in INTOV11 and SKOV3 cells. β-actin is shown as a control for protein loading. A representative experiment of 3 performed is shown.

Table 1. List of the top 15 differentially up or down regulated genes following CHKA silencing

Gene Symbol	Parametric p-value	FDR[a]	Geometric mean of intensities[b]	
CHKA	4,60E-06	0,0421	0,44	DOWN REGULATETED GENES
CCNA1	2,60E-06	0,0421	0,48	
KRT80	0,0005081	0,128	0,51	
IL6	0,0046555	0,213	0,51	
TAGLN	0,0064673	0,236	0,53	
IL8	9,30E-06	0,0467	0,54	
AKAP12	0,0009146	0,145	0,56	
H19	3,29E-05	0,106	0,59	
IDH2	5,34E-05	0,106	0,59	
TNFRSF25	0,0011795	0,148	0,61	
KRT7	0,0016046	0,163	0,61	
LIMK1	0,0054187	0,222	0,61	
MAD2L1	8,14E-05	0,124	0,62	
SEC23A	0,0001111	0,124	0,62	
SNX25	0,0007806	0,137	0,62	
ARFIP1	0,0009437	0,146	1,57	UP REGULATETED GENES
CA5B	0,0022191	0,169	1,57	
LAMC1	0,0002072	0,124	1,59	
C5	0,0013041	0,155	1,6	
PRSS35	0,0004709	0,128	1,62	
SPTLC3	0,0002098	0,124	1,63	
UBE2E3	4,63E-05	0,106	1,64	
BCMO1	0,0001368	0,124	1,64	
ID3	0,0032983	0,19	1,67	
PPAP2A	0,0001578	0,124	1,71	
LRRC31	0,0001612	0,124	1,72	
RTN4	3,78E-05	0,106	1,76	
FXYD2	0,0025975	0,175	1,84	
TNFRSF11B	0,0001958	0,124	1,85	
ACSM3	4,54E-05	0,106	2,11	

[a]: False Discovery Rate (FDR); [b]: for each specified probe represents the ratio between the mean intensity of the siCHKA vs. control cells

Table 1: List of the top 15 differentially up or downregulated genes following CHKA silencing

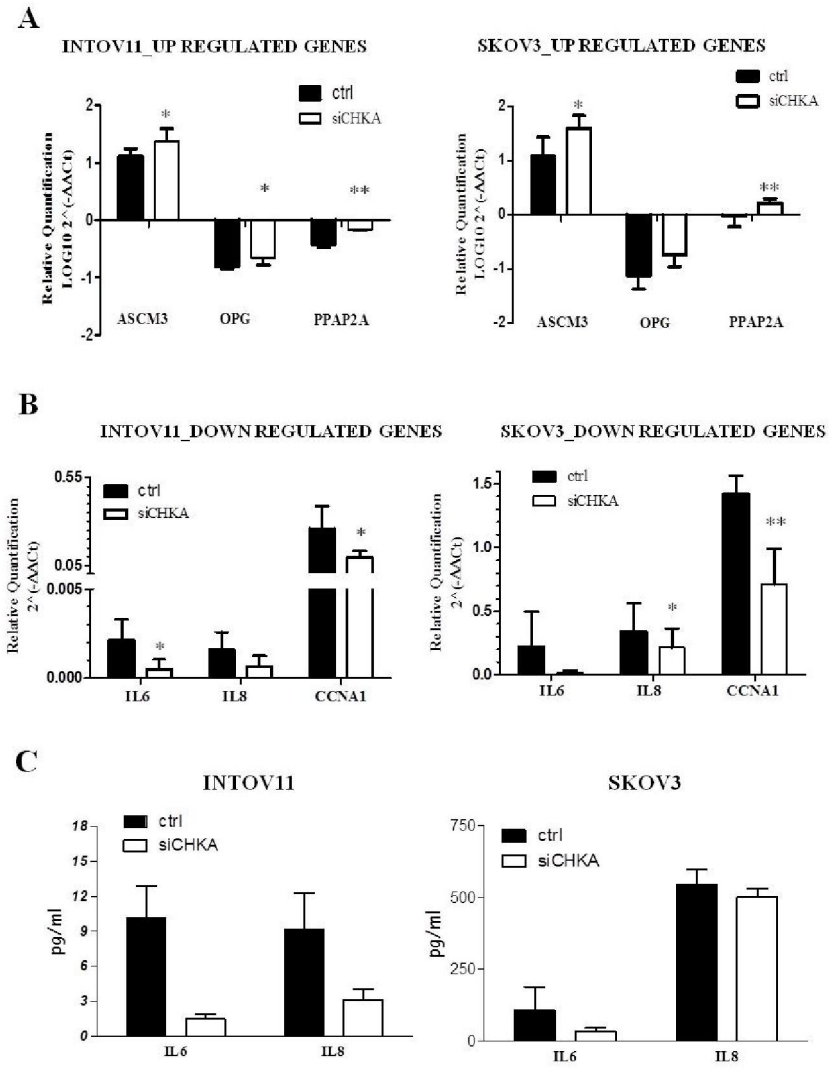

Figure 5: Validation of genes perturbed by CHKA silencing

RT-qPCR of selected up (**A**) and down (**B**) modulated genes in CHKA-silenced EOC cell lines. GAPDH was amplified as endogenous control and I64-hTERT cells preparations were used as calibrator. The mean of five independent experiments is reported. **C**) Evaluation of IL6 and IL8 release by bioplex assay on conditioned media from both EOC cell lines. Data are the mean±SD of 3 independent experiments.

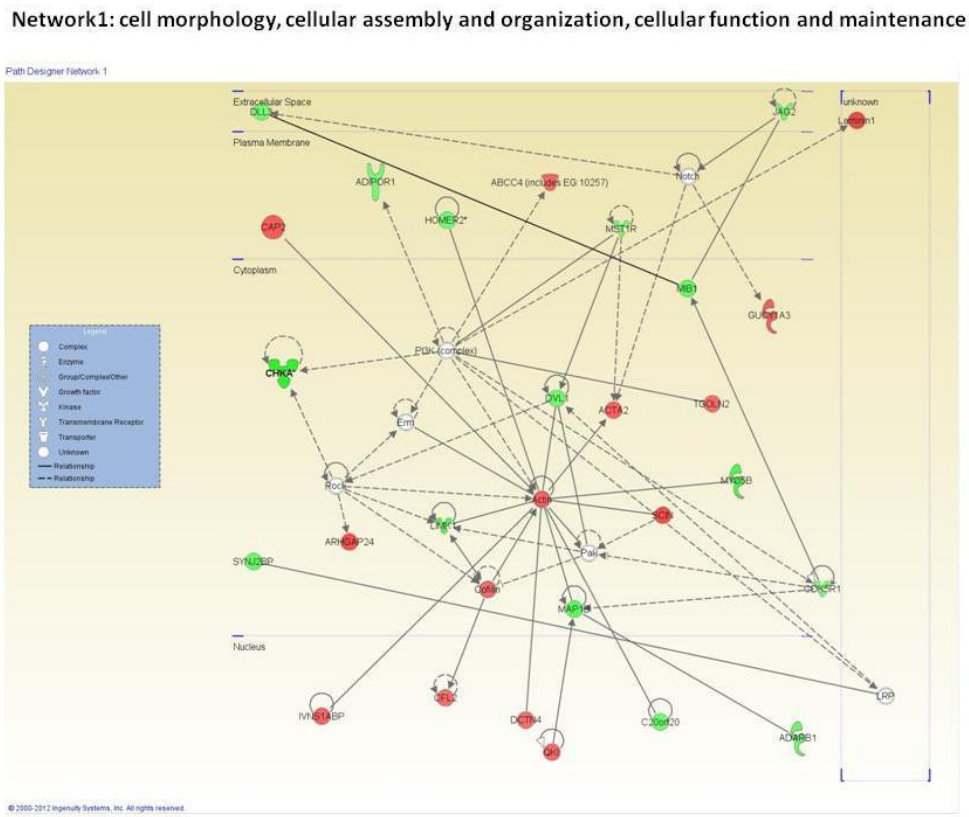

Figure 6: Graphical representation of the most highly rated network as obtained by Ingenuity Pathway Analysis (IPA).

The defined statistically significant genes are shaded and the intensity of the shading shows the degree of relative modulation. Red and green shading are for up- or down-regulated genes in CHKA-silenced cells. A solid line represents a direct interaction between the two gene products and a dotted line means there is an indirect interaction. All molecules participating to the network are listed below. The focus molecules of the network significantly affected by CHKA silencing are reported in red or green color, depending on their relative modulation as above described.

A

Molecular and Cellular Functions

Name	P-value	# Molecules
Cell Death	1.59E-08 - 7.98E-03	129
Cellular Growth and Proliferation	1.84E-07 - 7.36E-03	136
Cellular Movement	9.06E-06 - 7.98E-03	86
Cell-to-Cell Signaling and Interaction	1.00E-05 - 8.14E-03	43
Cellular Development	1.19E-05 - 7.42E-03	126

B

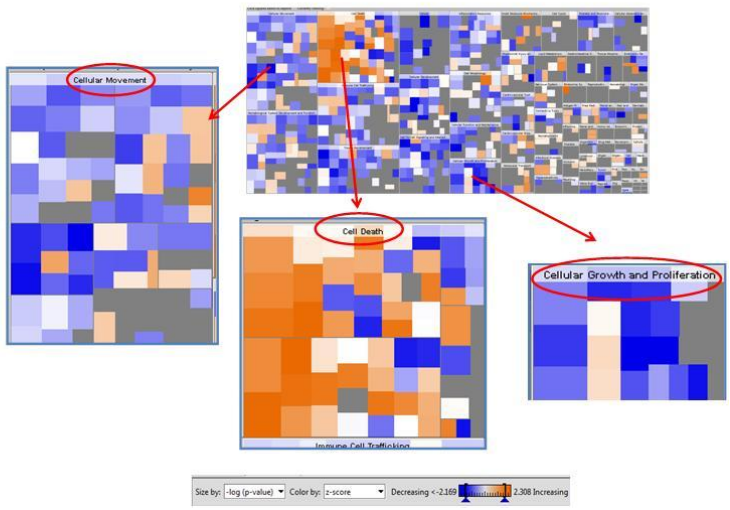

Figure 7. Prediction of cellular functions affected by CHKA silencing.

A: List of the cellular functions significantly affected by CHKA silencing by IPA analysis. For each of them the number of related molecules significantly altered upon CHK downregulation and their level (range) of significance is reported. B: Detailed z-score heatmap of the three most relevant altered cellular functions predicting their relative alteration in CHKA-silenced cells as compared to control. Square in the heatmap are divided in hierarchical levels from high-level functional category (listed in the bar) to mid level sub-functional categories and specific functions. Blue and orange shading represent a prediction of decrease or increase of the specified function, and the intensity of the shading indicates the prediction strength. The size of squares reflects the –log of the calculated P value, with larger square indicating more significant overlap between dataset observations and predicted function.

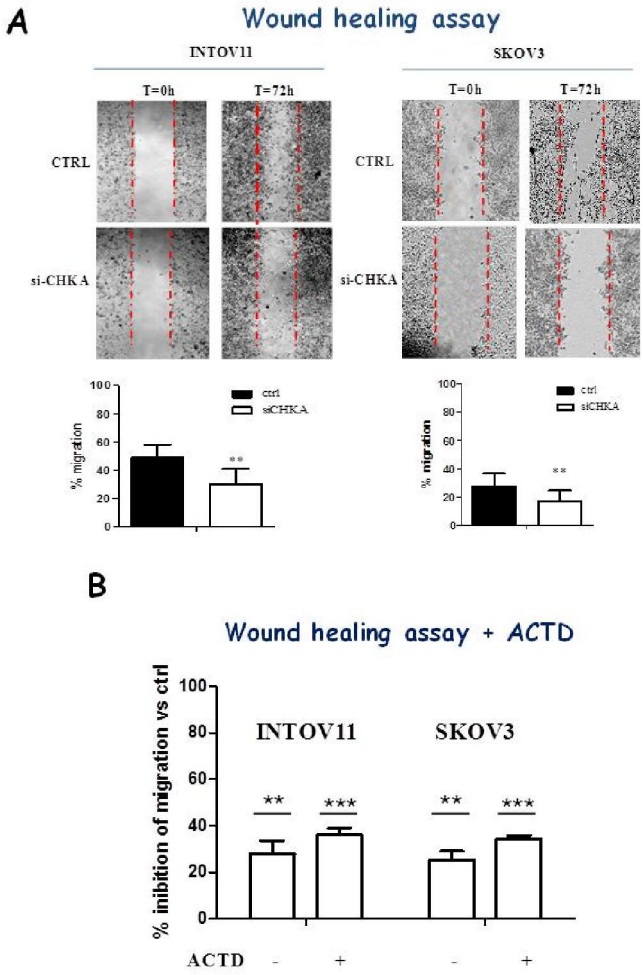

Figure 8. *CHKA* silencing regulates cell migration

A: Wound healing assay: photographs of a representative experiment of three performed taken at the time of scratch (t=0) and at t=72h. Magnification 200x; Mean percentage ± SD of migration at t=72h is reported in the graph for each cell line. **B:** mean percentage ± SD of inhibition of migration of silenced cells compared to control cells (100%) in absence or presence of Actinomycin D (ACTD) for both EOC cell lines is reported.

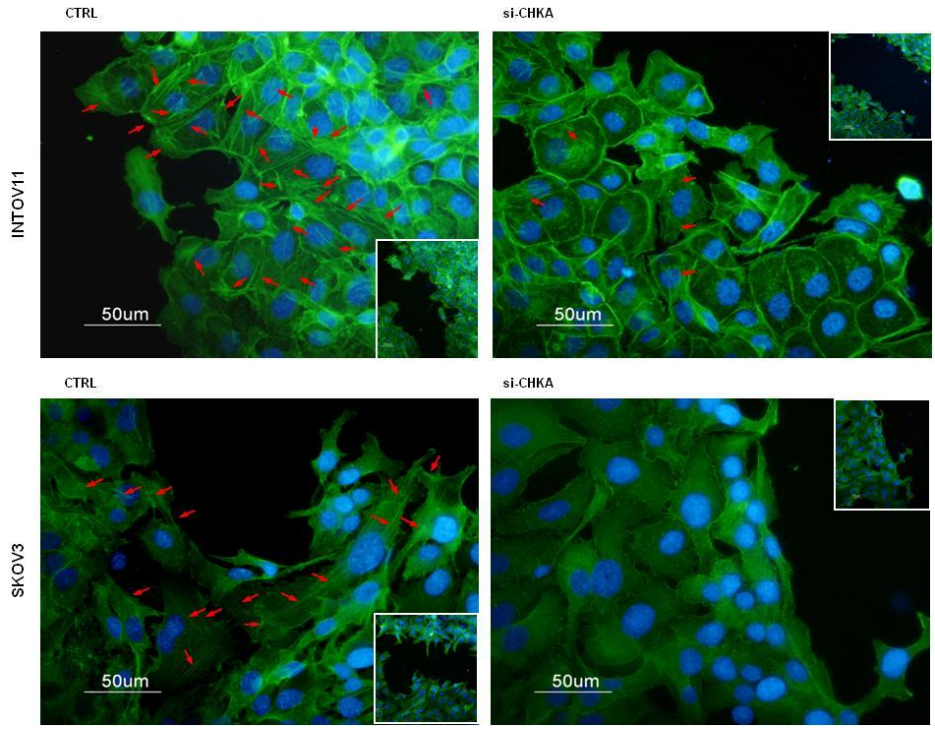

Figure 9. *CHKA* silencing induces alteration in F-actin organization

Representative immunofluorescence staining of INTOV11 and SKOV3 CHKA-silenced and control cells. Cells were wounded 72h after transfection and analyzed 24h later. F-actin filaments were visualized as green fluorescence through Alexa488–phalloidin binding, and cell nuclei were stained by DAPI. Actin stress fibers and focal adhesion sites are indicated by red arrows (Magnification: 300x). In each panel a picture of the wound border is reported in the inset (Magnification 200x).

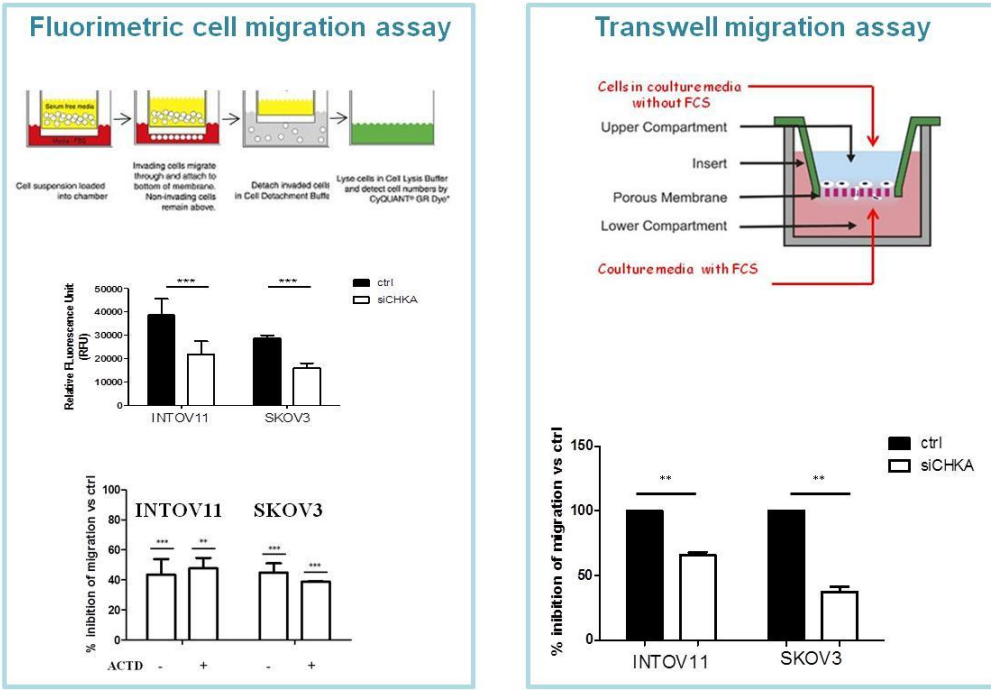

Figure 10. CHKA silenced cells display reduced motility

Cells migration capability was assessed using two assays both based on the Boyden chamber principle but having different detection methods: by relative fluorescence units (RFU) of CyQUANT dye binding by cellular nucleic acids in the lysates (***left panel***) or Odyssey Infrared laser scanner quantification after SRB staining (***right panel***). The fluorimetric assay was performed also in presence of Actinomycin D (ACTD) : mean percentage ± SD of inhibition of migration of silenced cells compared to control cells (100%) in absence or presence of Actinomycin D (ACTD) for both EOC cell lines is reported.

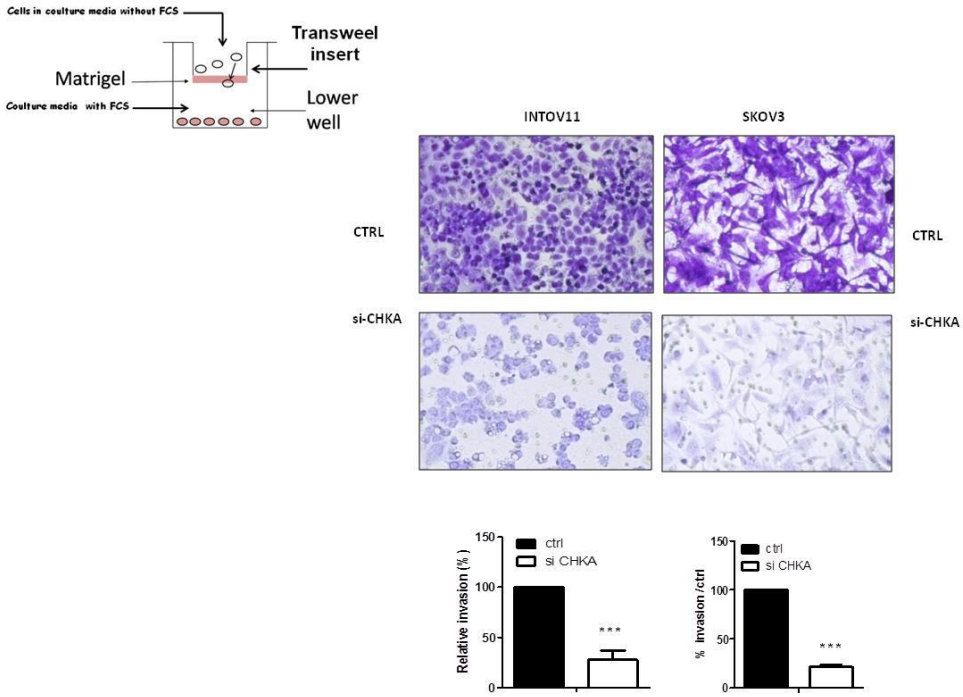

Figure 11. CHKA silenced cells display reduced invasion capability

Photographs of a representative experiment of the matrigel-coated membrane invading cells (Magnification 200X).Mean relative percentage ± SD of invasion capability calculated respect to control cells set to 100%.

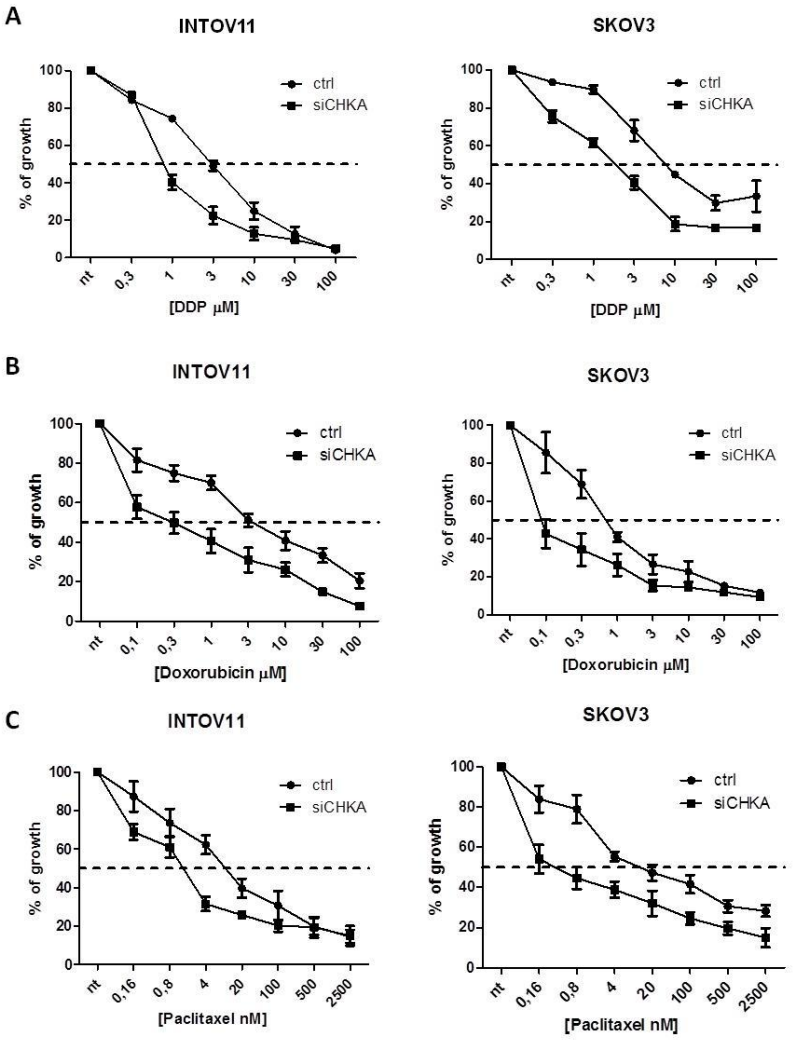

Figure 12. CHKA silencing induces sensitivity to drug treatment

Citotoxicity assay. Sensitivity to: **(A)** cisplatinum (DDP, from $1x10^{-4}$ to $3x10^{-7}$ M); **(B)** Doxorubicin (from $1x10^{-4}$ to $1x10^{-7}$ M); **(C)** Paclitaxel (from 2.5μM to 0.016 nM) was tested. Mean ± SD of growth percentage of treated vs. untreated cells is reported.

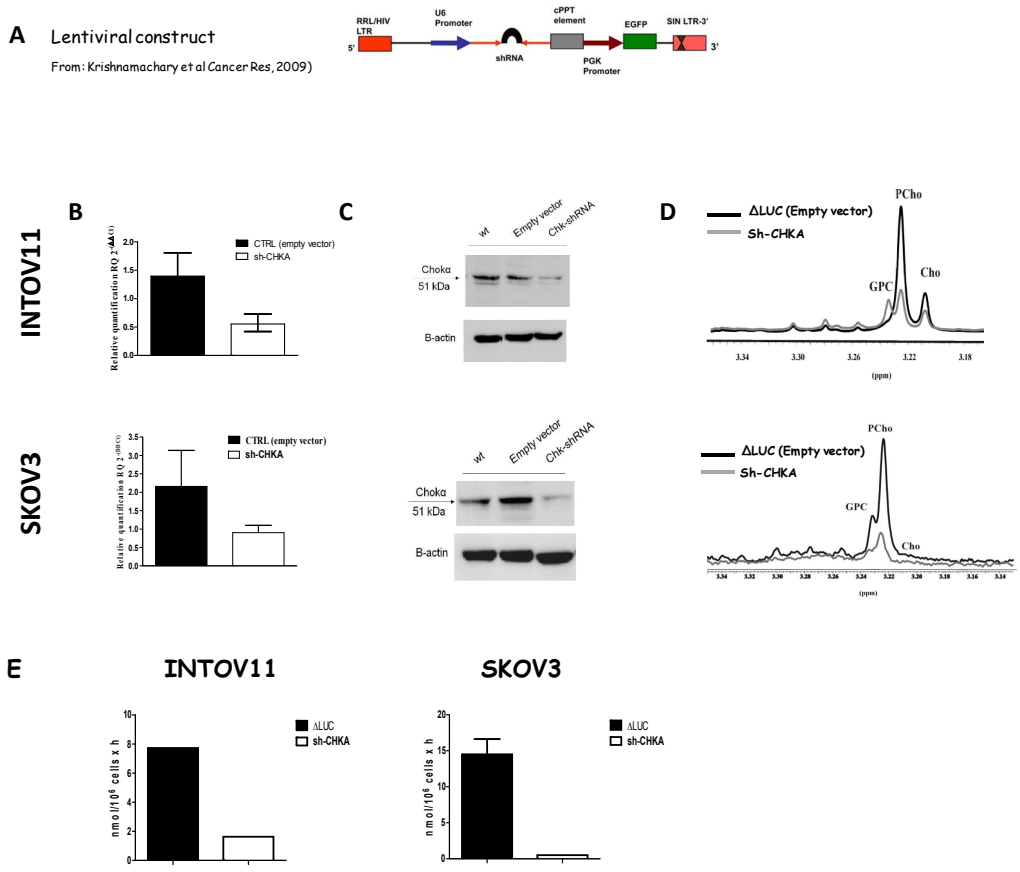

Figure 13: Molecular and functional characterization of CHKA stable transduced cells

A: structure of the lentiviral vector (Modified from: Krishnamachary et al Cancer Res, 2009). **B:** assessment of ChoKα mRNA and **C**:protein expression level in control and sh-CHKA transduced cells. **D:** Representative MRS spectra profile of the respective cell lines. **E:** Chokα enzymatic activity for both cell lines

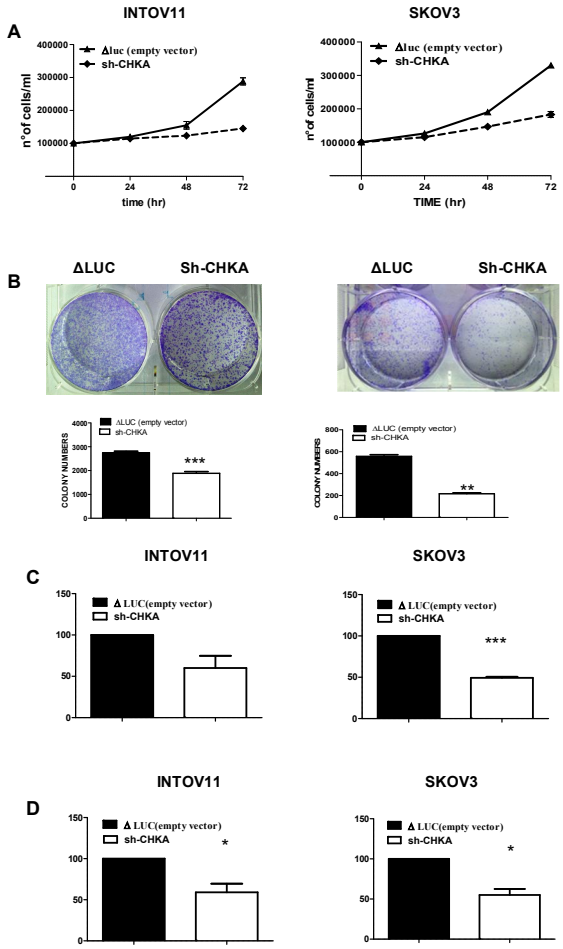

Figure 14: Biological characterization of CHKA stable silenced EOC cells.
A: Proliferation curves. Viable cells were counted 24, 48 and 72h post-seeding. Mean ± SD for three independent experiments of sh-CHKA transduced cells vs. control cells (cells transduced with ΔLuc-sh-RNA) is reported. **B:** Representative images of colony formation assay and related quantification. Lower panel: the bar graphs show the quantification of the number of colonies after 10 days of growth. Data are the mean ± SD of three independent experiments. **C:** Migration assay. Cells migrating through the membrane were measured by relative fluorescence units (RFU) of CyQUANT dye binding by cellular nucleic acids in the lysates. The percentage of inhibition of migration in sh-CHKA transduced INTOV11 and SKOV3 cells as compared to their relative controls (ΔLuc-sh-RNA) is reported. **D:** Invasion assay. Invasion capability was calculated respect to control transduced (ΔLuc-sh-RNA) cells set to 100%. Mean relative percentage ± SD of 3 independent experiments is reported

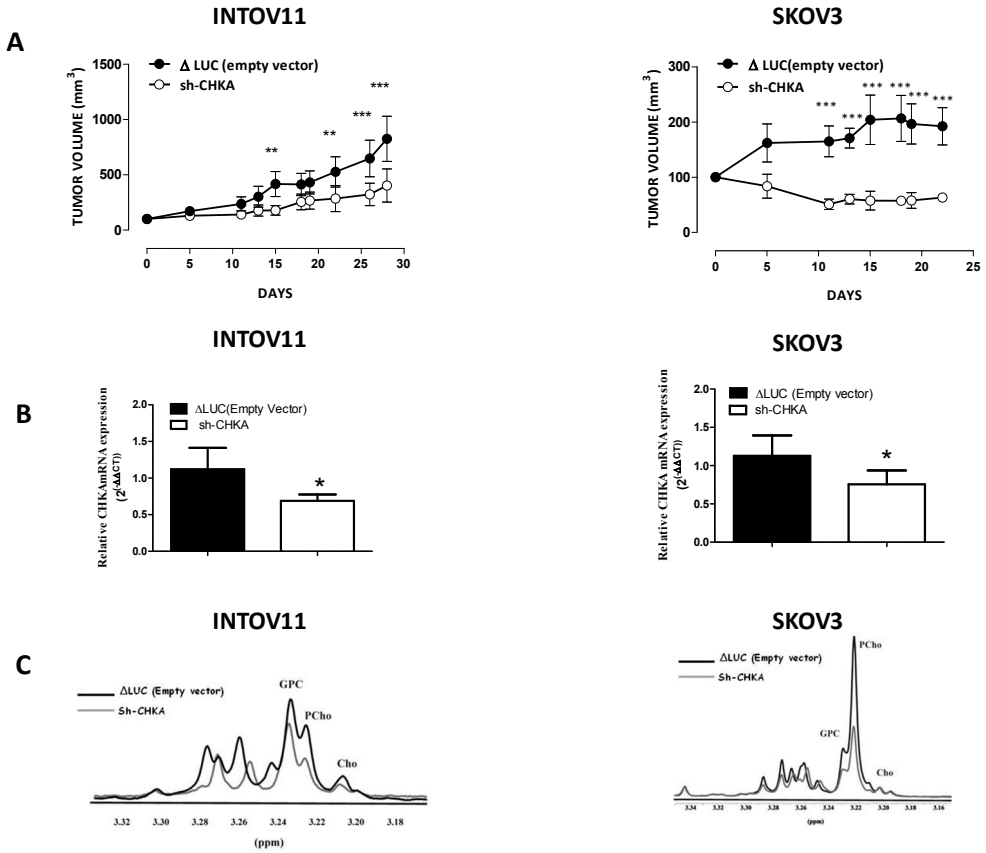

Figure 15: Effects of CHKA stable silencing in EOC xenotraplants

A: *in vivo* tumor growth of both transduced EOC cells. $3x10^6$ cells were injected sub-cutaneously into Nude mice. 5 animals per group (control and sh-CHKA) were treated. **B:** qRT-PCR for CHKA mRNA expression of tumors derived from INTOV11 and SKOV3 xenografts. Data are the mean ± SD of 5 tumors. GAPDH was used as endogenous control and the I64-hTERT cell preparations were used as calibrator. **C:** Representative expanded regions of 1H-MR spectra from INTOV11 and SKOV3 xenografts. Black lines: cells transduced with ΔLuc-sh-RNA; grey lines: cells transduced with CHKA-sh-RNA.

Summary Statistics				
ANOVA Contrasts shRNA / Mock	Total biochemicals $p \leq 0.05$	Biochemicals (↑|↓)	Total biochemicals $0.05 < p < 0.10$	Biochemicals (↑|↓)
INTOV11	89	8 | 81	29	2 | 20
SKOV3	32	0 | 32	29	0 | 29

Table 2: summary of biochemicals that differed significantly between experimental groups (control Δluc and stably silenced sh-CHKA) within each cell line 72h after plating. A summary of the numbers of biochemicals that achieved statistical significance ($p \leq 0.05$), as well as those approaching significance ($0.05 < p < 0.10$), is shown; downregulated metabolites are in green, upregulated are in red.

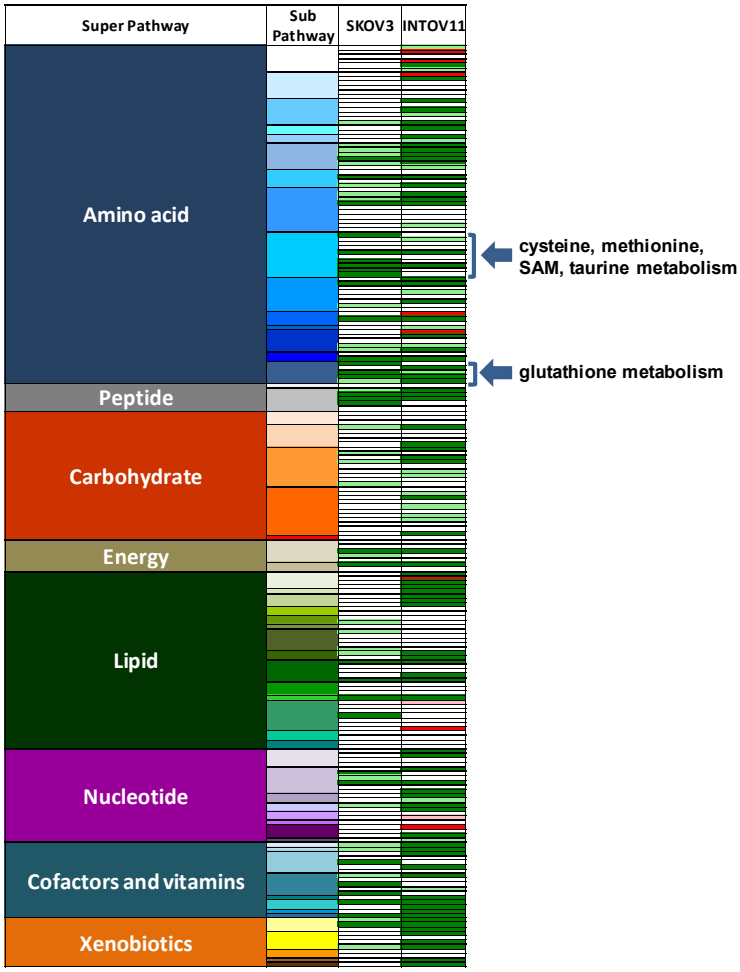

Table 3: Heatmap of the metabolites significantly altered in shCHKA INTOV11 and SKOV3 cell lines as compared to their controls. Downregulated biochemicals with statistical significance $p \leq 0.05$ are in dark green those approaching significance ($0.05 < p < 0.10$) are reported in light green. The same criteria are applied for up-regulated biochemicals, which are respectively in dark and light red.

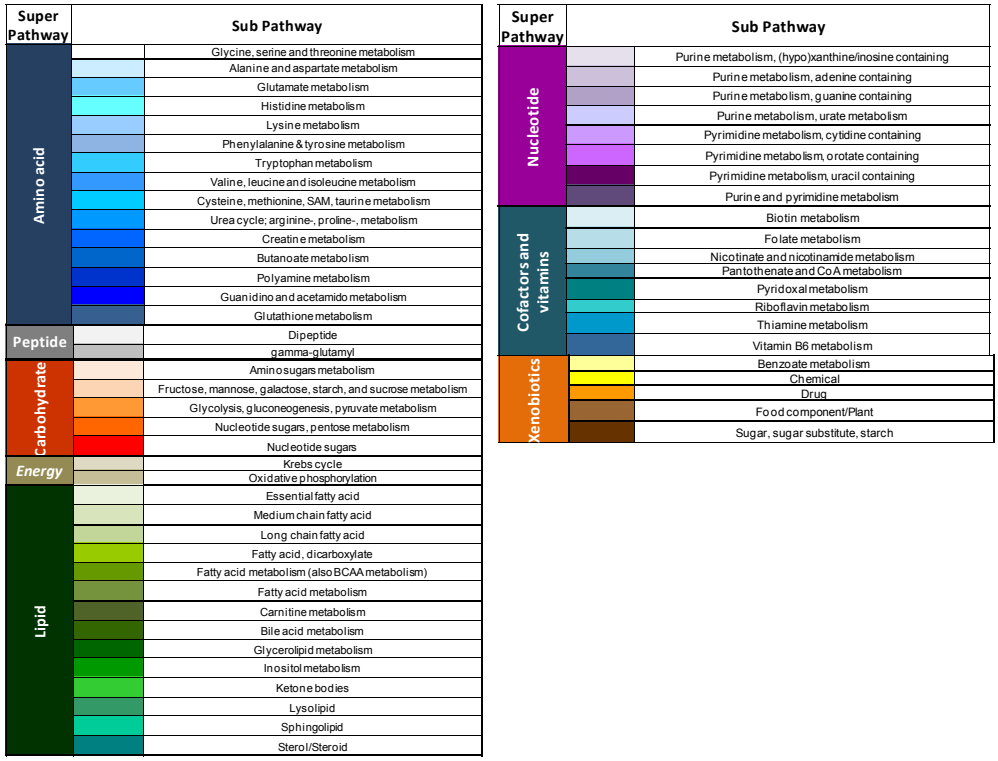

Table 4: Major metabolic pathways (Super pathway) altered following CHKA stable silencing

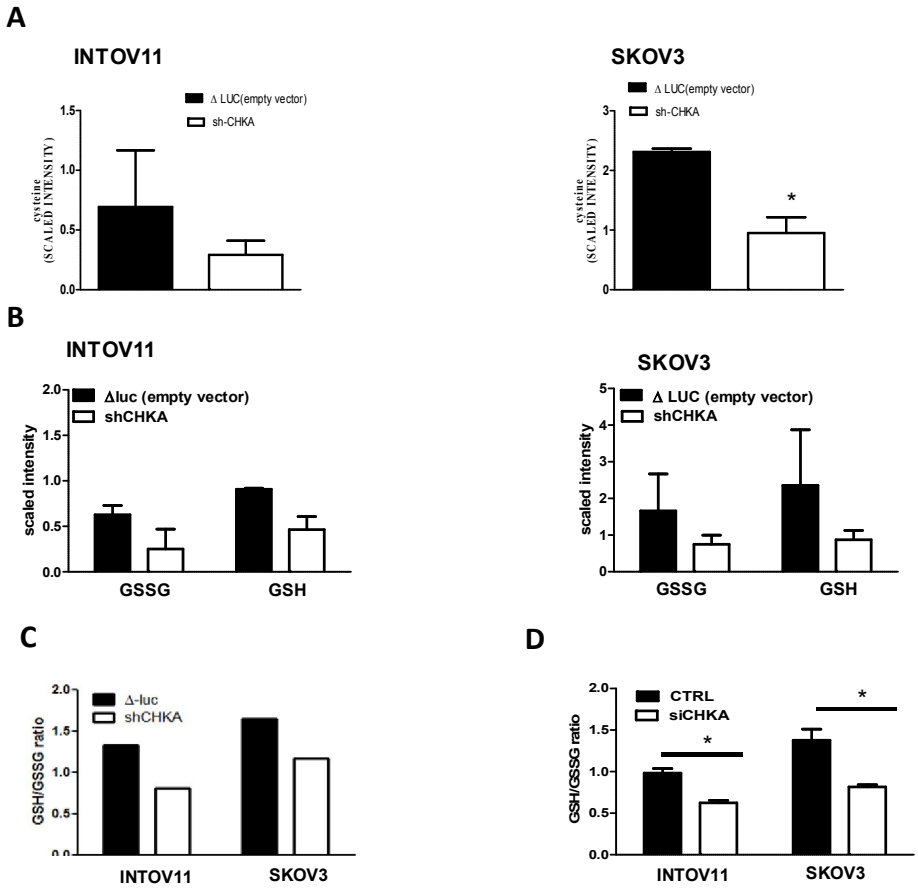

Figure 16: Effects of stable and transient CHKA silencing on cellular metabolism

Quantification of metabolic signals of control (ΔLuc) and sh-CHKA EOC cell lines: (**A**) Cysteine; (**B** left columns) GSSG; (**B** right columns) GSH signals. Data are mean ± SD of values obtained by mass spectrometry (Metabolon Technology) on 4 replicates analyzed 72h post seeding. **C**: GSH/GSSG ratio derived from Metabolon data. **D**: Validation of GSH and GSSG signals variations in transiently CHKA-silenced EOC cell lines using a luminescence-based assay.

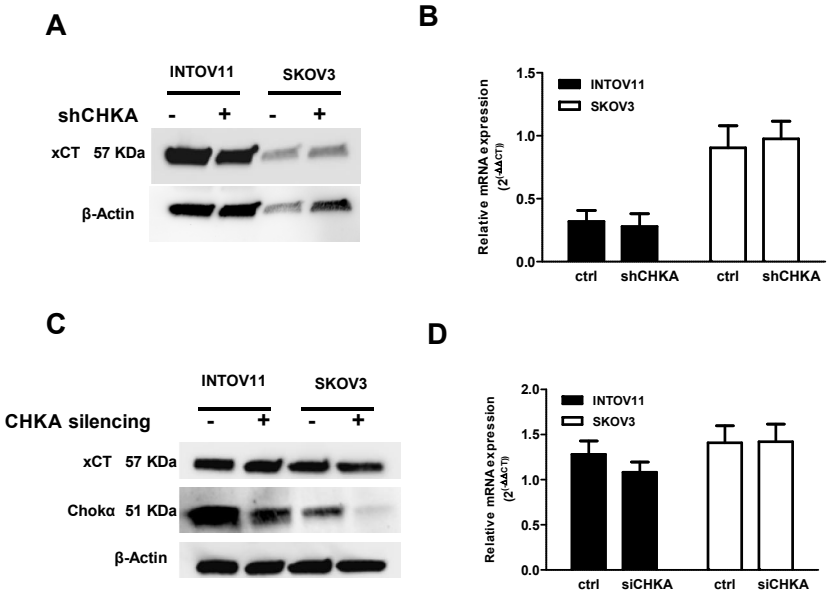

Figure 17: Analysis of xCT expression.

(A-C) Western Blot and **(B-D)** mRNA analysis of xCT expression in INTOV11and SKOV3 cell lines stably (**A,B**) or transiently (**C,D**) silenced for CHKA expression.

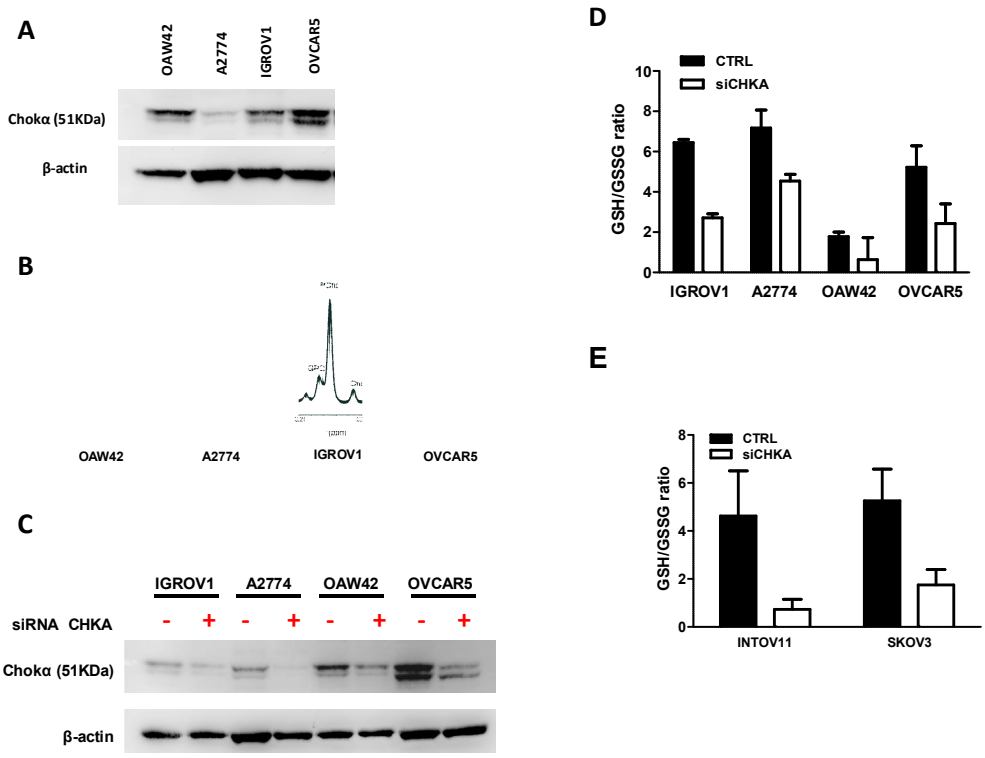

Figure 18: Alteration of GSH metabolism following CHKA silencing is a common feature of EOC cells.

Representative experiments in a panel of four EOC cell lines are shown: **A**: Immunoblot for CHKA protein expression. **B**: MRS spectra profile for PCho intracellular pooling **C**: Assessment of ChoKα downmodulation by Western blot analysis. β-actin was used as loading control. **D:** Quantification of GSH and GSSG concentration by luminescence-based assay in control and siCHKA-EOC cell lines. Data are mean ± SD of 3 independent experiments.

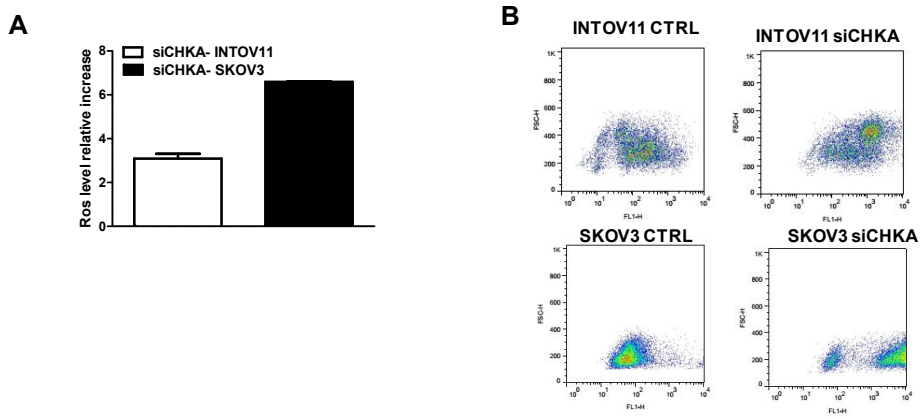

Figure 19: CHKA silencing regulates ROS activation.

ROS levels were measured by flow cytometry using the oxidation-sensitive probe CM-H2DCF-DA whose fluorescent signal intensity is directly proportional to production of reactive oxidants. To calculate the relative fold change of siCHKA signal vs control cells, the cells alone without fluorescent dye were used as negative control to derive the mean fluorescence index for each sample. **A:** Relative increase in intracellular ROS levels in si-CHKA silenced cells as compared to their controls. **B:** A representative experiment for each cell line is reported.

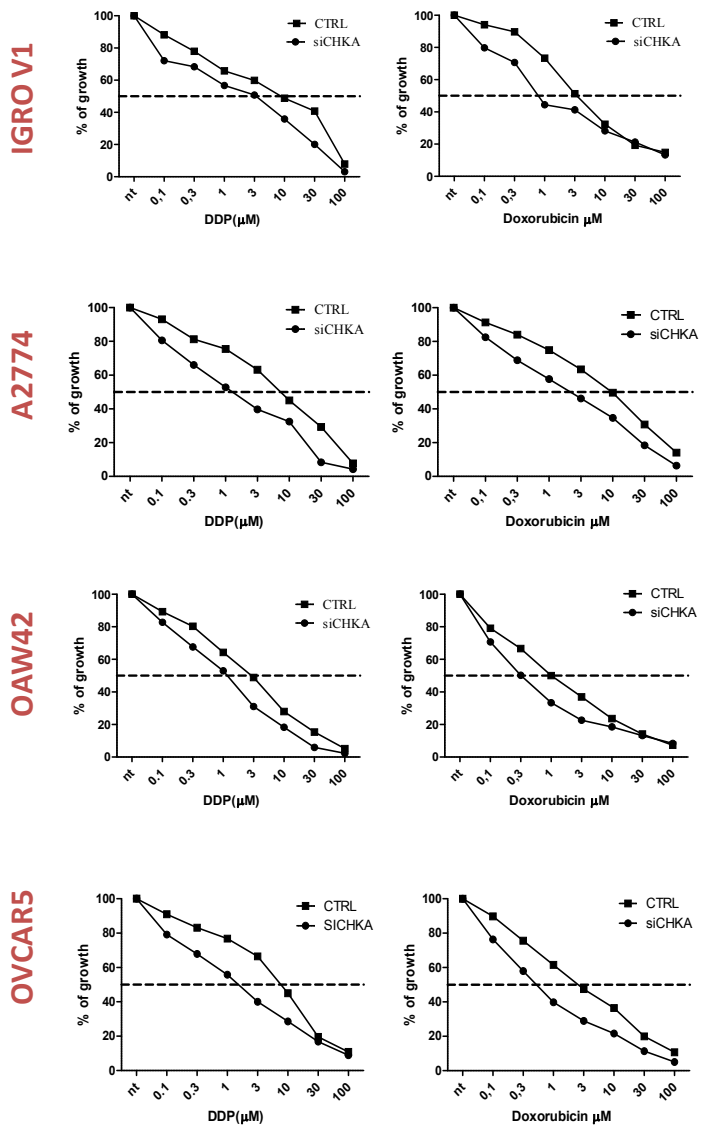

Figure 20: Increase of drug sensitivity upon CHKA silencing is a common feature of EOC cells. Sensitivity to DDP and Doxorubicin treatment were tested in a panel of EOC cell lines after CHKA transient silencing (siCHKA).

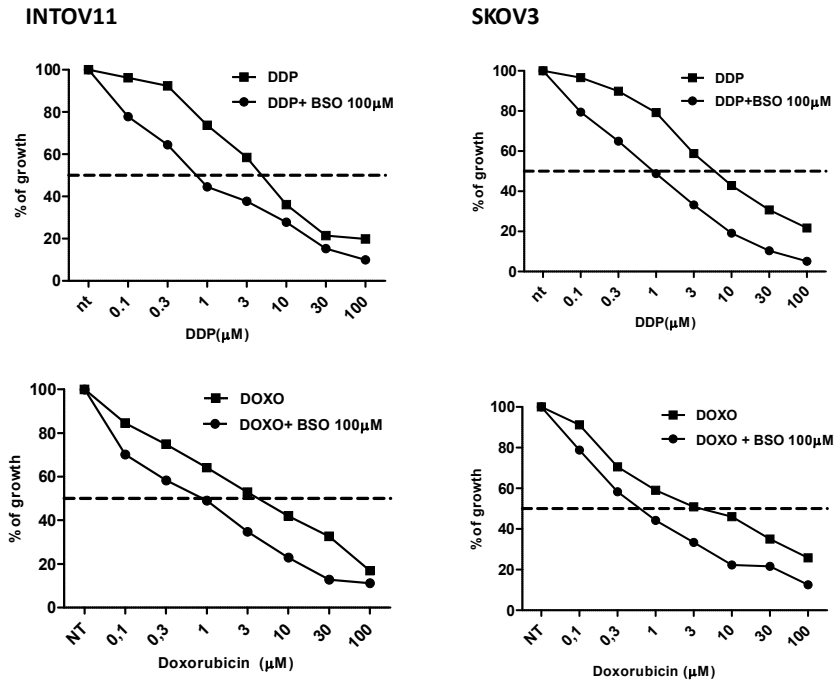

Figure 21: Sensitivity to drug treatment following exposure with BSO.

Sensitivity to DDP (upper panels) and doxorubicin (lower panels) in the presence or absence of 100 µM BSO in wild type INTOV11 and SKOV3 cells.

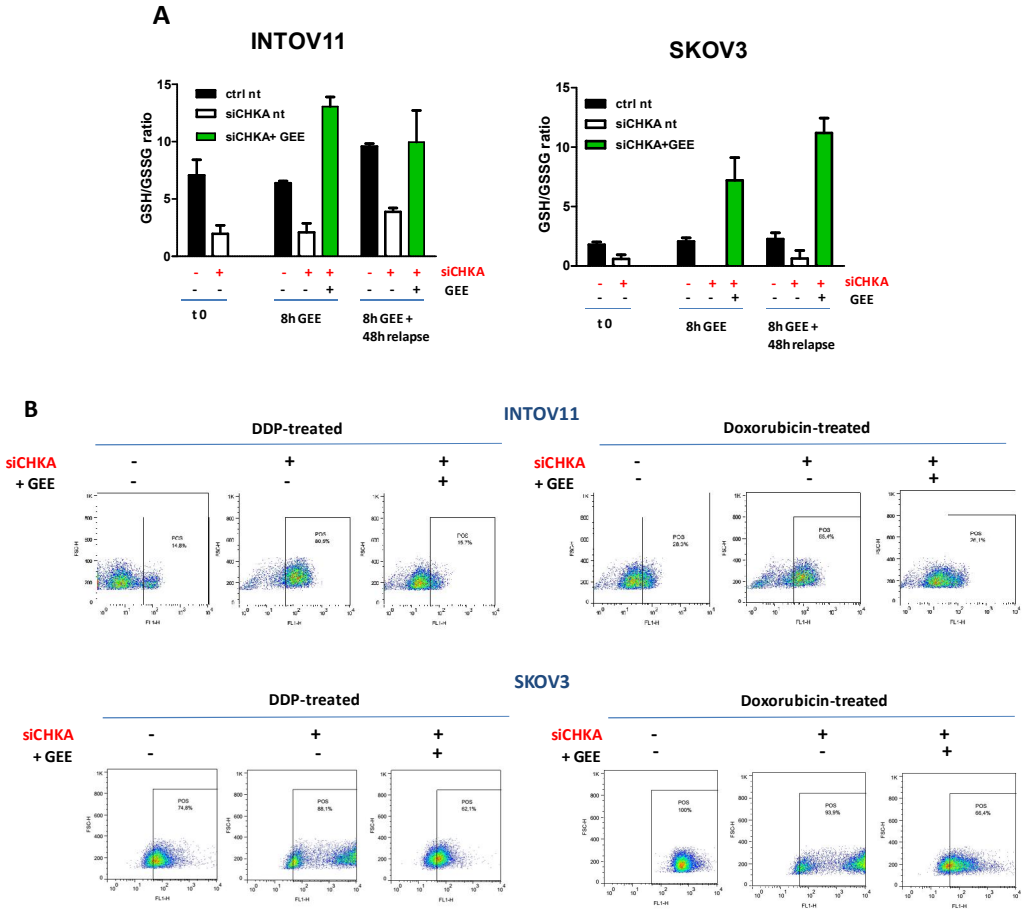

Figure 22: ROS levels and drug sensitivity are affected by modulations of intracellular GSH content mimicking CHKA silencing and/or expression.

A: Reloading of GSH content in siCHKA cells by 10mM GEE treatment. Intracellular levels of reduced and oxidized glutathione were monitored at the end of 72h of silencing, after GEE loading and relapse. **B.** GEE treatment decreases ROS levels in siCHKA- drug treated cells. Cells were treated with 10μM DDP or doxorubicin in presence or absence of GEE. Control (si-ctrl) drug-treated cells were used as negative control to measure the specific ROS level variation.

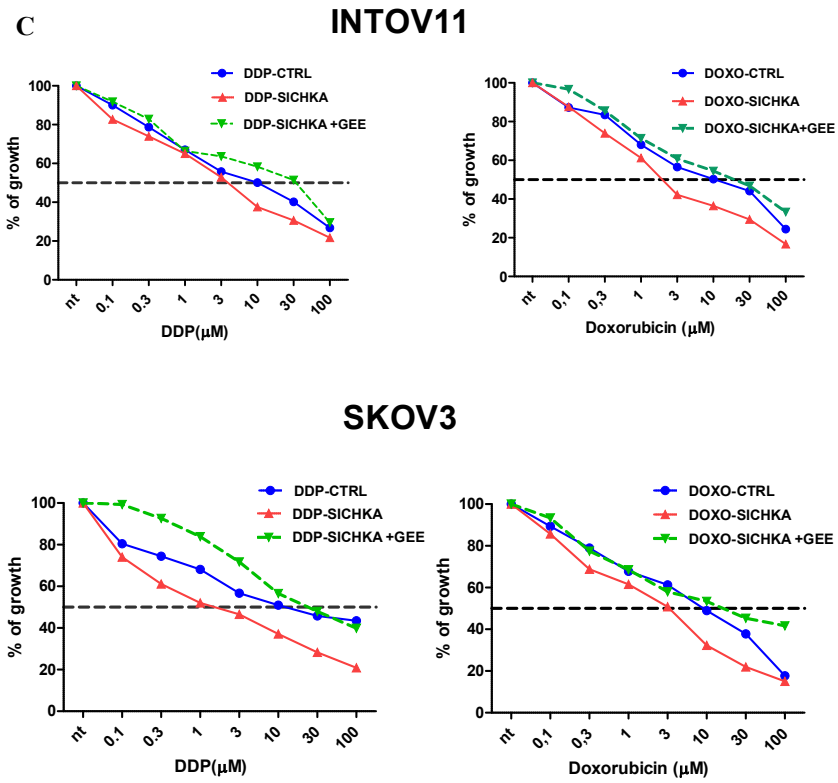

Figure 22: ROS levels and drug sensitivity are affected by modulations of intracellular GSH content mimicking CHKA silencing and/or expression.

C. Effects of GEE exposure on cell sensitivity to DDP and doxorubicin in INTOV11 and SKOV3 siCHKA-cells.

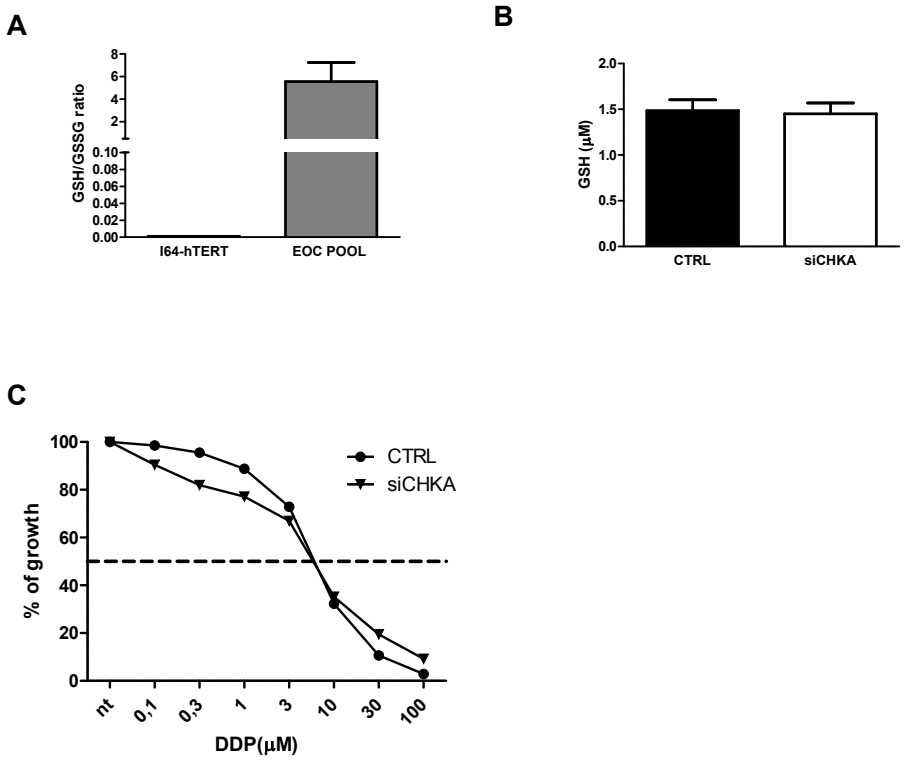

Figure 23: Alteration of Glutathione metabolism following CHKA silencing is a characteristic only of EOC tumoral cells

A: Quantification of GSH/GSSG ratio in I64-hTERT normal ovarian cell line and in a pool of EOC cells. **B:** Quantification of GSH concentration, in I64-hTERT CHKA transiently silenced and control cells. **C:** Sensitivity to DDP in CHKA silenced I64-hTERT.

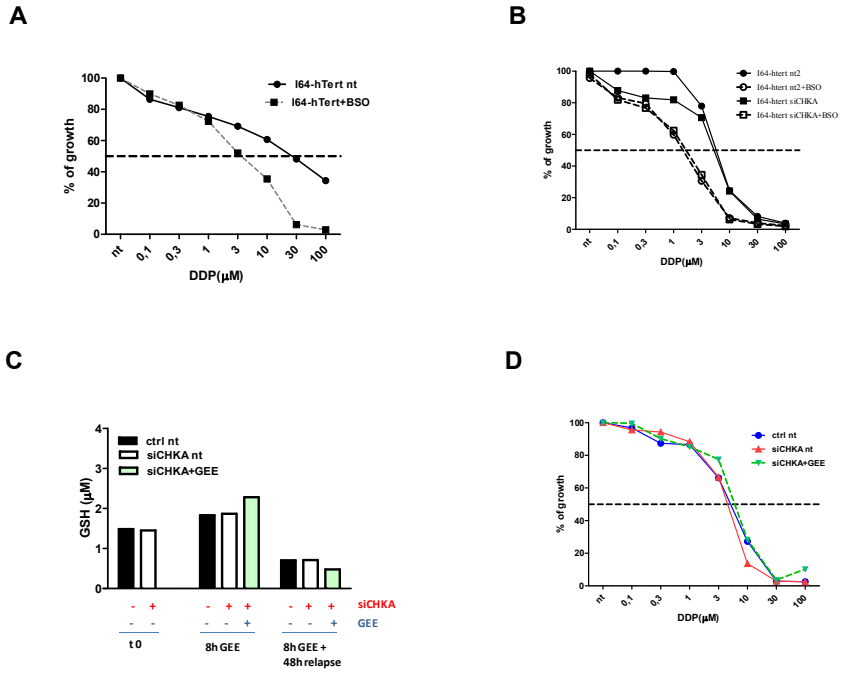

Figure 24: Effects of depletion and rescue of GSH in non tumoral I64-hTERT cells upon CHKA silencing.

A: Effects of BSO treatment on sensitivity to cisplatinum (DDP) of I64-hTERT wild type cells. Mean ± SD of growth percentage of treated vs. untreated cells is reported. **B:** Effects of BSO treatment on sensitivity to cisplatinum (DDP) of I64-hTERT control and silenced cells. Mean ± SD of growth percentage of treated vs. untreated cells is reported. **C:** Quantification of GSH concentration at the end of 72h of silencing, after GEE loading and at relapse. **D:** Effects of DDP treatment in presence or absence of GEE in siCHKA I64-hTERT cells. Mean ± SD of growth percentage of treated vs. untreated cells is reported for 3 independent experiments.

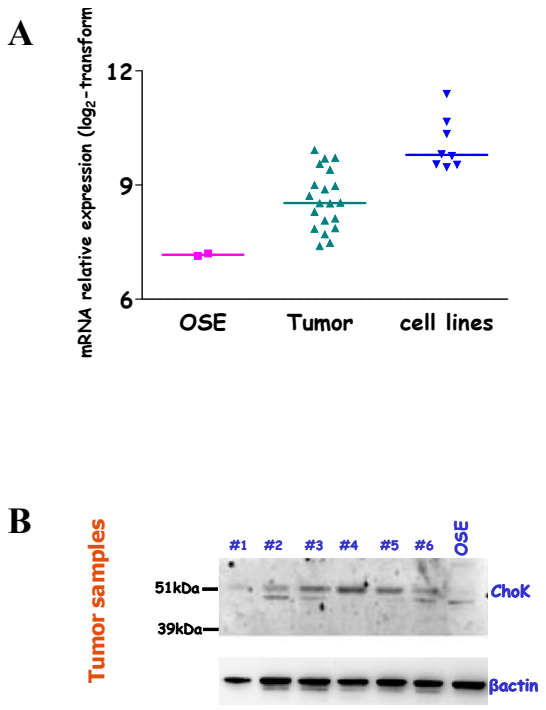

Figure 25: ChoKα detection in EOC surgical specimens

A: Gene expression analysis of ChoKα in OSE cells, surgical EOC specimens and EOC cell lines. Horizontal bars represent relative median expression for each group. **B:** Western blot analyses of total lysates of EOC surgical specimens and OSE cells are shown for ChoKα protein expression; β-actin was used as internal loading control.

DATASETS	EOC TUMOR CELLS	NORMAL EOC CELL LINES	LMP TUMORS	LOW GRADE TUMORS	HIGH GRADE TUMORS
Iorio (Cancer Res, 2010)	8	2	/	/	21
Berchuck (Clin Cancer Re, 2009)	/	/	19	4	73
King (Am J Surg Pathol, 2011)	/	6	8	13	22
Bonome (Cancer Res, 2008)	/	10	/	/	185
Bowen (BMC Med Genomics, 2010)	/	12	/	2	10
Mok (Cancer Cell, 2009)	/	10	/	/	53
Anglesio (Mol Cancer Res, 2008)	/	/	/	30	60
Tothill (Clin Cancer Res, 2008)	/	/	18	10	210

Table 5: Characteristics of publicly available gene-expression EOC datasets

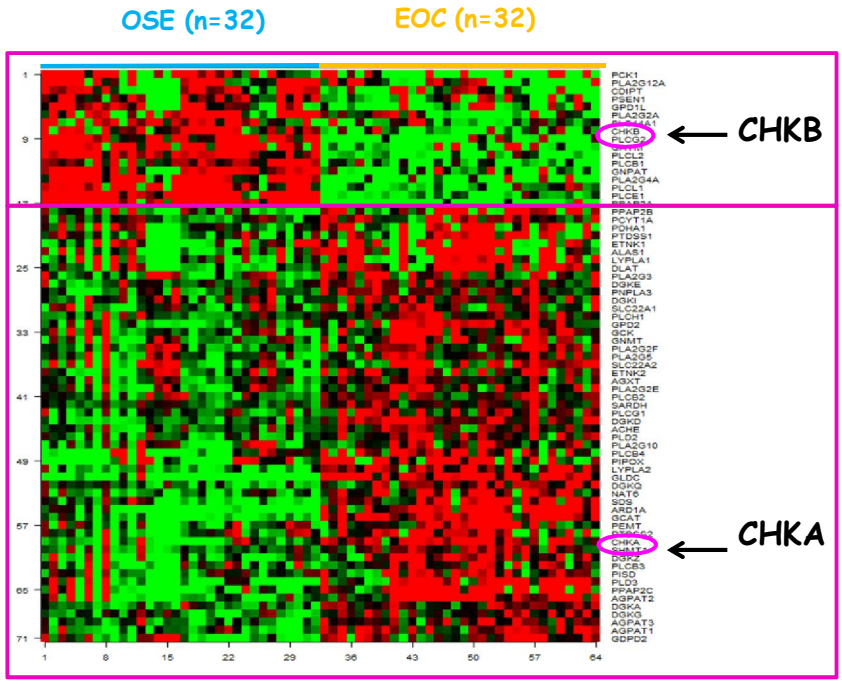

Figure 26 : Metanalysis of metabolism-related genes expression in high grade serous EOC vs OSE

Heat map of differentially expressed metabolism-related genes in EOC. Unsupervised hierarchical clustering was performed on gene expression profiles of three different datasets: Bowen (GSE14407, Affy HGU133 plus2;), Mok (GSE18520, Affy HGU133 plus2) and Bonome (GSE26712, Affy HGU133A). Samples were selected according to the following criteria: 12 OSE and 12 EOC for Bowen dataset, 10 OSE and 10 EOC for Mok and Bonome datasets. Each column represents a tumor sample and each row represents a gene Red color indicates genes that were upregulated and green color indicates genes that were downregulated. Black indicates genes whose expression is unchanged in tumors as compared to normal

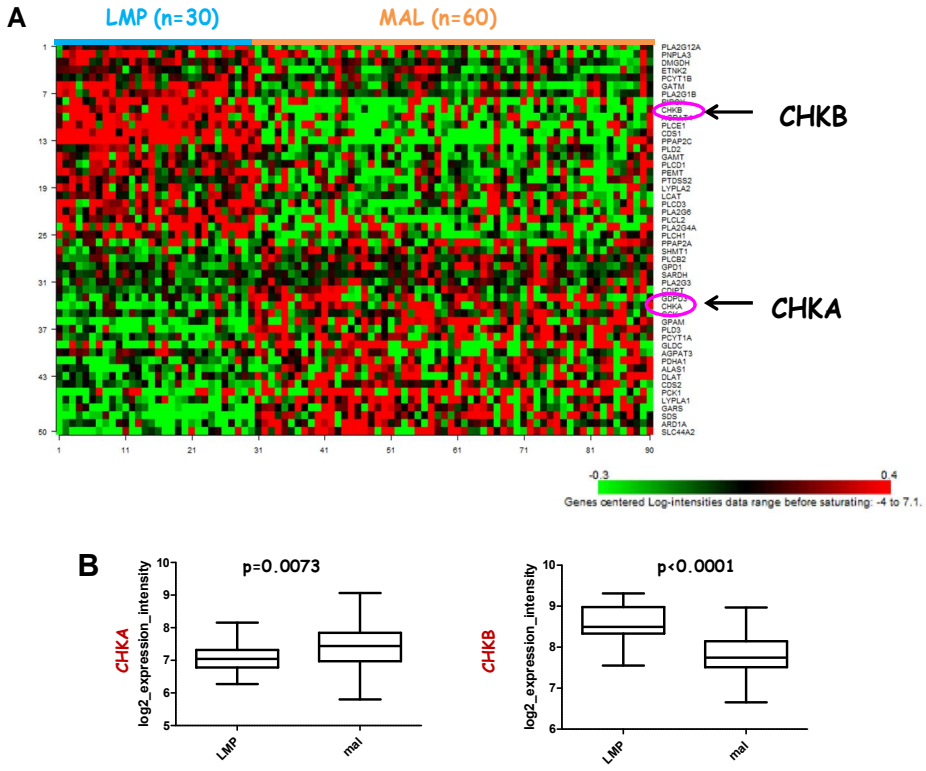

Figure 27: Metanalysis of metabolism-related genes LMP vs MAL tumors

A: Heat map of differentially expressesed metabolism-related genes in LMP vs malignant (MAL) EOC. Unsupervised hierarchical clustering was performed on gene expression profiles of tumor specimens selected from Anglesio dataset. Each column represents a tumor sample and each row represents a gene Red color indicates genes that were upregulated and green color indicates genes that were downregulated. Black indicates genes whose expression is unchanged in malignant EOC compared to LMP**. B:** Box-plot of CHKA and CHKB gene expression data from Anglesio dataset comparing LMP vs malignant EOC. Expression values are indicated in the boxes as the median of each group. Y-axis probe set expression values in log2 scale.

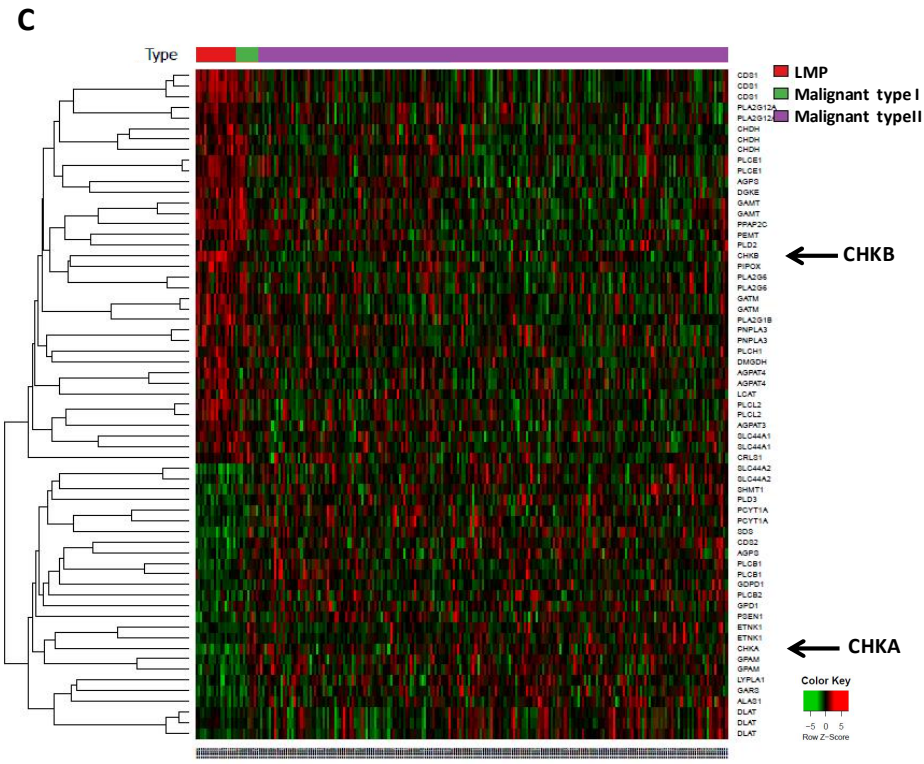

Figure 27: Metanalysis of metabolism-related genes LMP vs MAL tumors

C: Heat map of differentially expressesed metabolism-related genes in LMP vs malignant (MAL) typeI and type II EOC in Tothill dataset. Unsupervised hierarchical clustering was performed on gene expression profiles of tumor specimens. Each column represents a tumor sample and each row represents a gene. Red color indicates genes that were upregulated and green color indicates genes that were downregulated. Black indicates genes whose expression is unchanged in malignant EOC compared to LMP**.**

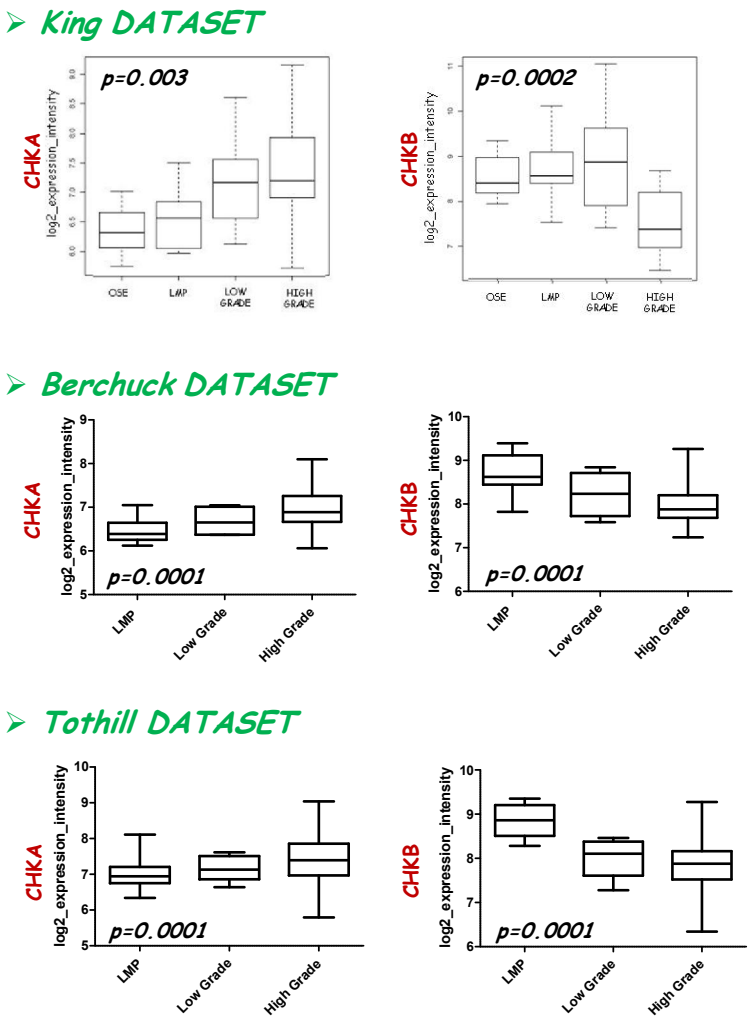

Figure 28: Evaluation of CHK genes expression according to EOC grading in others publicly available datasets

Box-plot of CHKA and CHKB gene expression data from three different datasets including OSE cells (only *King dataset*), LMP, Low Grade and High Grade EOC tumors (*King, Berchuck and Tothill* Datasets). Expression values are indicated in the boxes as the median of each group. Y-axis probe set expression values in log2 scale.

REFERENCES

(1) Jemal A, Bray F, Center MM, Ferlay J, Ward E, Forman D. Global cancer statistics. CA Cancer J Clin 2011 Mar;61(2):69-90.

(2) Heintz AP, Odicino F, Maisonneuve P, Quinn MA, Benedet JL, Creasman WT, Ngan HY, Pecorelli S, et al. Carcinoma of the ovary. FIGO 6th Annual Report on the Results of Treatment in Gynecological Cancer. Int J Gynaecol Obstet 2006 Nov;95 Suppl 1:S161-S192.

(3) Sandercock J, Parmar MK, Torri V. First-line chemotherapy for advanced ovarian cancer: paclitaxel, cisplatin and the evidence. Br J Cancer 1998 Dec;78(11):1471-8.

(4) Markman M, Bookman MA. Second-line treatment of ovarian cancer. Oncologist 2000;5(1):26-35.

(5) Banerjee S, Gore M. The future of targeted therapies in ovarian cancer. Oncologist 2009 Jul;14(7):706-16.

(6) Bookman MA. On the road to PARPi-platin. J Natl Cancer Inst 2014 Jun;106(6):dju119.

(7) Vaughan S, Coward JI, Bast RC, Jr., Berchuck A, Berek JS, Brenton JD, Coukos G, Crum CC, et al. Rethinking ovarian cancer: recommendations for improving outcomes. Nat Rev Cancer 2011 Sep 23;11(10):719-25.

(8) Kurman RJ, Shih I. Molecular pathogenesis and extraovarian origin of epithelial ovarian cancer--shifting the paradigm. Hum Pathol 2011 Jul;42(7):918-31.

(9) Jones PM, Drapkin R. Modeling High-Grade Serous Carcinoma: How Converging Insights into Pathogenesis and Genetics are Driving Better Experimental Platforms. Front Oncol 2013;3:217.

(10) The Cancer Genome Atlas database. [https://tcga-data.nci.nih.gov/]. 2012.

(11) Hanahan D, Weinberg RA. The hallmarks of cancer. Cell 2000 Jan 7;100(1):57-70.

(12) Hanahan D, Weinberg RA. Hallmarks of cancer: the next generation. Cell 2011 Mar 4;144(5):646-74.

(13) Glunde K, Bhujwalla ZM, Ronen SM. Choline metabolism in malignant transformation. Nat Rev Cancer 2011 Nov 17;11(12):835-48.

(14) Iorio E, Mezzanzanica D, Alberti P, Spadaro F, Ramoni C, D'Ascenzo S, Millimaggi D, Pavan A, et al. Alterations of choline phospholipid metabolism in ovarian tumor progression. Cancer Res 2005 Oct 15;65(20):9369-76.

(15) Yuan Z, Tie A, Tarnopolsky M, Bakovic M. Genomic organization, promoter activity, and expression of the human choline transporter-like protein 1. Physiol Genomics 2006 Jun 16;26(1):76-90.

(16) Wang T, Li J, Chen F, Zhao Y, He X, Wan D, Gu J. Choline transporters in human lung adenocarcinoma: expression and functional implications. Acta Biochim Biophys Sin (Shanghai) 2007 Sep;39(9):668-74.

(17) Eliyahu G, Kreizman T, Degani H. Phosphocholine as a biomarker of breast cancer: molecular and biochemical studies. Int J Cancer 2007 Apr 15;120(8):1721-30.

(18) Gibellini F, Smith TK. The Kennedy pathway--De novo synthesis of phosphatidylethanolamine and phosphatidylcholine. IUBMB Life 2010 Jun;62(6):414-28.

(19) Cui Z, Houweling M. Phosphatidylcholine and cell death. Biochim Biophys Acta 2002 Dec 30;1585(2-3):87-96.

(20) WITTENBERG J, Kornberg A. Choline phosphokinase. J Biol Chem 1953 May;202(1):431-44.

(21) Hosaka H, Nakamura H, Funakoshi H, Takaku H. Nucleoside phosphite,*O*-bis(1,1,1,3,3,3-hexafluoro-2-propyl) deoxyribonucleosid-3'-yl phosphites. A versatile synthetic intermediate for phosphonate modified nucleotide and oligonucleotide synthesis. Chem Lett 1992;1992:935-8.

(22) Aoyama C, Ohtani A, Ishidate K. Expression and characterization of the active molecular forms of choline/ethanolamine kinase-alpha and -beta in mouse tissues, including carbon tetrachloride-induced liver. Biochem J 2002 May 1;363(Pt 3):777-84.

(23) Gallego-Ortega D, Ramirez dM, Ramos MA, Valdes-Mora F, Barderas MG, Sarmentero-Estrada J, Lacal JC. Differential role of human choline kinase alpha and beta enzymes in lipid metabolism: implications in cancer onset and treatment. PLoS One 2009;4(11):e7819.

(24) Wu G, Sher RB, Cox GA, Vance DE. Differential expression of choline kinase isoforms in skeletal muscle explains the phenotypic variability in the rostrocaudal muscular dystrophy mouse. Biochim Biophys Acta 2010 Apr;1801(4):446-54.

(25) Ramirez de MA, Rodriguez-Gonzalez A, Gutierrez R, Martinez-Pineiro L, Sanchez J, Bonilla F, Rosell R, Lacal J. Overexpression of choline kinase is a frequent feature in human tumor-derived cell lines and in lung, prostate, and colorectal human cancers. Biochem Biophys Res Commun 2002 Aug 23;296(3):580-3.

(26) Ramirez dM, Sarmentero-Estrada J, Belda-Iniesta C, Taron M, Ramirez dM, V, Cejas P, Skrzypski M, Gallego-Ortega D, et al.

Expression of choline kinase alpha to predict outcome in patients with early-stage non-small-cell lung cancer: a retrospective study. Lancet Oncol 2007 Oct;8(10):889-97.

(27) Ahmed N, Thompson EW, Quinn MA. Epithelial-mesenchymal interconversions in normal ovarian surface epithelium and ovarian carcinomas: an exception to the norm. J Cell Physiol 2007 Dec;213(3):581-8.

(28) Ramirez de MA, Gutierrez R, Ramos MA, Silva JM, Silva J, Bonilla F, Sanchez JJ, Lacal JC. Increased choline kinase activity in human breast carcinomas: clinical evidence for a potential novel antitumor strategy. Oncogene 2002 Jun 20;21(27):4317-22.

(29) Iorio E, Ricci A, Bagnoli M, Pisanu ME, Castellano G, Di Vito M, Venturini E, Glunde K, et al. Activation of phosphatidylcholine cycle enzymes in human epithelial ovarian cancer cells. Cancer Res 2010 Mar 1;70(5):2126-35.

(30) Gadiya M, Mori N, Cao MD, Mironchik Y, Kakkad S, Gribbestad IS, Glunde K, Krishnamachary B, et al. Phospholipase D1 and choline kinase-alpha are interactive targets in breast cancer. Cancer Biol Ther 2014 May;15(5):593-601.

(31) Spadaro F, Ramoni C, Mezzanzanica D, Miotti S, Alberti P, Cecchetti S, Iorio E, Dolo V, et al. Phosphatidylcholine-specific phospholipase C activation in epithelial ovarian cancer cells. Cancer Res 2008 Aug 15;68(16):6541-9.

(32) Podo F, Canevari S, Canese R, Pisanu ME, Ricci A, Iorio E. MR evaluation of response to targeted treatment in cancer cells. NMR Biomed 2011 Jul;24(6):648-72.

(33) Cao MD, Dopkens M, Krishnamachary B, Vesuna F, Gadiya MM, Lonning PE, Bhujwalla ZM, Gribbestad IS, et al. Glycerophosphodiester phosphodiesterase domain containing 5 (GDPD5) expression correlates with malignant choline phospholipid metabolite profiles in human breast cancer. NMR Biomed 2012 Sep;25(9):1033-42.

(34) Lacal JC. Choline kinase: a novel target for antitumor drugs. IDrugs 2001 Apr;4(4):419-26.

(35) Ramirez de MA, Sarmentero-Estrada J, Belda-Iniesta C, Taron M, Ramirez dM, V, Cejas P, Skrzypski M, Gallego-Ortega D, et al. Expression of choline kinase alpha to predict outcome in patients with early-stage non-small-cell lung cancer: a retrospective study. Lancet Oncol 2007 Oct;8(10):889-97.

(36) Lloveras J, Hamza M, Chap H, Douste-Blazy L. Action of hemicholinium-3 on phospholipid metabolism in Krebs II ascites cells. Biochem Pharmacol 1985 Nov 15;34(22):3987-93.

(37) Cannon JG. Structure-activity aspects of hemicholinium-3 (HC-3) and its analogs and congeners. Med Res Rev 1994 Sep;14(5):505-31.

(38) de la CA, Ramirez de MA, varez-Ayerza N, Ramos MA, Cebrian A, Del Pulgar TG, Lacal JC. Combined 5-FU and ChoKalpha inhibitors as a new alternative therapy of colorectal cancer: evidence in human tumor-derived cell lines and mouse xenografts. PLoS One 2013;8(6):e64961.

(39) Hernandez-Alcoceba R, Saniger L, Campos J, Nunez MC, Khaless F, Gallo MA, Espinosa A, Lacal JC. Choline kinase inhibitors as a novel approach for antiproliferative drug design. Oncogene 1997 Nov 6;15(19):2289-301.

(40) Hernandez-Alcoceba R, Fernandez F, Lacal JC. In vivo antitumor activity of choline kinase inhibitors: a novel target for anticancer drug discovery. Cancer Res 1999 Jul 1;59(13):3112-8.

(41) Clem BF, Clem AL, Yalcin A, Goswami U, Arumugam S, Telang S, Trent JO, Chesney J. A novel small molecule antagonist of choline kinase-alpha that simultaneously suppresses MAPK and PI3K/AKT signaling. Oncogene 2011 Jul 28;30(30):3370-80.

(42) Glunde K, Raman V, Mori N, Bhujwalla ZM. RNA interference-mediated choline kinase suppression in breast cancer cells induces differentiation and reduces proliferation. Cancer Res 2005 Dec 1;65(23):11034-43.

(43) Krishnamachary B, Glunde K, Wildes F, Mori N, Takagi T, Raman V, Bhujwalla ZM. Noninvasive detection of lentiviral-mediated choline kinase targeting in a human breast cancer xenograft. Cancer Res 2009 Apr 15;69(8):3464-71.

(44) Mori N, Gadiya M, Wildes F, Krishnamachary B, Glunde K, Bhujwalla ZM. Characterization of choline kinase in human endothelial cells. NMR Biomed 2013 Jun 18;10.

(45) Holohan C, Van SS, Longley DB, Johnston PG. Cancer drug resistance: an evolving paradigm. Nat Rev Cancer 2013 Oct;13(10):714-26.

(46) Bohlig L, Rother K. One function--multiple mechanisms: the manifold activities of p53 as a transcriptional repressor. J Biomed Biotechnol 2011;2011:464916.

(47) Dean M. Cancer stem cells: Implications for cancer causation and therapy resistance. Discov Med 2005 Jun;5(27):278-82.

(48) Bagnoli M, Balladore E, Luison E, Alberti P, Raspagliesi F, Marcomini B, Canevari S, Mezzanzanica D. Sensitization of p53-mutated epithelial ovarian cancer to CD95-mediated apoptosis is synergistically induced by cisplatin pretreatment. Mol Cancer Ther 2007;6(2):762-72.

(49) Mezzanzanica D, Balladore E, Turatti F, Luison E, Alberti P, Bagnoli M, Figini M, Mazzoni A, et al. CD95-mediated apoptosis is impaired at receptor level by cellular FLICE-inhibitory protein (long form) in wild-type p53 human ovarian carcinoma. Clin Cancer Res 2004 Aug 1;10(15):5202-14.

(50) Bagnoli M, Ambrogi F, Pilotti S, Alberti P, Ditto A, Barbareschi M, Galligioni E, Biganzoli E, et al. c-FLIPL expression defines two ovarian cancer patient subsets and is a prognostic factor of adverse outcome. Endocr Relat Cancer 2009 Jun;16(2):443-53.

(51) Sonego M, Schiappacassi M, Lovisa S, Dall'Acqua A, Bagnoli M, Lovat F, Libra M, D'Andrea S, et al. Stathmin regulates mutant p53 stability and transcriptional activity in ovarian cancer. EMBO Mol Med 2013 May;5(5):707-22.

(52) Kang J, D'Andrea AD, Kozono D. A DNA repair pathway-focused score for prediction of outcomes in ovarian cancer treated with platinum-based chemotherapy. J Natl Cancer Inst 2012 May 2;104(9):670-81.

(53) Matei D, Fang F, Shen C, Schilder J, Arnold A, Zeng Y, Berry WA, Huang T, et al. Epigenetic resensitization to platinum in ovarian cancer. Cancer Res 2012 May 1;72(9):2197-205.

(54) Zhao Y, Butler EB, Tan M. Targeting cellular metabolism to improve cancer therapeutics. Cell Death Dis 2013;4:e532.

(55) Sabharwal SS, Schumacker PT. Mitochondrial ROS in cancer: initiators, amplifiers or an Achilles' heel? Nat Rev Cancer 2014 Oct 24;14(11):709-21.

(56) Singh S, Khan AR, Gupta AK. Role of glutathione in cancer pathophysiology and therapeutic interventions. J Exp Ther Oncol 2012;9(4):303-16.

(57) Glasauer A, Chandel NS. Targeting antioxidants for cancer therapy. Biochem Pharmacol 2014 Jul 28.

(58) Traverso N, Ricciarelli R, Nitti M, Marengo B, Furfaro AL, Pronzato MA, Marinari UM, Domenicotti C. Role of glutathione in cancer progression and chemoresistance. Oxid Med Cell Longev 2013;2013:972913.

(59) Gorrini C, Harris IS, Mak TW. Modulation of oxidative stress as an anticancer strategy. Nat Rev Drug Discov 2013 Dec;12(12):931-47.

(60) Meister A. Glutathione metabolism and its selective modification. J Biol Chem 1988 Nov 25;263(33):17205-8.

(61) Sies H. Glutathione and its role in cellular functions. Free Radic Biol Med 1999 Nov;27(9-10):916-21.

(62) Calvert P, Yao KS, Hamilton TC, O'Dwyer PJ. Clinical studies of reversal of drug resistance based on glutathione. Chem Biol Interact 1998 Apr 24;111-112:213-24.

(63) Estrela JM, Ortega A, Obrador E. Glutathione in cancer biology and therapy. Crit Rev Clin Lab Sci 2006;43(2):143-81.

(64) Godwin AK, Meister A, O'Dwyer PJ, Huang CS, Hamilton TC, Anderson ME. High resistance to cisplatin in human ovarian cancer cell lines is associated with marked increase of glutathione synthesis. Proc Natl Acad Sci U S A 1992 Apr 1;89(7):3070-4.

(65) Cossa G, Gatti L, Zunino F, Perego P. Strategies to improve the efficacy of platinum compounds. Curr Med Chem 2009;16(19):2355-65.

(66) Gamcsik MP, Kasibhatla MS, Teeter SD, Colvin OM. Glutathione levels in human tumors. Biomarkers 2012 Dec;17(8):671-91.

(67) Granata A, Nicoletti R, Tinaglia V, De CL, Pisanu ME, Ricci A, Podo F, Canevari S, et al. Choline kinase-alpha by regulating cell aggressiveness and drug sensitivity is a potential druggable target for ovarian cancer. Br J Cancer 2014 Jan 21;110(2):330-40.

(68) Chua BT, Gallego-Ortega D, Ramirez dM, Ullrich A, Lacal JC, Downward J. Regulation of Akt(ser473) phosphorylation by Choline kinase in breast carcinoma cells. Mol Cancer 2009;8:131.

(69) Yalcin A, Clem B, Makoni S, Clem A, Nelson K, Thornburg J, Siow D, Lane AN, et al. Selective inhibition of choline kinase simultaneously attenuates MAPK and PI3K/AKT signaling. Oncogene 2010 Jan 7;29(1):139-49.

(70) Banez-Coronel M, de Molina AR, Rodriguez-Gonzalez A, Sarmentero J, Ramos MA, Garcia-Cabezas MA, Garcia-Oroz L, Lacal JC. Choline kinase alpha depletion selectively kills tumoral cells. Curr Cancer Drug Targets 2008 Dec;8(8):709-19.

(71) Gruber J, See Too WC, Wong MT, Lavie A, McSorley T, Konrad M. Balance of human choline kinase isoforms is critical for cell cycle regulation: implications for the development of choline kinase-targeted cancer therapy. FEBS J 2012 Jun;279(11):1915-28.

(72) Rodriguez-Gonzalez A, Ramirez de MA, Fernandez F, Ramos MA, del Carmen NM, Campos J, Lacal JC. Inhibition of choline kinase as a

specific cytotoxic strategy in oncogene-transformed cells. Oncogene 2003 Dec 4;22(55):8803-12.

(73) Rodriguez-Gonzalez A, Ramirez de MA, Banez-Coronel M, Megias D, Lacal JC. Inhibition of choline kinase renders a highly selective cytotoxic effect in tumour cells through a mitochondrial independent mechanism. Int J Oncol 2005 Apr;26(4):999-1008.

(74) Fang X, Yu S, Bast RC, Liu S, Xu HJ, Hu SX, LaPushin R, Claret FX, et al. Mechanisms for lysophosphatidic acid-induced cytokine production in ovarian cancer cells. J Biol Chem 2004 Mar 5;279(10):9653-61.

(75) So J, Navari J, Wang FQ, Fishman DA. Lysophosphatidic acid enhances epithelial ovarian carcinoma invasion through the increased expression of interleukin-8. Gynecol Oncol 2004 Nov;95(2):314-22.

(76) Nilsson MB, Langley RR, Fidler IJ. Interleukin-6, secreted by human ovarian carcinoma cells, is a potent proangiogenic cytokine. Cancer Res 2005 Dec 1;65(23):10794-800.

(77) Aoki J, Inoue A, Okudaira S. Two pathways for lysophosphatidic acid production. Biochim Biophys Acta 2008 Sep;1781(9):513-8.

(78) Iorio E, Di VM, Spadaro F, Ramoni C, Lococo E, Carnevale R, Lenti L, Strom R, et al. Triacsin C inhibits the formation of 1H NMR-visible mobile lipids and lipid bodies in HuT 78 apoptotic cells. Biochim Biophys Acta 2003 Oct 20;1634(1-2):1-14.

(79) Roberts RZ, Morris AJ. Role of phosphatidic acid phosphatase 2a in uptake of extracellular lipid phosphate mediators. Biochim Biophys Acta 2000 Aug 24;1487(1):33-49.

(80) Rivera A, Mavila A, Bayless KJ, Davis GE, Maxwell SA. Cyclin A1 is a p53-induced gene that mediates apoptosis, G2/M arrest, and

mitotic catastrophe in renal, ovarian, and lung carcinoma cells. Cell Mol Life Sci 2006 Jun;63(12):1425-39.

(81) Mori N, Glunde K, Takagi T, Raman V, Bhujwalla ZM. Choline kinase down-regulation increases the effect of 5-fluorouracil in breast cancer cells. Cancer Res 2007 Dec 1;67(23):11284-90.

(82) Vander Heiden MG. Targeting cancer metabolism: a therapeutic window opens. Nat Rev Drug Discov 2011 Aug 31;10(9):671-84.

(83) Fong MY, McDunn J, Kakar SS. Identification of metabolites in the normal ovary and their transformation in primary and metastatic ovarian cancer. PLoS One 2011;6(5):e19963.

(84) Galluzzi L, Kepp O, Vander Heiden MG, Kroemer G. Metabolic targets for cancer therapy. Nat Rev Drug Discov 2013 Nov;12(11):829-46.

(85) Raj L, Ide T, Gurkar AU, Foley M, Schenone M, Li X, Tolliday NJ, Golub TR, et al. Selective killing of cancer cells by a small molecule targeting the stress response to ROS. Nature 2011 Jul 14;475(7355):231-4.

(86) Hernando E, Sarmentero-Estrada J, Koppie T, Belda-Iniesta C, Ramirez dM, V, Cejas P, Ozu C, Le C, et al. A critical role for choline kinase-alpha in the aggressiveness of bladder carcinomas. Oncogene 2009 Jul 2;28(26):2425-35.

(87) Moestue SA, Borgan E, Huuse EM, Lindholm EM, Sitter B, Borresen-Dale AL, Engebraaten O, Maelandsmo GM, et al. Distinct choline metabolic profiles are associated with differences in gene expression for basal-like and luminal-like breast cancer xenograft models. BMC Cancer 2010;10:433.

(88) Bowen NJ, Walker LD, Matyunina LV, Logani S, Totten KA, Benigno BB, McDonald JF. Gene expression profiling supports the hypothesis that human ovarian surface epithelia are multipotent and capable of serving as ovarian cancer initiating cells. BMC Med Genomics 2009;2:71.

(89) Mok SC, Bonome T, Vathipadiekal V, Bell A, Johnson ME, Wong KK, Park DC, Hao K, et al. A gene signature predictive for outcome in advanced ovarian cancer identifies a survival factor: microfibril-associated glycoprotein 2. Cancer Cell 2009 Dec 8;16(6):521-32.

(90) Bonome T, Levine DA, Shih J, Randonovich M, Pise-Masison CA, Bogomolniy F, Ozbun L, Brady J, et al. A gene signature predicting for survival in suboptimally debulked patients with ovarian cancer. Cancer Res 2008 Jul 1;68(13):5478-86.

(91) Anglesio MS, Arnold JM, George J, Tinker AV, Tothill R, Waddell N, Simms L, Locandro B, et al. Mutation of ERBB2 provides a novel alternative mechanism for the ubiquitous activation of RAS-MAPK in ovarian serous low malignant potential tumors. Mol Cancer Res 2008 Nov;6(11):1678-90.

(92) Berns EM, Bowtell DD. The changing view of high-grade serous ovarian cancer. Cancer Res 2012 Jun 1;72(11):2701-4.

(93) Bast RC, Jr., Hennessy B, Mills GB. The biology of ovarian cancer: new opportunities for translation. Nat Rev Cancer 2009 Jun;9(6):415-28.

(94) Tothill RW, Tinker AV, George J, Brown R, Fox SB, Lade S, Johnson DS, Trivett MK, et al. Novel molecular subtypes of serous and endometrioid ovarian cancer linked to clinical outcome. Clin Cancer Res 2008 Aug 15;14(16):5198-208.

(95) King ER, Tung CS, Tsang YT, Zu Z, Lok GT, Deavers MT, Malpica A, Wolf JK, et al. The anterior gradient homolog 3 (AGR3) gene is associated with differentiation and survival in ovarian cancer. Am J Surg Pathol 2011 Jun;35(6):904-12.

(96) Berchuck A, Iversen ES, Luo J, Clarke JP, Horne H, Levine DA, Boyd J, Alonso MA, et al. Microarray analysis of early stage serous ovarian cancers shows profiles predictive of favorable outcome. Clin Cancer Res 2009 Apr 1;15(7):2448-55.

Acknowledgements

I would like to thank many people who helped me during my graduate study. My dearest and most sincere appreciation goes to each of them:

- Dr. Delia Mezzanzanica, my supervisor, for her wonderful mentoring and huge support during my PhD project.
- Dr. Marina Bagnoli for her helpful deductions, suggestions and criticism.
- My husband Lorenzo for his infinite patience and unconditional love.
- My mother for her loving encouragements.
- Palumbo's family and Stefania, a part of family which doesn't make me feel alone.
- Barbara, Katia, Roberta e Valentina for their friendship and important motivation during these years.
- Katia e Alessandro for sharing these three years of PhD school.
- Alessandro for his technical assistance in the writing of the thesis.
- Patrizia for her help in bioinformatics analysis.

PART II

PUBLISHED PAPER

Alterations of choline phospholipid metabolism in ovarian cancer: study of the activity and expression of choline kinase as a prognostic value.

FULL PAPER

BJC

British Journal of Cancer (2014) 110, 330–340 | doi: 10.1038/bjc.2013.729

Keywords: choline kinase-alpha; phosphocholine; cancer metabolism; ovarian cancer; drug sensitivity

Choline kinase-alpha by regulating cell aggressiveness and drug sensitivity is a potential druggable target for ovarian cancer

A Granata[1], R Nicoletti[1], V Tinaglia[1], L De Cecco[2], M E Pisanu[3], A Ricci[3], F Podo[3], S Canevari[1,2], E Iorio[3], M Bagnoli[*,1,4] and D Mezzanzanica[*,1,4]

[1]*Unit of Molecular Therapies, Department of Experimental Oncology and Molecular Medicine, Fondazione IRCCS Istituto Nazionale dei Tumori, Via Amadeo 42, 20133 Milan, Italy;* [2]*Unit of Functional Genomics, Department of Experimental Oncology and Molecular Medicine, Fondazione IRCCS Istituto Nazionale dei Tumori, Via Amadeo 42, 20133 Milan, Italy and* [3]*Department of Cell Biology and Neurosciences, Istituto Superiore di Sanità, Viale Regina Elena 299, 00161 Rome, Italy*

Background: Aberrant choline metabolism has been proposed as a novel cancer hallmark. We recently showed that epithelial ovarian cancer (EOC) possesses an altered MRS-choline profile, characterised by increased phosphocholine (PCho) content to which mainly contribute over-expression and activation of choline kinase-alpha (ChoK-alpha).

Methods: To assess its biological relevance, ChoK-alpha expression was downmodulated by transient RNA interference in EOC *in vitro* models. Gene expression profiling by microarray analysis and functional analysis was performed to identify the pathway/functions perturbed in ChoK-alpha-silenced cells, then validated by *in vitro* experiments.

Results: In silenced cells, compared with control, we observed: (I) a significant reduction of both *CHKA* transcript and ChoK-alpha protein expression; (II) a dramatic, proportional drop in PCho content ranging from 60 to 71%, as revealed by ^{1}H-magnetic spectroscopy analysis; (III) a 35–36% of cell growth inhibition, with no evidences of apoptosis or modification of the main cellular survival signalling pathways; (IV) 476 differentially expressed genes, including genes related to lipid metabolism. Ingenuity pathway analysis identified cellular functions related to cell death and cellular proliferation and movement as the most perturbed. Accordingly, *CHKA*-silenced cells displayed a significant delay in wound repair, a reduced migration and invasion capability were also observed. Furthermore, although *CHKA* silencing did not directly induce cell death, a significant increase of sensitivity to platinum, paclitaxel and doxorubicin was observed even in a drug-resistant context.

Conclusion: We showed for the first time in EOC that *CHKA* downregulation significantly decreased the aggressive EOC cell behaviour also affecting cells' sensitivity to drug treatment. These observations open the way to further analysis for ChoK-alpha validation as a new EOC therapeutic target to be used alone or in combination with conventional drugs.

Altered metabolism has been recently linked to cancer development, progression and poor clinical outcome (Hanahan and Weinberg, 2011; Ward and Thompson, 2012). In the past years, the introduction of magnetic resonance spectroscopy (MRS) for tumour studies, helped to recognise activated phosphatidyl choline (PtdCho) metabolism as one emerging metabolic hallmark associated with oncogenesis and tumour progression (Podo, 1999; Podo *et al*, 2011).

Altered choline (Cho) metabolism is characterised by increase in total choline-(tCho) containing metabolites levels essentially due to intracellular pooling of phosphocholine (PCho) that is both a precursor and a breakdown product of PtdCho, one of the major

*Correspondence: Dr M Bagnoli; E-mail: marina.bagnoli@istitutotumori.mi.it or Dr D Mezzanzanica; E-mail: delia.mezzanzanica@istitutotumori.mi.it
[4]These authors contributed equally to this work.

Revised 23 October 2013; accepted 24 October 2013; published online 26 November 2013

components of cellular membranes, required for structural stability and cell proliferation (Podo, 1999; Vance and Vance, 2004; Podo *et al*, 2011). Among the multiple enzymes involved in both the biosynthetic and catabolic pathways leading to PtdCho synthesis (Ishidate, 1997), evidences grew to support choline kinase (ChoK) as also being rate limiting and regulatory in some circumstances, in particular in transformed cells (Aoyama *et al*, 2004). Choline kinas catalyses the phosphorylation of free Cho to PCho, and, in mammalian cells, only the alpha-isoform (synthesised by *CHKA* gene) has a central role in sustaining PtdCho biosynthesis, indeed ChoK-beta alone cannot compensate this activity (Wu *et al*, 2008). Choline kinase is an interesting enzyme at the crossroads of the main growth factor-triggered survival signalling pathways (Ras activation, PI3K signalling) and constitutively activated in some human tumour cells and tissues (see (Glunde *et al*, 2011a)). Furthermore, a large body of work in cancer cells suggests that ChoK-alpha expression and activity are directly associated not only with increased cancer cell proliferation but also with malignancy, making it a potential prognostic marker of some cancers, such as non-small-cell lung cancer (Ramirez *et al*, 2007) as well as a potential novel target for image-guided cancer therapy (Glunde *et al*, 2011b). Addiction of cancer cell survival to metabolic changes opened new therapeutic windows suggesting the possibility of targeting specific metabolic alterations (Vander Heiden, 2011). The choline phenotype, characterised by increased ChoK-alpha activity and expression, renders this enzyme an attractive new therapeutic target. The feasibility of ChoK-alpha inhibition as antitumoural therapy is being pursued through the development of chemical inhibitors of its enzymatic activity (Hernandez-Alcoceba *et al*, 1999; Rodriguez-Gonzalez *et al*, 2003; Clem *et al*, 2011) and by silencing *CHKA* expression by RNA interference (Glunde *et al*, 2005; Krishnamachary *et al*, 2009).

Epithelial ovarian cancer (EOC) remains one of the most challenging areas of cancer research. In spite of progress in diagnosis and treatment, EOC incidence and mortality rates have remained unchanged over the last 30 years, mainly because of late diagnosis and disease recurrence with development of chemoresistance (Vaughan *et al*, 2011), with a resulting 5-year overall survival around 30% (Siegel *et al*, 2013). Considering the great molecular heterogeneity of the disease (Kurman and Shih, 2010), and, in the attempt to design and develop more sensitive diagnostic tools as well as novel treatment approaches, a deeper understanding of critical molecules and pathways specifically involved in EOC tumourigenesis and progression is needed (Konstantinopoulos *et al*, 2008; Chon and Lancaster, 2011; Vaughan *et al*, 2011). We previously reported that alteration of the tCho MRS profile, with a characteristic increase in the content of intracellular PCho, is a common feature during the progression from non-tumoural or immortalised ovarian cells to EOC cells (Iorio *et al*, 2005, 2013). By a combined biochemical, functional and genomic approach, we recently showed that these alterations are sustained by activation of enzymes involved in PtdCho biosynthetic as well as catabolic pathways: ChoK-alpha and PtdCho-specific phospholipase C (PtdCho-plc) (Spadaro *et al*, 2008; Iorio *et al*, 2010) strongly suggesting a main role for ChoK-alpha in sustaining the PCho increase in EOC cells as well as in EOC growth and progression.

Aiming to assess the biological relevance of Chok-alpha expression and activity in EOC cells, here we specifically silenced *CHKA* gene expression by transient RNA interference in two EOC cell lines and evaluated the main biological effects related to alterations of tCho-metabolic profiles, global gene expression as well as general cancer cell behaviour.

MATERIALS AND METHODS

Cell lines. INTOV11 (obtained in our laboratory from a serous high-grade EOC) and SKOV3 (from ATCC) cell lines were maintained in RPMI 1640 (Sigma, St Louis, MO, USA) supplemented with 10% (v/v) FCS and 2 mmol l^{-1} L-glutamine (Sigma). Normal ovary cell lines (I64-hTERT) immortalised with hTERT obtained as described (Iorio *et al*, 2005) were maintained in 199-MCDB105 medium (Sigma) supplemented with 10% FCS, 2 mmol l^{-1}-glutamine, 200 μg ml^{-1} G418. Cells were maintained at 37 °C in a humidified incubator under 5% CO_2. Cells were genotyped at the fragment analysis facility of our Institute, using Stem Elite ID System (Promega, Madison, WI, USA), according to manufactures instructions and ATCC guidelines. Cells were routinely confirmed to be mycoplasma-free using the Hoechst staining and MycoAlert Mycoplasma Detection Kit (Lonza, Walkersville, MD, USA).

Transient ChoK silencing. A total of 180 000 cells per well were seeded on six-well plates and transfected with a final concentration of 40 nM specific small interfering RNA (siRNA) against *CHKA*, NM_212469 and NM_001277 (siGENOME Smart Pool, Thermo Scientific, Dharmacon Inc., Chicago, IL, USA), whereas a non-targeting siRNA was used as control (siGENOME non-targeting siRNA no. 2, Dharmacon). Transfection was carried out using Lipofectamine2000 (Invitrogen, Life Technologies, Carlsbad, CA, USA), according to the manufacturers' protocol. The efficacy of *CHKA* silencing as well as its related biological effects were assessed at day 3 (72 h) after 7 h transfection, unless otherwise specified.

FlexiTube Gene Solution (Qiagen, Hilden, Germany) siRNA pool targeting *CHKA* (NM_001277), together with their relative negative controls siRNA (Qiagen), were used in the experiments aimed to exclude off-target non-specific effects, applying the same transfection protocols and siRNA concentration.

Nuclear magnetic resonance spectroscopy. Cells grown to 60–70% confluence were trypsinised 24 h after culture medium change, counted and assessed for cell viability (80–90%) and membrane integrity by trypan blue staining. Cell aqueous extracts (from 5 to 10×10^6 cells per sample) were prepared in EtOH 70% according to an established protocol (Iorio *et al*, 2010). Briefly, after ultrasonication at 20 kHz, supernatants were lyophilised twice and the residue resuspended in 0.7 ml D_2O (Sigma-Aldrich) containing 0.1 mM 3-(trimethylsilyl)-propionic-2,2,3,3-d4 acid sodium salt as internal chemical shift and peak area standard. High-resolution NMR experiments (25 °C) were performed at 9.4 T (Bruker AVANCE spectrometer, Karlsruhe, Germany). Proton nuclear magnetic resonance spectroscopy spectra of cell extracts were acquired using 90° flip angle, 30 s repetition time, 32 K time domain data points and 128 transients (Iorio *et al*, 2005).

Western blotting. Western blot analysis was performed as previously described (Iorio *et al*, 2010) by separating proteins (30 μg) on a 4–12% SDS–PAGE gel (Invitrogen, Life Technologies). For primary antibodies used see Supplementary Materials. Blots were acquired with a Bio-Rad apparatus using ChemiDoc XRS (Bio-Rad Laboratories Srl) and analysed using Quantity One software (Bio-Rad, Hercules, CA, USA). For densitometric analysis, protein levels were normalised to β-actin. Relative percentage of expression reported is expressed respective to control oligo-treated cells, set to 100%.

Quantitative Real-Time PCR. Total RNA was extracted from EOC cell lines using the RNA Spin Mini Isolation Kit (GE Healthcare Europe GmbH) following the manufacturer's protocol. Complementary DNA was generated from 2 μg of RNA using High-Capacity cDNA Archive Kit (Applied Biosystems-Life Technologies, Carlsbad, CA, USA), and RT-qPCR was carried out in triplicate using the 7900 HT FAST Real-Time PCR System (Applied Biosystems-Life Technologies). Specific probes are indicated in Supplementary Materials. The ΔΔCT method was used to determine the quantity of the target sequences. In all

Alterations of choline phospholipid metabolism in ovarian cancer: study of the activity and expression of choline kinase as a prognostic value.

RT-qPCR experiments, *GAPDH* was amplified as endogenous control and I64-hTERT cells were used as calibrator. Analyses were performed using SDS software 2.2.2 (Applied Biosystems-Life Technologies).

Proliferation and drug treatment assays. Cells were seeded in triplicates at 1×10^5 per well on 12-well plates. After transfection, proliferation was assessed at each time point by Trypan Blue exclusion assay using Countess automated cell counter (Invitrogen, Life Technologies). Cell viability was evaluated as percentage of alive cells in the total cell population. For cytotoxicity assays, the day after transfection 5000 cells per well were seeded in 96-well flat-bottom plates and exposed for 7 h to cisplatinum (DDP) (TEVA Italia s.r.l, Milan, Italy) at serial dilution starting from 1×10^{-4} to 3×10^{-7} M, or doxorubicin hydrochloride (Pfizer Italia s.r.l, Rome, Italy) at serial dilution starting from 1×10^{-4} to 1×10^{-7} M, and for 48 h to Paclitaxel (Sigma) at serial dilution starting from 2.5 to 0.016 nM. The effects of DDP treatment on cell proliferation were assessed 48 h later by Sulforhodamine B (SRB) assay as described (Bagnoli *et al*, 2011). Optical density was measured at 550 nm in a microplate reader (Bio-Rad model 550). The effects of Doxorubicin (assessed 48 h after drug treatment) and Paclitaxel were measured using a CellTiter-GLO luminescent cell viability assay performed according to the manufacturer's instructions (Promega).

Cell cycle analysis. Seventy-two hours post transfection, cells were pulsed with 10 μM 5′-bromo-2′-deoxyuridine (BrdU) for 1 h at 37 °C, collected and serially washed in PBS. Following fixing with 70% ethanol, cells were processed using BrdU Labelling and detection kit (Roche Diagnostic Corp. Indianapolis, IN, USA) according to manufacturer's protocol. Samples were double-stained by incubation with 5 μg ml^{-1} propidium iodide (Sigma) and 0.5 mg ml^{-1} RNAse (Sigma) for 30 min at 4 °C in the dark, then they were analysed with FACSCanto (Becton–Dickinson, Franklin Lakes, NJ, USA) and the data were processed using FlowJo 7.6.4 Analysis Software (Becton–Dickinson).

Gene expression and Bioinformatic analysis. Total RNA was isolated as described from triplicate cultures of *CHKA*-silenced and control cells of both EOC cellular models. Five hundred nanograms of quality-checked (Agilent BioAnalyzer, Agilent Technologies Italia, SpA, Milan, Italy) RNA were analysed for global gene expression profiling using HumanHT12_v3 BeadChips (Illumina Inc., San Diego, CA, USA) microarrays and the Illumina BeadArray Reader. Data were collected and analysed using the supplied scanner software and the BeadStudio Version 3 software package. Following hybridisation quality check, the data set was normalised using quantile algorithm. The expression profiles of the 12 samples have been deposited in NCBI's Gene Expression Omnibus (GEO) with GSE accession number GSE39943.

We used BRB Array Tool (v4.2.1; http://linus.nci.nih.gov/BRB-ArrayTools.html) to identify the 18 308 genes that crossed the threshold of detection *P*-value ⩽0.05 among all the samples and to derive by class comparison analysis (silenced *vs* control cells) the list of 476 differentially expressed genes with *P*-value<0.01 and FDR <0.25. For genes identified by multiple probesets, the probeset with the best-performing FDR was selected.

A data set consisting of the 476 differentially expressed genes was imported into the Ingenuity Pathway Analysis Tool (IPA Tool; IngenuitySystems, Redwood City, CA, USA; http://www.ingenuity.com) based on the Ingenuity Pathway Knowledge Base, derived from known and published genes interactions and functions. Differentially expressed genes are mapped into genetic networks that are ranked according to the number of significantly expressed genes they contain (focus molecules).

Bioplex analysis. Triplicate culture supernatants, from both EOC silenced and control cells, were collected 72 h post transfection by centrifugation at 1500 r.p.m. for 10 min. A multiplex biometric ELISA-based immunoassay, containing dyed microspheres conjugated to monoclonal antibodies specific for IL6 and IL8 was used according to the manufacturer's instructions (Bioplex, Bio-Rad Lab Inc.). Cytokines quantifications, referred to a standard curve, were determined using a Bio-Plex array reader (Luminex, Austin, TX, USA) with software provided by the manufacturer (Bio-Plex Manager Software).

Immunofluorescence microscopy. Cells were fixed in 4% (w/v) paraformaldehyde in PBS for 20 min at room temperature, washed twice with PBS and permeabilised for 10 min at room temperature with 0.1% Triton X-100 (Sigma) in PBS. After rinsing twice in PBS-0.1% Tween (v/v), cells were incubated with Alexa-488 conjugated phalloidin (Invitrogen, Life Technologies) (1 : 150) in PBS with 1% BSA for 1 h to visualise F-actin. After washing twice in PBS-0.1% Tween slides were mounted with ProLong Gold antifade reagent with DAPI (Invitrogen, Life Technologies) for nuclei staining. Images were acquired using a Nikon Eclipse Te-2000 phase-contrast microscope.

Wound-healing assay. A scratch was made with a micropipette tip across a confluent monolayer of 2.5×10^5 transfected cells, seeded directly in 24-well plates or on glass coverslip when assayed by immunofluorescence. Cells were then incubated in serum-free culture medium after removing floating cells. Wound healing was visualised by comparing photographs taken at the time of scratch and 24, 48 and 72 h later, by a Nikon Eclipse Te-2000 inverted microscope. The distance travelled by the cells was the wound width at each times of observation subtracted from the wound width at time 0. The values obtained were then expressed as percentage of migration, setting the gap width at t0 as 100%. The assay was also performed in presence of Actinomycin D (Sigma) at 2 ng ml^{-1} concentration that we observe to inhibit cell proliferation without inducing cell death.

Migration assay. To account for methodological variability, migration assays were performed using two assays both based on the Boyden chamber principle but having different detection methods: 24-well Transwell chamber system (Costar Corning Inc., Corning, NY, USA) and 24-Well Fluorimetric Cell Migration Assay (Merck Millipore, Billerica, MA, USA).

For the first assay, 1.5×10^5 transfected cells were seeded in the upper chamber in 0.3 ml serum-free culture media. Media supplemented with 10% fetal bovine serum was placed in the bottom well in a volume of 0.7 ml (used as a chemoattractant). After incubation for 24 h at 37 °C in an atmosphere containing 5% CO2, migrated cells on the lower surface were stained with SRB. Migration was quantified using Odyssey Infrared laser scanner (Li-Cor Biosciences, Lincoln, NE, USA) at Infrared wavelength of 700 nm, after removing the noninvading cells on the upper side of the membrane with cotton swabs. For fluorimetric assay, transfected cells were seeded in the upper chamber at 5×10^5 cells/ml in 0.3 ml serum-free culture media. Media supplemented with 10% fetal bovine serum was placed in the bottom well in a volume of 0.5 ml (used as a chemoattractant). After incubation for 24 h at 37 °C in an atmosphere containing 5% CO2, assay was performed according to the manufacturer's instructions (Merck Millipore). The migrating cells were determined by fluorescence and reported as relative fluorescence units (RFUs). The assay was also carried out by adding 2 ng ml^{-1} of Actinomycin D (Sigma).

Cell invasion Assay. Cell invasion was tested using a BD BioCoat Matrigel Invasion Chamber (Cat no. 354480 Becton–Dickinson). The inserts were transferred into the wells containing serum-free medium. Then, cells were harvested 72 h after transfection and resuspended in fresh medium were added at a density of 5×10^4 cells per well. Cell invasion into the Matrigel was determined after 22 h of culture at 37 °C. The membrane with invading cells was

fixed with absolute methanol and stained with 1% crystal violet in methanol. Invasion was quantified using Odyssey Infrared laser scanner (Li-Cor Biosciences) at Infrared wavelength of 700 nm, after removing the noninvading cells on the upper side of the membrane with cotton swabs.

Statistical analysis. Data were analysed using Prism GraphPad Software Version 5. Statistical significance of differences was determined by one-way ANOVA or by Student's *t*-test, as specified. Differences were considered significant at $P<0.05$. Asterisks in all figures denote a statistically significant difference in comparison with the relative control $^{*}P<0.05$; $^{**}P<0.01$; $^{***}P<0.001$. Data reported are the mean ± s.d. of at least three independent experiments unless otherwise indicated.

RESULTS

Transient CHKA silencing drastically reduces ChoK-alpha expression and activity. Choline kinase-alpha expression was inhibited by specific transient RNA interference in two EOC cell lines, INTOV11 and SKOV3, with known ChoK-alpha expression and overactivation (see (Iorio *et al*, 2005, 2010) for SKOV3 and Supplementary Figure 1 for INTOV11). Silencing efficacy was evaluated 72 h after transfection both at transcript and protein level. We obtained a significant reduction of 68 ± 12% and 75 ± 10.7% of *CHKA* mRNA transcript in si*CHKA*-INTOV11 and si*CHKA*-SKOV3, respectively, as compared with their relative control (Figure 1A). A drastic inhibitory effect of si*CHKA* was observed also at the protein level (Figure 1A lower panel), where the densitometric analysis showed a consistent and significant protein downmodulation of 83 ± 11% and 80 ± 3.5% on INTOV11 and SKOV3 cell lines, respectively ($P<0.01$). To confirm the specificity of our siRNA pool as regard to the ChoK isoform silenced, we analysed the ChoK-beta isoform mRNA expression levels in the *CHKA*-silenced cells. In both *CHKA*-silenced EOC cell lines, levels of *CHKB* transcript remained unchanged as compared with the control (Figure 1B).

Proton magnetic resonance spectroscopy spectra on cellular ethanolic extracts revealed in both si*CHKA*-cell lines an overall reduction of PCho content as a consequence of *CHKA* silencing in all the performed experiments (two representative examples are in Figure 1C). The protein downmodulation (inset of Figure 1C, lower panel), as an indirect measure of ChoK-alpha activity, reflected the decrease in PCho content as shown in expanded regions of the corresponding ^{1}H-MRS spectra profiles. Despite the biological variability and the spread due to deconvolution analyses, we observed consistent decreases of 60.4 ± 9.7 and 70.8 ± 10.9% in the PCho content of silenced INTOV11 and SKOV3 cells, respectively. Accordingly, the overall tCho contents also decreased (41.4 ± 21.4% and 44 ± 26.5% in silenced INTOV11 and SKOV3 cells, respectively). Glycerophosphocholine absolute concentration, although highly variable, was not significantly changed by *CHKA* knockdown being 3.7 ± 4.0 nmol per 10^{8}cells in silenced SKOV3 cells compared with 0.8 ± 0.6 nmol per 10^{8}cells in the corresponding controls. The slight (if any) increase of GPC in silenced cells is in agreement with a similar observation previously reported for ChoK-alpha depleted MD-MBA-231 breast cancer cells (Glunde *et al*, 2005) and it could be due to lipases' activation, associated with neutral lipid accumulation particularly seen in breast and ovary carcinoma. No changes were observed in GPC in CHKA-silenced INTOV11 cells compared with their controls (1.8 ± 2.2 *vs* 1.8 ± 1.4 nmol per 10^{8}cells). Similar results were obtained for free choline, whose mean levels were maintained at 2 ± 1 nmol per 10^{8}cells in all experiments.

Choline kinase-alpha downregulation inhibits cell proliferation without affecting survival signalling pathways. Kinetics of cell proliferation after transfection showed a cell growth inhibition in si*CHKA* cells already detectable at 24 h and with a significant 35% reduction at 72 h in both models (Figure 2A). No relevant changes in cell viability were observed between si*CHKA* and control cells, being >95% cells viable in all analysed models, whereas, a 35–38% reduction in the S-phase BrdU incorporation, proportional to growth inhibition, was determined in both siCHKA cells. A representative experiment is shown in Figure 2B. Analysis of

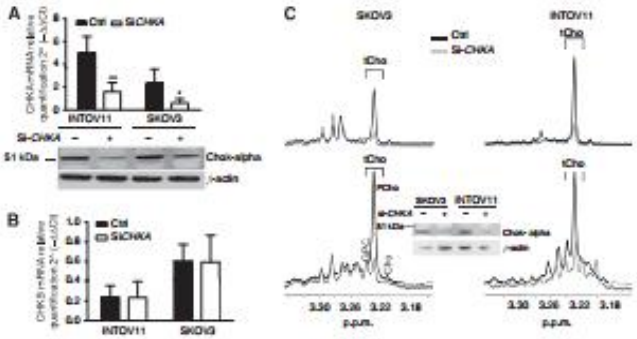

Figure1. Transient *CHKA* silencing efficiently downmodulates ChoK-alpha and intracellular PCho content in EOC cell lines. (A): *CHKA* silencing was confirmed at mRNA (RT-qPCR, upper panel; data are the mean ± s.d. of five independent experiments) and protein expression level (lower panel: western blotting of a representative experiment is reported). (B): RT-qPCR for ChoK β-isoform. Data are the mean ± s.d. of five independent experiments. GAPDH was amplified as endogenous control and I64-hTERT cells preparations were used as calibrator. (C): Representative examples of alterations induced by si*CHKA* on the ^{1}H-MRS tCho profile and its PCho component. Black lines: control cells; grey lines: silenced cells. Inset in lower panel: western blot of control and siCHKA EOC cells probed with specific antibody to ChoK-alpha. GPC, glycerophosphocholine; PCho, phosphocholine; tCho, total choline-containing compounds. The PCho/tCho ratio was 0.75 ± 0.20 in both cell types before silencing.

Alterations of choline phospholipid metabolism in ovarian cancer: study of the activity and expression of choline kinase as a prognostic value.

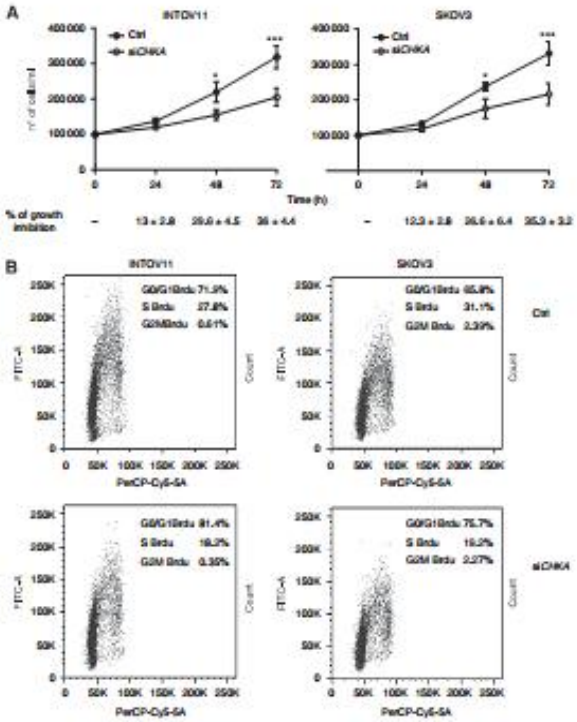

Figure 2. Cell proliferation upon *CHKA* silencing. (A): Proliferation curves. Viable cells were counted 24, 48 and 72 h post-transfection. Mean percentage of growth inhibition of *CHKA*-silenced *vs* control cells is reported below. (B): Representative experiment of BrdU incorporation at 72 h after transfection.

cell cycle also showed a slight G1 cell-cycle arrest in silenced cells compared with controls (12 ± 4% in both models). Cells with hypodiploid DNA content, suggestive of activation of apoptotic signalling, were not observed (data not shown).

To assess the specific biological impact in EOC cells lines, *CHKA* silencing was performed also on the non-tumoural ovarian cell line 184-hTERT (Iorio *et al*, 2005). siCHKA transfection in 184-hTERT decreased ChoK-alpha expression at both mRNA and protein levels (Supplementary Figure 2A and B) and dropped cellular PCho content (Supplementary Figure 2C). It has to be noted that the basal level of PCho in 184-hTERT is 2.3 ± 1.3 nmol per 10^7 cells, consistent with our previously published data (Iorio *et al*, 2005) and significantly lower than that measured in EOC. *CHKA* silencing induced a consistent decrease in PCho content. However, no significant effects on cell proliferation were observed in the non-tumoural cell line 184-hTERT (Supplementary Figure 2D) in spite of a cell turnover comparable to EOC cells (Figure 2A and Supplementary Figure 2D), thus confirming that ChoK-alpha sustains the cholinic phenotype only in EOC cells.

Given the effects on cell proliferation and the data available in literature for cancer others than ovary (Yalcin *et al*, 2010; Clem *et al*, 2011) reporting a positive feed-back signalling loop existing among ChoK-alpha and the main cellular survival signalling pathways, we evaluated the effects of *CHKA* silencing on AKT and MAPK activation immediately after siRNA transfection and at 24–72 h of relapse. No consistent differences of phosphorylation levels of pAkt (S473) and pMAPK (p44-42) or in total Akt and ERK1/2 protein levels were observed in both *CHKA*-silenced cells compared with controls (Supplementary Figure 3).

Modulation of gene profiling associated to CHKA silencing. As the biological outcomes observed in siCHKA EOC cell lines were not super imposable to features described in other tumour models, we investigated alteration of global gene expression profile upon *CHKA* silencing to possibly identify the main pathways affected.

By class comparison analysis of INTOV11- and SKOV3-*CHKA* silenced *vs* control cells, we identified 476 differentially expressed genes in *CHKA* silenced as compared with control cells, 252 of them being downregulated (Supplementary Table 1). Importantly, *CHKB* gene was not included among the modulated genes thus confirming the data obtained by RT-qPCR (see Figure 1B). Furthermore, none of the genes associated to the biosynthetic Kennedy's Pathway resulted differentially expressed between *CHKA*-silenced and control cells apart from a weak decrease (0.8-fold change in expression, FDR = 0.21 and $P = 0.0049$) of the *GDPD5* gene, involved in the catabolic pathway leading to Choline

Table 1. List of the top 15 differentially up or downregulated genes following CHKA silencing

Gene symbol	Parametric P-value	FDR[a]	Geometric mean of intensities[b]	
CHKA	4.60E-06	0.0421	0.44	Downregulated genes
CCNA1	2.60E-06	0.0421	0.48	
KRT80	0.0009081	0.128	0.51	
IL6	0.0046555	0.213	0.51	
TAGLN	0.0064673	0.236	0.53	
IL8	9.30E-06	0.0467	0.54	
AKAP12	0.0009146	0.145	0.56	
H19	3.29E-05	0.106	0.59	
IDH2	5.34E-05	0.106	0.59	
TNFRSF25	0.0011795	0.148	0.61	
KRT7	0.0016046	0.163	0.61	
LIMK1	0.0054187	0.222	0.61	
MAD2L1	8.14E-05	0.124	0.62	
SEC23A	0.0001111	0.124	0.62	
SNX25	0.0007806	0.137	0.62	
ARFIP1	0.0009437	0.146	1.57	Upregulated genes
CASB	0.0022191	0.169	1.57	
LAMC1	0.0003072	0.124	1.59	
C5	0.0013041	0.155	1.6	
PRSS35	0.0004709	0.128	1.62	
SPTLC3	0.0003098	0.124	1.63	
UBE2E3	4.63E-05	0.106	1.64	
BCMO1	0.0001368	0.124	1.64	
ID3	0.0032983	0.19	1.67	
PPAP2A	0.0001578	0.124	1.71	
LRRC31	0.0001612	0.124	1.72	
RTN4	3.78E-05	0.106	1.76	
FXYD2	0.0025975	0.175	1.84	
TNFRSF11B	0.0001958	0.124	1.85	
ACSM3	4.54E-05	0.106	2.11	

[a]FDR, false discovery rate.
[b]For each specified probe represents the ratio between the mean intensity of the siCHKA vs control cells.

formation (Supplementary Table 1). The 15 genes most consistently up or downregulated following *CHKA* silencing are reported in Table 1. Among the most relevant co-repressed genes, we focused our attention on Cyclin A1 (CCNA1), related to regulation of cell cycle progression and cytokines genes (IL6 and IL8) related to inflammation and EOC aggressiveness. Among the most upregulated genes, we identified as gene of interest Acyl-CoA synthetase (ASCM3) needed for fatty acid synthesis, phosphatidic acid phosphatase 2A (PPAP2A), a member of the phosphatidic acid phosphatase (PAP) family and osteoprotegerin (TNFRSF11B; OPG), a soluble decoy receptor for receptor activator of nuclear factor-kappa B ligand (RANKL).

Microarray data showing differential expression of selected genes were biologically validated by three independent silencing experiments for each cell line. ASCM3 and PPAP2A were confirmed to be upmodulated in both *CHKA*-silenced cell lines by RT-qPCR. Osteoprotegerin instead was significantly upregulated only in INTOV11 *CHKA*-silenced cells, whereas only a trend was observed in the SKOV3 model ($P = 0.07$) (Figure 3A). Considering the co-repressed genes, significant downregulation of CCNA1 was confirmed in both SKOV3- and INTOV11-silenced cells (Figure 3B). Cyclin A1 downmodulation was evident also at the protein level with a 25% and 77% reduction in SKOV3 and INTOV11 cells, respectively (Supplementary Figure 4). Downmodulation of IL6 resulted statistically significant only in INTOV11-silenced cell line. On the contrary, downmodulation of IL8 was statistically significant only in SKOV3 with only a trend for the INTOV11 model ($P = 0.08$). Evaluation of IL6 and IL8 cytokine content in the conditioned medium of transfected cells showed a decrease in the release generally proportional to the efficacy of *CHKA* silencing. The modulation was more consistent in INTOV11 *CHKA*-silenced cells as we observed 86% reduction for IL6 and 66% for IL8 release in spite of the low-level of the cytokine production, whereas in the si*CHKA*-SKOV3 model, we observed a 70% of inhibition of IL6 release and only a slight reduction of IL8 release (10% of decrease). To exclude that these observations could be due to nonspecific off-target effects, *CHKA*-specific silencing and co-modulation of selected genes were validated by RT-qPCR using a second independent *CHKA*-specific siRNA pool (Supplementary Figure 5A and 5B).

CHKA silencing modulates cell functions related to cell movement and affects drug sensitivity. To derive the possibly deregulated pathways a data set consisting of the 476 differentially expressed genes was analysed with IPA Tool, revealing 25 significantly altered pathways (the top 10 networks, all with a score greater than 20, are reported in Supplementary Table 2). Significantly, the network identified with the highest score included *CHKA* among the focus molecules. The biological functions associated to this network were related to cell morphology, cellular assembly and organisation, cellular function and maintenance (See Figure 4 for details).

When exploring the molecular and cellular functions affected by *CHKA* silencing, the functions named as '*Cell Death*', '*Cellular Growth and Proliferation*' and '*Cellular Movement*' were found as the most significantly perturbed (Supplementary Figure 6A). Interestingly, as shown by the z-score heatmaps (Supplementary Figure 6B), *Cellular Movement* and *Cellular Growth and Proliferation* functions were predicted to be decreased, whereas *Cell Death* function was predicted to be increased in *CHKA*-silenced cells as compared with their control. Indeed, following *CHKA* knockdown, a decreased proliferation was evident (see Figure 2B) and, as expected, a clear delay in wound closure was observed in both *CHKA*-silencing cell lines using the classic scratch assay (Figure 5A). As the significantly reduced cell motility observed in *CHKA*-silenced cells as compared with their control cells could be partially due to a reduced proliferation capacity, to possibly exclude effects of CHKA silencing related to proliferation rather than migration, scratch assay was also performed in the presence of Actinomycin D obtaining comparable inhibitory effects. Indeed, we observed an inhibition of wound repair of 46% ± 5.6 and 45% ± 5.4 in INTOV11 and SKOV3 CHKA-silenced cell line as compared with their relative control and of 37% ± 2.7 and 37% ± 2.9 in the presence of Actinomycin D in the same cell lines; thus suggesting that results observed were mostly related to alterations of the migratory rather than proliferative phenotype. In addition, CHKA-silenced cells showed a dramatic rearrangement of F-actin fibres with a significant reduction of oriented actin stress fibres and focal adhesion sites (Figure 5B, red arrows), further suggesting that CHKA-silenced cells are less prone to movement and migration as compared with their control cells.

Alterations of choline phospholipid metabolism in ovarian cancer: study of the activity and expression of choline kinase as a prognostic value.

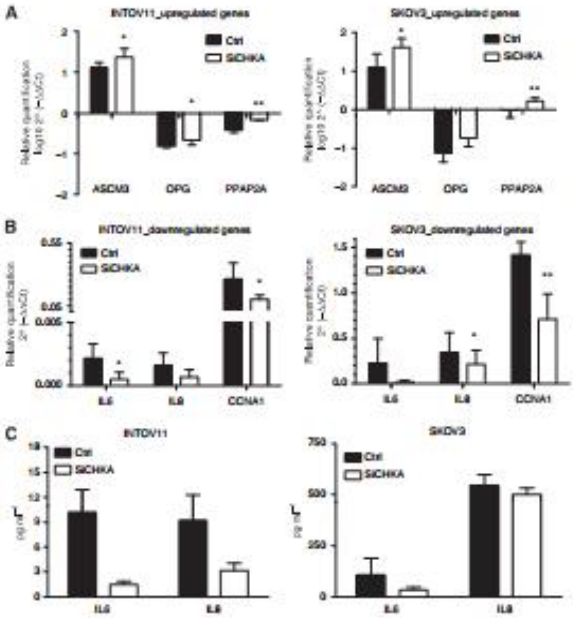

Figure 3. Validation of genes perturbed by CHKA silencing. RT-qPCR of selected up (A) and down (B) modulated genes in CHKA-silenced EOC cell lines. GAPDH was amplified as endogenous control, and I64-hTERT cells preparations were used as calibrator. The mean of five independent experiments is reported. (C) Evaluation of IL6 and IL8 release by bioplex assay on conditioned media from both EOC cell lines. Data are the mean ± s.d. of three independent experiments.

To confirm these observations, we then assessed migration capability by using two assays both based on the Boyden chamber principle but having different detection methods to account for methodological variability and in presence or absence of Actinomycin D to exclude bias related to proliferative effects. Results obtained (see Figure 6A and B) showed a 43–47% inhibition of migration in INTOV11 and SKOV3 CHKA-silenced cells as compared with their relative controls when migration was detected by Fluorimetric assay; comparable results were obtained when Actinomycin D was added to culture medium (Figure 6A). In addition, a 37–65% inhibition of migration was detected in INTOV11 and SKOV3 cells as compared with their relative controls when migration was detected by quantification of SRB staining (Figure 6B).

Furthermore, *CHKA*-silenced cells showed a significantly reduced (72% and 79% in silenced INTOV11 and SKOV3, respectively) invasive potential through Matrigel as compared with their control cells (Figure 6C).

Our observations on *CHKA*-silenced cells did not show any direct effect of ChoK downregulation on cell death. However, to possibly confirm the IPA-predicted modulation, we evaluated sensitivity to drug treatments upon *CHKA* silencing. As compared with their relative untreated cells, we observed a significant increase of sensitivity to DDP treatment associated with *CHKA* silencing in both INTOV11- and in the DDP-resistant SKOV3 cell lines (Figure 7A). CHKA-silenced cells showed also a significantly increased sensitivity to Doxorubicin and Paclitaxel (Figure 7B and C), two drugs currently used in EOC treatment.

DISCUSSION

Cancer cells are able to activate signalling pathways that change their metabolism. Aberrant choline metabolism, characterised by an increased intracellular PCho pooling mainly related to increased ChoK activity, is a fairly new metabolic hallmark able to discriminate cancer cells having a cholinic phenotype (Glunde *et al*, 2011a). Our recent works showed an increased expression and over activation of ChoK-alpha in EOC cells that we already characterised for their increased PCho content. Here we show for the first time in EOC that, by using siRNA specific for ChoK-alpha, the expression and the activity of the enzyme can be down-modulated in two models of EOC affecting cell behaviour and sensitivity to drug treatment. The biological effects were evident only in EOC cell lines and not in the non-tumoural ovarian I64-hTERT cell line in spite of the comparable cellular turnover of the two cellular models (Iorio *et al*, 2005 and present results). Our results, in agreement with those by Mori *et al* (2013) in other type of non-tumoural cells (i.e., endothelial), further support the concept of ChoK-alpha as the major player in supporting cholinic phenotype only in tumour cells (Glunde *et al*, 2011a). All together these observations strongly suggest a possible reliance of EOC cells survival on the abnormal ChoK-alpha activity and expression (Iorio *et al*, 2005, 2010; Spadaro *et al*, 2008; Podo *et al*, 2011) that if verified, could be successfully exploited for therapeutic purpose. Epithelial ovarian cancer conventional approaches (aggressive debulking surgery followed by platinum-taxane chemotherapy)

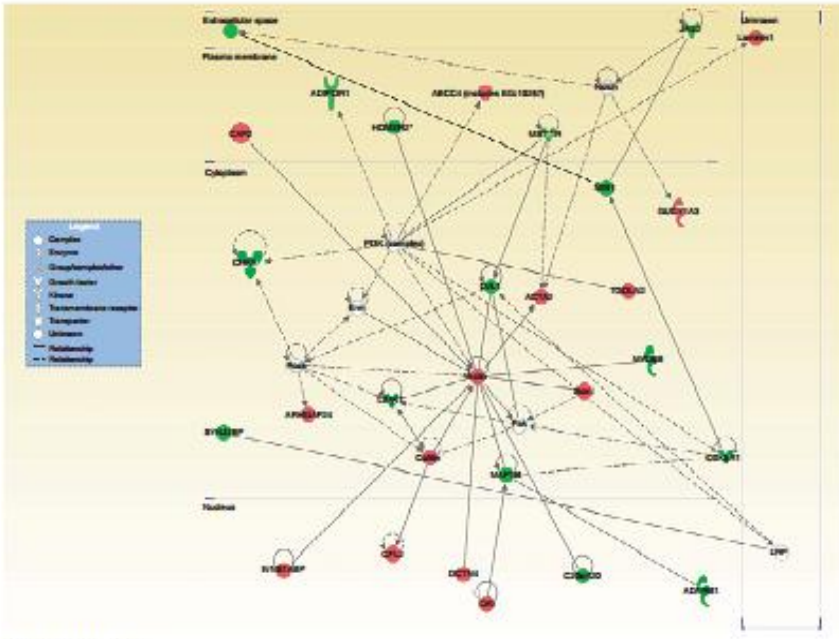

Molecules of the network:
ABCC4, ACTA2, Actin, ADARB1, ADIPOR1, ARHGAP24, C20orf20, CAP2, CDK5R1, CFL2, CHKA, Collin, DCTN4, DLL3, DVL1, Erm, GUCY1A3, HOMER2, IVNS1ABP, JAG2, Laminin1, LIMK1, LRP, MAP1B, MIB1, MST1R, MYO5B, Notch, Pak, PI3K(complex), GKL Rock, SGN, SYNJ2BP, TGOLN2

Figure 4. Graphical representation of the most highly rated network as obtained by IPA. The defined statistically significant genes are shaded and the intensity of the shading shows the degree of relative modulation. Red and green shading are for up or downregulated genes in *CHKA*-silenced cells. A solid line represents a direct interaction between the two gene products and a dotted line means there is an indirect interaction. All molecules participating to the network are listed below. The focus molecules of the network significantly affected by CHKA silencing are reported in red or green colour, depending on their relative modulation as above described.

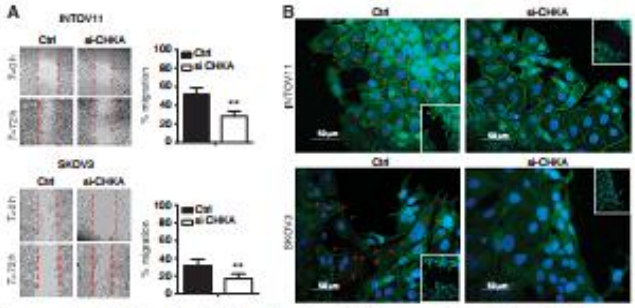

Figure 5. CHKA silencing regulates cell migration and induces alteration in F-actin organisation. (A): Wound-healing assay: photographs of a representative experiment of three performed taken at the time of scratch ($t = 0$) and at $t = 72$ h. Magnification × 200: mean percentage ± s.d. of migration at $t = 72$ h is reported in the graph for each cell line. (B): Representative immunofluorescence staining of INTOV11 and SKOV3 CHKA-silenced and control cells. Cells were wounded 72 h after transfection and analysed 24 h later. F-actin filaments were visualised as green fluorescence through Alexa-488–phalloidin binding, and cell nuclei were stained by DAPI. Actin stress fibers and focal adhesion sites are indicated by red arrows (Magnification: × 300). In each panel, a picture of the wound border is reported in the inset (Magnification × 200).

Alterations of choline phospholipid metabolism in ovarian cancer: study of the activity and expression of choline kinase as a prognostic value.

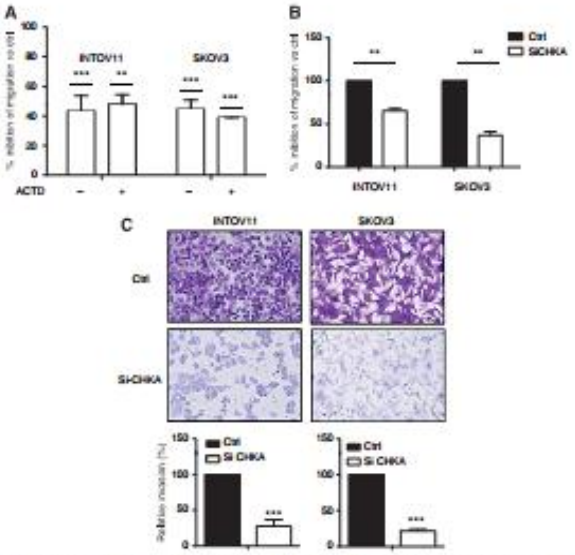

Figure 6. CHKA-silenced cells display reduced motility and invasion. Cells migrating through the membrane were measured by (A). RFU of CyQUANT dye binding to cellular nucleic acids in the lysates or (B). Odyssey infrared laser scanner quantification after SRB staining. In the graphs is reported the percentage of inhibition of migration in CHKA-silenced INTOV11 and SKOV3 cells as compared with their relative controls (oligo-treated cells), to which significance is referred. Data are the mean ± s.d. of three to six independent experiments. (C): upper panels. photographs of a representative experiment of the matrigel-coated membrane invading cells. Magnification ×200. lower panel: mean relative percentage ± s.d. of invasion capability calculated respect to control oligo-treated cells set to 100%.

(Sandercock *et al*, 2002) have shown to be largely ineffective in achieving patients' cure (Agarwal and Kaye, 2003), especially due to the occurrence of chemoresistant relapse. Although ChoK-alpha impairment by siRNA might have some limitations when transferred in a clinical context essentially due to the stability of the effect and delivery of siRNA, it, however, represents the most effective way to assess the central role of ChoK-alpha in favoring EOC cell survival and its druggability; thus fostering the development of new chemical drugs with higher specificity and lower systemic toxicity.

The effects related to *CHKA* transient silencing in EOC appeared to have perturbation on EOC cell behaviour different than that observed in other cellular models. For instance, neither we observed a reduction of Akt phosphorylation in a PI3K-independent way (Chua *et al*, 2009) nor an attenuation of MAPK and PI3K/AKT signalling (Yalcin *et al*, 2010). Furthermore, although cell proliferation was reduced in both cell lines after *CHKA* silencing, neither decrease of cell viability nor apoptosis were observed in silenced cells. In this respect, EOC seems to behave differently than other tumour types in which targeting ChoK by siRNA technology (Banez-Coronel *et al*, 2008; Gruber *et al*, 2012) or by pharmacological inhibitors (Rodriguez-Gonzalez *et al*, 2003, 2005) was able to induce an apoptotic effect. Nevertheless, the efficacy of transient *CHKA* silencing in our two cellular models in inducing a dramatic drop in PCho content, as observed in si*CHKA* cells by ^{1}H-MRS analysis, especially confirmed the dependence of EOC cholinic phenotype on elevated ChoK-alpha expression and activity. Indeed, apart from *CHKA* downmodulation, none of the genes associated to the biosynthetic Kennedy's Pathway resulted perturbed after transient *CHKA* silencing.

However, when gene expression analysis was performed on silenced *CHKA* cells, perturbations of the most comodulated genes were overall suggestive of a less aggressive phenotype. From a metabolic point of view, comodulatted genes were especially related to fatty acids (such as triacylglycerides (TAG)) synthesis and accumulation of cytoplasmic lipid droplets (*ACSM3*, (Iorio *et al*, 2003; Glunde *et al*, 2005)) as well as biolipid mediators (*PPAP2A*). Interestingly, *PPAP2A* converts phosphatidic acid (PA) that participates in a number of signalling functions to diacylglycerol. It has been reported that an increase in *PPAP2A* activity, due to a gene upmodulation, could terminate the Raf-1 and the MAP-kinase pathway signalling overall affecting cell proliferation (Roberts and Morris, 2000). Although we did not observe consistent modulation of these signalling in our experimental setting, we observed a consistent and reproducible decrease of *IL6* and *IL8* mRNA levels associated to a decrease of protein release in conditioned supernatant of si*CHKA* cells. It is now established that in EOC IL6 and IL8 expression is induced by lysophosphatidic acid (LPA) (Fang *et al*, 2004; So *et al*, 2004; Nilsson *et al*, 2005) a biolipid that, by upregulating these cytokines, stimulates tumour cell invasion and metastasis. Interestingly, LPA can be produced by breakdown of PA generated by the activity of phospholipase D, an enzyme involved in the catabolic pathway of PtdCho (see (Iorio *et al*, 2005) and (Aoki *et al*, 2008)). Downmodulation of these cytokine might be then related to a lower availability of LPA as a consequence of a decreased PtdCho synthesis and subsequent degradation by the catabolic pathway.

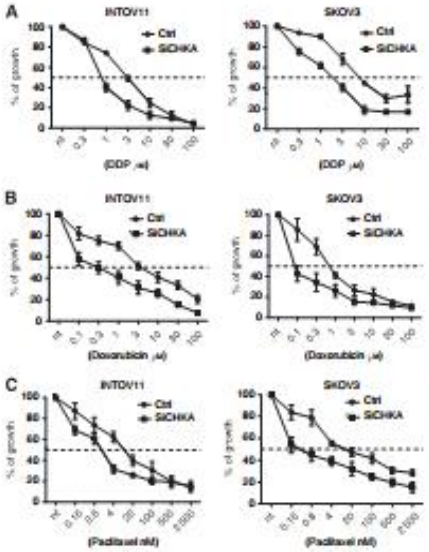

Figure 7. CHKA silencing induce sensitivity to drug treatment. Cytotoxicity assay: Sensitivity to: (A) cisplatinum (DDP, from 1×10^{-4} to 3×10^{-7} M); (B) Doxorubicin (from 1×10^{-4} to 1×10^{-7} M); (C) Paclitaxel (from 2.5 to 0.016 nM) was tested. Mean ± s.d. of growth percentage of treated vs untreated cells is reported.

Consistently with the preliminary biological indications derived from the most *CHKA*-comodulated genes, IPA functional analysis, identified as the most perturbed cellular functions those related to cell death and cellular proliferation and movement. The predicted alterations of these pathways were supposed to lead EOC cells towards a less tumourigenic behaviour.

Interestingly, LIMK1 was one of the genes downmodulated following *CHKA* silencing (see Table 1) and a reduced phosphorylation of the LIMK1/cofilin pathway at later time point after scratching was observed in *CHKA*-silenced cells (data not shown), suggesting that a long lasting dephosphorilation by impairing actin polimerisation might ultimately reduce cell migration (Mizuno, 2013). In this perspective, we indeed validated this prediction by showing a reduction of cell migration upon *CHKA* silencing. Furthermore, although we did not observe an increase in apoptosis, we could demonstrate in si*CHKA* cells an increased sensitivity to the main chemotherapeutic agent used for EOC treatment (platinum compounds) also in the highly platinum-resistant SKOV3 cell line. Importantly, we also observed a sensitisation of the CHKA-silenced cells to the other two drugs Paclitaxel and Doxorubicin that are currently in use in the clinical practice for EOC treatment in combination with platinum compounds. In agreement with the increased drug sensitivity, CCNA1 downmodulation following *CHKA* silencing might then impair the ability of cells to arrest cell cycle to repair DNA following DNA damage. Cyclin A1 is indeed a down-stream target of p53 able to mediate a G2/M cell-cycle arrest (Rivera *et al*, 2006). A cell sensitisation to drug treatment (5-fluoruracil) after *CHKA* silencing has been already reported also in the breast (Mori *et al*, 2007) and colorectal (de la Cueva *et al*, 2013) cancer cells.

When considering the biological relevance of *CHKA* knock-down it should be taken into account that the specific EOC molecular context may require longer time and a more persistent *CHKA* downregulation to achieve a more effective modulation of cell behaviour. A transient inhibition of *CHKA* in EOC could be not sufficient alone to maintain overtime the biological effect of its silencing. Indeed by a multidisciplinary approach, we showed that the alterations of the tCho MRS spectral profile observed in EOC cells is sustained also by the activation of other enzymes involved in PtdCho pathways such as PtdCho-plc (Iorio *et al*, 2005, 2010; Spadaro *et al*, 2008; Podo *et al*, 2011). It has also been shown that the decreased GPC to PCho ratio reported in several tumours could also be due to an increased cleavage of GPC to produce Cho by mean of the newly identified enzyme EDI3 (endometrial differential 3) (Stewart *et al*, 2012), which remain to be analysed in EOC. Then, both a *CHKA* stable inhibition as well as a simultaneous inhibition of the enzymes involved in both the biosynthetic as well as catabolic pathways could be more appropriated in these cellular models to obtain a stronger biological effect. Finally, the understanding of the possible different role of ChoK isoforms in carcinogenesis is at the moment a research great challenge (Gallego-Ortega *et al*, 2011; Gruber *et al*, 2012) that deserve to be further investigated in the next future.

In conclusion, the biological relevance of our results rests in the rescue to drug sensitivity of EOC cell lines when interfering with the ChoK-alpha expression and activity. This supports the concept of targeting metabolism to improve efficacy of existing standard chemotherapeutic approaches (Vander Heiden, 2011) and opens the way to validate ChoK-alpha as a druggable target.

ACKNOWLEDGEMENTS

We thank Mrs Paola Alberti, Mrs Donata Penso, Mrs G Abolafio and Mr Edoardo Marchesi for their excellent technical support; Dr Maria Teresa Comito for her efforts in the initial setting of the experiments and Dr Zaver Bhujwalla for helpful discussion of our data. We also thank the NMR Joint facility (ISS, INFM, UniTV) at the Department of Chemistry of the University of Rome Tor Vergata for the good maintenance of the 16.4 T spectrometer. This study is supported by grants from the Italian Association for Cancer Research (IG-9147/2009 and 12976/2012 to DM).

REFERENCES

Agarwal R, Kaye SB (2003) Ovarian cancer: strategies for overcoming resistance to chemotherapy. *Nat Rev Cancer* **3**: 502–516.

Aoki J, Inoue A, Okudaira S (2008) Two pathways for lysophosphatidic acid production. *Biochim Biophys Acta* **1781**: 513–518.

Aoyama C, Liao H, Ishidate K (2004) Structure and function of choline kinase isoforms in mammalian cells. *Prog Lipid Res* **43**: 266–281.

Bagnoli M, De Cecco L, Granata A, Nicoletti R, Marchesi E, Alberti P, Valeri B, Libra M, Barbareschi M, Raspaglioni F, Mezzanzanica D, Canevari S (2011) Identification of a chrXq27.3 microRNA cluster associated with early relapse in advanced stage ovarian cancer patients. *Oncotarget* **2**: 1265–1278.

Banez-Coronel M, de Molina AR, Rodriguez-Gonzalez A, Sarmentero J, Ramos MA, Garcia-Cabezas MA, Garcia-Orue I, Lacal JC (2008) Choline kinase alpha depletion selectively kills tumoral cells. *Curr Cancer Drug Targets* **8**: 709–719.

Chen HS, Lancaster JM (2011) Microarray-based gene expression studies in ovarian cancer. *Cancer Control* **18**: 8–15.

Chua BT, Gallego-Ortega D, Ramirez dM, Ullrich A, Lacal JC, Downward J (2009) Regulation of Akt(ser473) phosphorylation by Choline kinase in breast carcinoma cells. *Mol Cancer* **8**: 131.

Clem BF, Clem AL, Yalcin A, Goswami U, Arumugam S, Telang S, Trent JO, Chesney J (2011) A novel small molecule antagonist of choline kinase-alpha

Alterations of choline phospholipid metabolism in ovarian cancer: study of the activity and expression of choline kinase as a prognostic value.

that simultaneously suppresses MAPK and PI3K/AKT signaling. *Oncogene* 30: 3570–3580.
de la Cueva A, Ramírez de Molina A, Varez-Ayerza N, Ramos MA, Cebrian A, Del Pulgar TG, Lacal JC (2013) Combined 5-FU and ChoKalpha inhibitors as a new alternative therapy of colorectal cancer: evidence in human tumor-derived cell lines and mouse xenografts. *PLoS One* 8: e64961.
Fang X, Yu S, Bast RC, Liu S, Xu HJ, Hu SX, LaPushin R, Claret FX, Aggarwal BB, Lu Y, Mills GB (2004) Mechanisms for lysophosphatidic acid-induced cytokine production in ovarian cancer cells. *J Biol Chem* 279: 9653–9661.
Gallego-Ortega D, Gomez del PT, Valdes-Mora F, Cebrian A, Lacal JC (2011) Involvement of human choline kinase alpha and beta in carcinogenesis: a different role in lipid metabolism and biological functions. *Adv Enzyme Regul* 51: 183–194.
Glunde K, Bhujwalla ZM, Ronen SM (2011a) Choline metabolism in malignant transformation. *Nat Rev Cancer* 11: 835–848.
Glunde K, Jiang L, Moestue SA, Gribbestad IS (2011b) MRS and MRSI guidance in molecular medicine: targeting and monitoring of choline and glucose metabolism in cancer. *NMR Biomed* 24: 673–690.
Glunde K, Raman V, Mori N, Bhujwalla ZM (2005) RNA interference-mediated choline kinase suppression in breast cancer cells induces differentiation and reduces proliferation. *Cancer Res* 65: 11034–11043.
Gruber J, See Too WC, Wong MT, Lavie A, McSorley T, Konrad M (2012) Balance of human choline kinase isoforms is critical for cell cycle regulation: implications for the development of choline kinase-targeted cancer therapy. *FEBS J* 279: 1915–1928.
Hanahan D, Weinberg RA (2011) Hallmarks of cancer: the next generation. *Cell* 144: 646–674.
Hernandez-Alcoceba R, Fernandez F, Lacal JC (1999) *In vivo* antitumor activity of choline kinase inhibitors: a novel target for anticancer drug discovery. *Cancer Res* 59: 3112–3118.
Iorio E, Di VM, Spadaro F, Ramoni C, Locosco E, Carnevale R, Lenti L, Strom R, Podo F (2003) Triacsin C inhibits the formation of 1H NMR-visible mobile lipids and lipid bodies in HuT 78 apoptotic cells. *Biochim Biophys Acta* 1634: 1–14.
Iorio E, Mezzanzanica D, Alberti P, Spadaro F, Ramoni C, D'Ascenzo S, Millimaggi D, Pavan A, Dolo V, Canevari S, Podo F (2005) Alterations of choline phospholipid metabolism in ovarian tumor progression. *Cancer Res* 65: 9369–9376.
Iorio E, Ricci A, Bagnoli M, Pisanu ME, Castellano G, Di Vito M, Venturini E, Glunde K, Bhujwalla ZM, Mezzanzanica D, Canevari S, Podo F (2010) Activation of phosphatidylcholine cycle enzymes in human epithelial ovarian cancer cells. *Cancer Res* 70: 2126–2135.
Iorio E, Ricci A, Pisanu ME, Bagnoli M, Podo F, Canevari S (2013) Choline metabolic profiling by magnetic resonance spectroscopy. *Methods Mol Biol* 1049: 255–270.
Ishidate K (1997) Choline/ethanolamine kinase from mammalian tissues. *Biochim Biophys Acta* 1348: 70–78.
Konstantinopoulos PA, Spentzos D, Cannistra SA (2008) Gene-expression profiling in epithelial ovarian cancer. *Nat Clin Pract Oncol* 5: 577–587.
Krishnamachary B, Glunde K, Wildes F, Mori N, Takagi T, Raman V, Bhujwalla ZM (2009) Noninvasive detection of lentiviral-mediated choline kinase targeting in a human breast cancer xenograft. *Cancer Res* 69: 3464–3471.
Kurman RJ, Shih I (2010) The origin and pathogenesis of epithelial ovarian cancer: a proposed unifying theory. *Am J Surg Pathol* 34: 433–443.
Mizuno K (2013) Signaling mechanisms and functional roles of cofilin phosphorylation and dephosphorylation. *Cell Signal* 25: 457–469.
Mori N, Gadiya M, Wildes F, Krishnamachary B, Glunde K, Bhujwalla ZM (2013) Characterization of choline kinase in human endothelial cells. *NMR Biomed* 26: 1501–1507.
Mori N, Glunde K, Takagi T, Raman V, Bhujwalla ZM (2007) Choline kinase down-regulation increases the effect of 5-fluorouracil in breast cancer cells. *Cancer Res* 67: 11284–11290.
Nilsson MB, Langley RR, Fidler IJ (2005) Interleukin-6, secreted by human ovarian carcinoma cells, is a potent proangiogenic cytokine. *Cancer Res* 65: 10794–10800.
Podo F (1999) Tumour phospholipid metabolism. *NMR Biomed* 12: 413–439.
Podo F, Canevari S, Canese R, Pisanu ME, Ricci A, Iorio E (2011) MR evaluation of response to targeted treatment in cancer cells. *NMR Biomed* 24: 648–672.
Ramírez dM, Sarmentero-Estrada J, Belda-Iniesta C, Taron M, Ramírez dM V, Cejas P, Skrzypski M, Gallego-Ortega D, de Castro J, Casado E, Garcia-Cabezas MA, Sanchez JJ, Nistal M, Rosell R, Gonzalez-Baron M, Lacal JC (2007) Expression of choline kinase alpha to predict outcome in patients with early-stage non-small-cell lung cancer: a retrospective study. *Lancet Oncol* 8: 889–897.
Rivera A, Mavila A, Bayless KJ, Davis GE, Maxwell SA (2006) Cyclin A1 is a p53-induced gene that mediates apoptosis, G2/M arrest, and mitotic catastrophe in renal, ovarian, and lung carcinoma cells. *Cell Mol Life Sci* 63: 1425–1439.
Roberts RZ, Morris AJ (2000) Role of phosphatidic acid phosphatase 2a in uptake of extracellular lipid phosphate mediators. *Biochim Biophys Acta* 1487: 33–49.
Rodriguez-Gonzalez A, Ramirez de MA, Ramos-Coronel M, Megias D, Lacal JC (2005) Inhibition of choline kinase renders a highly selective cytotoxic effect in tumour cells through a mitochondrial independent mechanism. *Int J Oncol* 26: 999–1008.
Rodriguez-Gonzalez A, Ramirez de MA, Fernandez F, Ramos MA, del Carmen NM, Campos J, Lacal JC (2003) Inhibition of choline kinase as a specific cytotoxic strategy in oncogene-transformed cells. *Oncogene* 22: 8803–8812.
Sandercock J, Parmar MK, Torri V, Qian W (2002) First-line treatment for advanced ovarian cancer: paclitaxel, platinum and the evidence. *Br J Cancer* 87: 815–824.
Siegel R, Naishadham D, Jemal A (2013) Cancer statistics, 2013. *CA Cancer J Clin* 63: 11–30.
So J, Navari J, Wang FQ, Fishman DA (2004) Lysophosphatidic acid enhances epithelial ovarian carcinoma invasion through the increased expression of interleukin-8. *Gynecol Oncol* 95: 314–322.
Spadaro F, Ramoni C, Mezzanzanica D, Miotti S, Alberti P, Cecchetti S, Iorio E, Dolo V, Canevari S, Podo F (2008) Phosphatidylcholine-specific phospholipase C activation in epithelial ovarian cancer cells. *Cancer Res* 68: 6541–6549.
Stewart JD, Marchan R, Lesjak MS, Lambert J, Hergenroeder R, Ellis JK, Lau CH, Keun HC, Schmitz G, Schiller J, Eibisch M, Hedberg C, Waldmann H, Lausch E, Tanner B, Schrenk J, Sagemueller J, Staude H, Steiner E, Hengstler JG (2012) Choline-releasing glycerophosphodiesterase EDI3 drives tumor cell migration and metastasis. *Proc Natl Acad Sci USA* 109: 8155–8160.
Vance JE, Vance DE (2004) Phospholipid biosynthesis in mammalian cells. *Biochem Cell Biol* 82: 113–128.
Vander Heiden MG (2011) Targeting cancer metabolism: a therapeutic window opens. *Nat Rev Drug Discov* 10: 671–684.
Vaughan S, Coward JI, Bast Jr RC, Berchuck A, Berek JS, Brenton JD, Coukos G, Crum CC, Drapkin R, Etemadmoghadam D, Friedlander M, Gabra H, Kaye SB, Lord CJ, Lengyel E, Levine DA, McNeish IA, Menon U, Mills GB, Nephew KP, Oza AM, Sood AK, Stronach EA, Walczak H, Bowtell DD, Balkwill FR (2011) Rethinking ovarian cancer: recommendations for improving outcomes. *Nat Rev Cancer* 11: 719–725.
Ward PS, Thompson CB (2012) Metabolic reprogramming: a cancer hallmark even warburg did not anticipate. *Cancer Cell* 21: 297–308.
Wu G, Aoyama C, Young SG, Vance DE (2008) Early embryonic lethality caused by disruption of the gene for choline kinase alpha, the first enzyme in phosphatidylcholine biosynthesis. *J Biol Chem* 283: 1456–1462.
Yalcin A, Clem B, Makoni S, Clem A, Nelson K, Thornburg J, Siow D, Lane AN, Brock SE, Goswami U, Eaton JW, Telang S, Chesney J (2010) Selective inhibition of choline kinase simultaneously attenuates MAPK and PI3K/AKT signaling. *Oncogene* 29: 139–149.

Supplementary Information accompanies this paper on British Journal of Cancer website (http://www.nature.com/bjc)